The role of nutrient signaling in the regulation of pancreatic α-cell mass and glucagon secretion

by

Nadejda Ivanova Bozadjieva

A dissertation submitted in partial fulfillment
of the requirements for the degree of
Doctor of Philosophy
(Cellular and Molecular Biology)
in the University of Michigan
2016

Doctoral Committee:

Professor Ernesto Bernal-Mizrachi, Co-Chair
Professor Charles Burant, Co-Chair
Professor Ken Inoki
Associate Professor Lei Yin
Professor John A. Williams

Dedication

This work is dedicated to my family. Thank you for your limitless love, support, encouragement, and for the sacrifices you made to give me the opportunity to pursue my career goals.

Acknowledgements

I wish to thank my parents, Kalina Bozadjieva and Ivan Bozadjiev, for their limitless love, support, encouragement, and for the sacrifices they have made to give me many opportunities. My deepest appreciation goes to Mark Kramer who has lived through this experience with me and has patiently listened and supported me through numerous failed experiments and “great-data day” celebrations.

I would like to extend my sincere appreciation to my advisor, Dr. Ernesto Bernal-Mizrachi, for his guidance through this project, for developing me into the scientist I am today and for always believing in me and my abilities even when I didn’t. I also wish to thank my thesis committee, Dr. Charles Burant, Dr. John Williams, Dr. Ken Inoki and Dr. Lei Yin for their support and guidance through my development as a scientist and the progression of my studies. I want to recognize the Graduate Program in Cellular and Molecular Biology at the University of Michigan for giving me the opportunity and the means to develop as a scientist.

Preface

Type 2 Diabetes (T2D) is characterized by defective adaptation of β-cells to insulin resistance. Most of the research effort has focused on elucidating the physiological, molecular, and genetic components that regulate β-cell mass and insulin secretion, presenting diabetes as a unihormonal disorder. Contrary to this current approach, clinical data and animal experiments have shown that increased glucagon secretion by pancreatic α-cells play a role in the pathogenesis of hyperglycemia in diabetes. Physiological and genetic models of obesity show an increase in α-cell mass and glucagon secretion, but the signaling mechanisms responsible for these changes are not completely understood. Glucagon secretion is regulated by nutrients (glucose, amino acids) and growth factors (insulin). Studies in mice with loss of the insulin receptor in α-cells and studies in glucagon-secreting cell lines demonstrate that insulin receptor signaling regulates α-cell mass and glucagon secretion through AKT activation. Alpha cell proliferation is reduced by treatment with the mTOR Complex 1 (mTORC1) inhibitor, rapamycin, suggesting that downstream of the insulin receptor, Tuberous Sclerosis Complex (TSC1/2) and mTORC1 are important candidates in regulating α-cell mass and glucagon secretion. Most recently, studies using glucagon receptor deficient mice report increased α-cell proliferation and this was associated with a significant increase of circulating amino acids (known activators of mTORC1) suggesting that certain amino acids could induce α-cell mass in this mouse model. However, how downstream nutrient or insulin signaling regulates α-cell mass and glucagon secretion *in vivo* is currently unknown.

We hypothesize that mTORC1 signaling plays an essential role in nutrient-dependent regulation of α-cell mass maintenance and glucagon secretion. The following projects will test the hypothesis:

Chapter 1: **Determine how loss of mTORC1 signaling regulates α-cell mass, glucagon secretion and adaptation of α-cells to diabetogenic conditions**. The hypothesis for this project is that mTORC1 signaling is necessary for the proper maintenance of α-cell mass and glucagon secretion. The approach used to test this hypothesis includes *in vivo* and *in vitro* experiments using a genetic model of loss of mTORC1 signaling by ablating *raptor* in α-cells.

Chapter 2: Establish the role of gain of mTORC1 function on the regulation of α-cell mass, glucagon secretion and adaptation of α-cells to diabetogenic conditions. The working hypothesis is that gain in mTORC1 in α-cells potentiates α-cell mass expansion and increases glucagon levels as observed in diabetic patients. The approach used to test this hypothesis includes *in vivo* and *in vitro* experiments using a genetic model of gain of mTORC1 signaling by ablating *TSC2* in α-cells.

Uncovering the roles of mTOR Complex 1 in the regulation of α-cell mass and function using animal models and further examining these mechanisms using *in vitro* approaches will expand our understanding of how this pathway contributes to regulation of glucose homeostasis during normal and diabetogenic conditions. Finally, these studies will provide novel potential targets for therapeutic approaches in the maintenance of normoglycemia in diabetes.

Table of Contents

List of Figures

List of Tables

Abstract

Increased α-cell mass and aberrant glucagon response play major roles in the pathogenesis and complications associated with diabetes. In these studies, we determined that mTOR Complex 1 (mTORC1) is a major regulator of α-cell mass and glucagon secretion. Using mice deficient of *raptor* exclusively in α-cells we revealed that mTORC1 signaling promotes glucagon secretion during fasting by positively regulating K_{ATP} channels and glucagon expression. A novel mTORC1/FoxA2 axis provided a link between mTORC1 and transcriptional regulation of key genes responsible for α-cell function. Furthermore, we also found that mTORC1 signaling positively modulates the maintenance of islet α-cells by an autophagy-mediated process. In proceeding studies, we demonstrated that activation of mTORC1 signaling in α-cells is sufficient to induce α-cell mass expansion and hyperglucagonemia as observed in diabetic patients. We increased mTORC1 activity in α-cells by deletion of *TSC2*, a negative mTORC1 regulator. Our results revealed that gain of mTORC1 signaling in α-cells leads to increased fed and fasting glucagon levels and increased α-cell mass. Despite hyperglucagonemia, these mice were normoglycemic and had improved glucose tolerance and decreased hepatic glucose production. The results of these studies support a role for increased mTORC1 signaling in promoting the increase in α-cell mass and glucagon secretion observed in diabetic patients. Overall, our results revealed a novel function of mTORC1 in nutrient-dependent regulation of glucagon secretion and support a role for mTORC1 in controlling α-cell mass and function in patients treated with rapamycin analogs.

INTRODUCTION*

The discovery of glucagon

In 1907, Michael Lane described his anatomical observations of the pancreatic islets of Langerhans as cells with distinctive anatomical properties versus the earlier theory as those of “exhausted acini” (Lane, 1907). In his characterization of stained hamster pancreatic sections, Lane described the existence of two distinct types of cells within the islet, which he referred to as the large α and smaller β-cells (Lane, 1907). Four decades later, Sutherland and de Duve established that the α-cells of the pancreatic islet are the primary source of glucagon (Sutherland and De Duve, 1948a, b). Initially labeled as a contaminant, the physiological role of glucagon was first described in 1921, when Banting and Best conducted their classical experiments of insulin’s actions. Banting and Best tested their first pancreatic extracts in depancreatized dogs and observed an initial transient rise in blood glucose followed by the insulin-induced hypoglycemia (Gromada et al., 2007). Several years later, Murlin and his colleagues credited this transient rise in blood glucose to a hormone they named “Glucagon” or “Hyperglycemic-Glycogenolytic Factor” (Foa PP, 1952; Gromada et al., 2007; Murlin JR, 1923). Insights into the regulation of glucagon release came from elegant cross-circulation experiments performed by Foa and his colleagues in the 1950s, showing that hypoglycemia triggered by the injection of insulin in a donor dog induces the release of glucagon, which secreted through the donor blood *via* a pancreatic-femoral anastomosis causes a hyperglycemic response in a recipient dog (Foa PP, 1952). Bensley and Woerner added to these observations with their suggestion that glucagon

* Bozadjieva, Nadejda. Williams, John. Bernal-Mizrachi, Ernesto. (2013). Glucagon. *Pancreapedia: Exocrine Pancreas Knowledge Base*, DOI: 10.3998/panc.2013.23

induces liver glycogenolysis and thereby promotes a rise in blood glucose levels (Bensley S.H., 1939).

Glucagon

Glucagon is a 29-amino acid peptide derived from the tissue-specific processing of proglucagon in pancreatic α-cells through cleavage by prohormone convertase 2 (PC2) (Figure 1) (Furuta et al., 2001). In contrast, processing of proglucagon to glucagon-like peptides (GLP-1, GLP-2), oxyntomodulin and glicentin occurs in intestinal enteroendocrine cells by prohormone convertase 1 (PC1) (Figure 1) (Lefebvre, 1995). Glucagon plays a major role in antagonizing the effects of insulin and maintaining glucose homeostasis by promoting hepatic gluconeogenesis and glycogenolysis and inhibiting glycogen synthesis. Therefore, the secretion of glucagon is normally induced in states of decreasing blood glucose, such as fasting and increased energy expenditure, to sufficiently induce a rapid, yet transient rise in blood glucose.

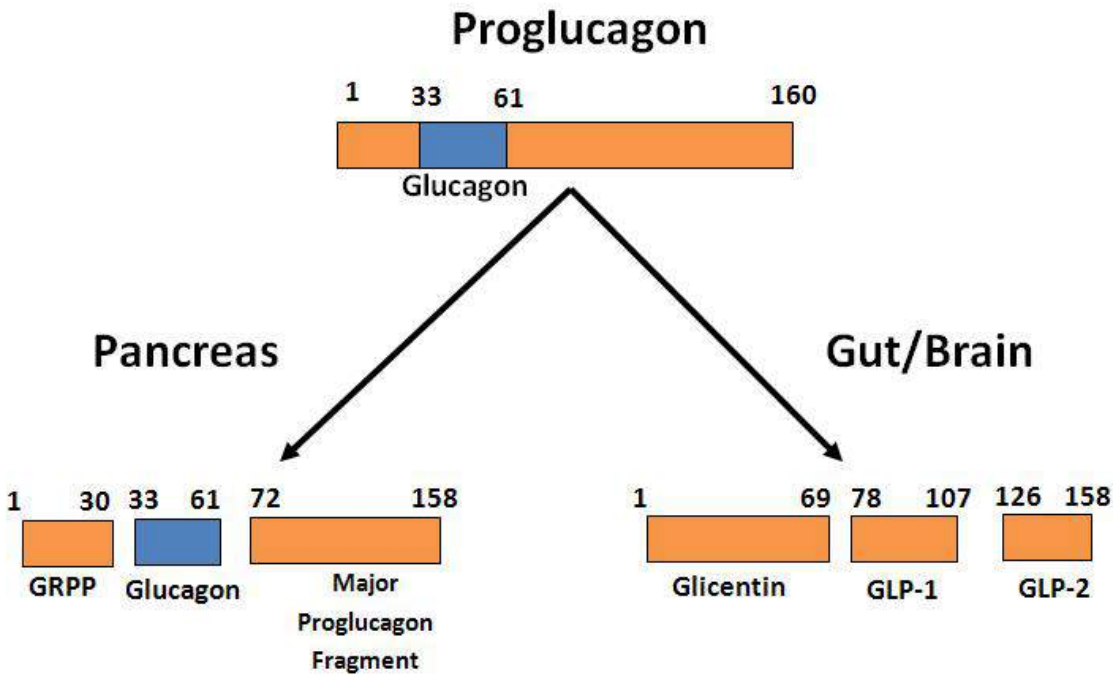

Figure 1. Diagram of differential processing of the proglucagon gene product in α-cells of the pancreas, gut (L-cells) and brain. Glucagon is a 29-amino acid peptide derived from the tissue-specific processing of proglucagon in pancreatic α-cells through cleavage by prohormone convertase 2 (PC2) In contrast, processing of proglucagon to glucagon-like peptides (GLP-1, GLP-2), oxyntomodulin and glicentin occurs in intestinal

enteroendocrine cells by prohormone convertase 1 (PC1) Only biologically active products are shown. For further details of cleavage sites and processing see reference (Lefebvre, 1995).

Glucagon and the endocrine pancreas

The pancreatic islet comprises five major types of polypeptide-secreting cells: insulin-secreting β-cells (65-80% of total islet cells), the glucagon secreting α-cells (15-20%), somatostatin-secreting δ-cells (3-10%) and pancreatic polypeptide-secreting cells (3-5%), along with ghrelin-positive cells which are mostly observed in early development (Wierup et al., 2004). The five major islet cell types are aligned on blood vessels at no particular order or structured organization within the human islet (Cabrera et al., 2006) (Figure 2A). In contrast, the rodent islet shows a more-defined architecture placing the β-cells in the core and the α, δ and PP-cells lying at the mantle of the islet (Figure 2B). This unique structure in the rodent islet suggests an organized system allowing paracrine interactions between the peptides released. This is supported by studies showing that arterial blood is directed from the core of the rodent islet (insulin-secreting β-cells) to the periphery (Bonner-Weir and Orci, 1982). Therefore, during a rise in blood glucose, the pancreatic α-cells are exposed to high levels of secreted insulin leading to the inhibition of glucagon secretion and glucagon gene transcription.

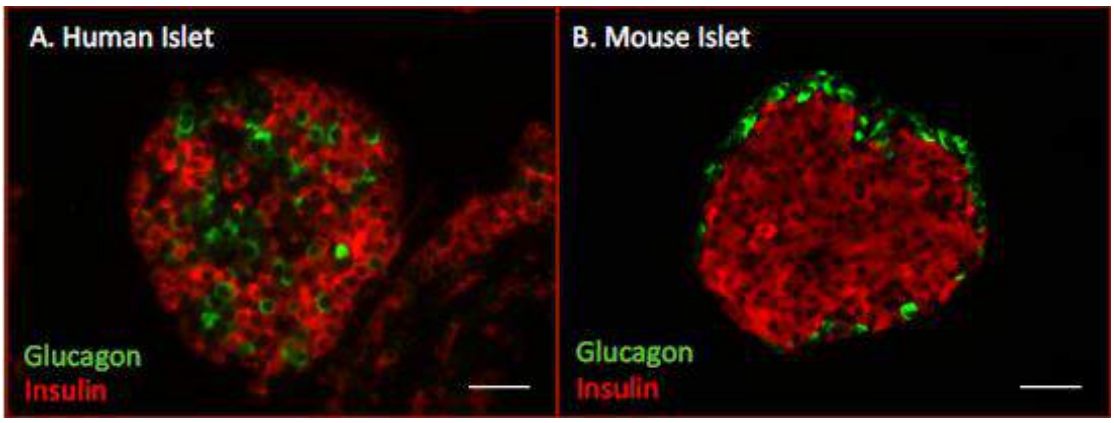

Figure 2. Immunofluorescent labeling of human and mouse islets. A. Human islet: glucagon-positive α-cells (green) are randomly dispersed among insulin-positive β-cells (red) within the human islet (scale 50 μm). **B.** Mouse islet: glucagon-positive α-cells (green) are concentrated on the mantle and insulin-positive β-cells (red) make-up the core of the mouse islet (scale 50 μm).

Transcriptional regulation of α-cell development, maintenance and glucagon gene transcription

A cascade of transcriptional factor regulators, starting from pancreatic progenitors expressing Pdx1, Ptf1a and Sox9, mediate the differentiation of α-cells. The pancreatic endocrine progenitors that give rise to islet cells express Neurog3 at embryonic day (E) 8.5. The newly formed endocrine cells accumulate along the ducts and blood vessels and undergo rapid expansion *via* self-replication during the neonatal period. The final committed α-cell lineage is defined by the expression of the transcription factors Arx, Foxa1/2, Pou3f4 (Brn4), MafB, Pax6 and Isl1. Glucagon is expressed at E12.5.

The loss of α-cell transcription factors Arx and Pax6 results in loss of α-cells and circulating glucagon levels. The specific loss of Arx is sufficient to promote the conversion of α to β–cells at any stage, and is independent of Pax4 expression (Courtney et al., 2013). Loss of Pax4 results in dramatic loss of β and δ-cells and increase in α-cells (Sosa-Pineda et al., 1997). In contrast, ectopic expression of Pax4 drives endocrine precursor cells and mature α-cells to adopt a β-cell fate by suppressing Pax6-mediated transcription (Collombat et al., 2003; Collombat et al., 2009; St-Onge et al., 1997). Pax6 also has been shown to play a key role in the regulation of proglucagon gene expression and processing, as well as glucagon biosynthesis and secretion (Gosmain et al., 2012; Katz et al., 2009; Ritz-Laser et al., 2002).

Foxa1 and Foxa2 play major roles in α-cell development and glucagon expression. Foxa1 null mice lack key islet genes, including glucagon, and die shortly after birth due to hypoglycemia (Kaestner et al., 1999; Shih et al., 1999). Ablation of Foxa2 in the gut endoderm leads to major reduction in the number of mature α-cells and proglucagon expression (Lee et al., 2005). Pou3f4 (Brn4) is dispensable for α-cell development and maintenance, but this transcription factor promotes the expression of glucagon by directly binding to the proglucagon promoter. Isl1 and MafB have also been shown to promote glucagon expression by directly binding to the proglucagon promoter (Artner et al., 2006; Conrad et al., 2015).

Regulation of glucagon release

The secretion of glucagon by the α-cells is regulated by the effects of paracrine and autocrine factors as wells as neuronal inputs. Glucagon release is inhibited after carbohydrate-rich meal and the consequent rise in blood glucose (hyperglycemia) and insulin secretion. However, a meal rich in amino acids induces glucagon release. Parasympathetic (Adrenaline) and sympathetic (Epinephrine, Norepinephrine, Galanin, Neuropeptide Y) nerve stimulations induce the secretion of glucagon from the pancreatic α-cells.

Nutrients (Amino Acids and Glucose)

Nutrients play primary role in the regulation of glucagon secretion, in part by modulating cell mass and glucagon expression (reviewed in (Marroqui et al., 2014). The amino acids arginine, alanine, glutamine and low levels of leucine potentiate glucagon secretion and it has been shown that this effect is suppressed during high glucose in an insulin-independent manner (Pipeleers et al., 1985). In turn, lysine and high levels of leucine inhibit glucagon release.

Glucagon is secreted by the pancreatic α-cells in states of decreasing blood glucose; however, whether changes in glucose concentrations alone can regulate glucagon secretion still remains unclear. Contrary to the regulation of glucagon release in the fed state, it has been strongly suggested that extrinsic paracrine signals (insulin/GABA, somatostatin) do not play a role in regulating glucagon secretion during fasting (1-6 mM glucose) (Walker et al., 2011).

Rat α-cells express glucokinase and glucose transporter GLUT1, an isoform with a lower capacity compared to GLUT2 - the predominant form in insulin-secreting mouse β-cells (Heimberg et al., 1996). Despite differences in metabolism of glucose by the two cells types, studies have shown that they share similar inherent mechanisms of activation (Olsen et al., 2005). Alpha cells have high ATP concentrations under low glucose, which rise further after stimulation with high glucose. In contrast to β-cells, net K_{ATP}-channel activity at low (1 mM) glucose is significantly inhibited (Rorsman et al.,

2014; Rorsman et al., 2008). This renders K_{ATP}-channel partly open, shifting the membrane potential enough to activate low-voltage-activated L-type Ca^{2+}-channels. Ca^{2+} influx activates Na^{+}-channels to further depolarize membrane potential triggering Ca^{2+} entry through P/Q type channels (Leclerc et al., 2011; Rorsman et al., 2014; Rorsman et al., 2008; Zhang et al., 2013). Influx of Ca^{2+} triggers glucagon granule exocytosis. In contrast, glucose elevation inhibits remaining α-cell K_{ATP} channel activity causing further depolarization that partially inactivates voltage-dependent Na^{+}-channels, decreases spike height and results in low P/Q Ca^{2+} channel activity. This depolarization ultimately results in inhibition of secretion (Leclerc et al., 2011; Rorsman et al., 2014; Rorsman et al., 2008; Zhang et al., 2013). Elegant studies have shown that K_{ATP} channels play an essential role in potentiating glucagon release and their activity is altered in diabetic islets (Gopel et al., 2000; MacDonald et al., 2007; Zhang et al., 2013). Also, these studies have shown that glucose-mediated regulation of glucagon secretion is dependent on K_{ATP} channel function (Rorsman et al., 2008; Zhang et al., 2013).

Paracrine Regulation by Insulin and GABA

Pancreatic α-cells are exposed to high levels of insulin secreted from the β-cells in the islet. Insulin is a potent inhibitor of glucagon secretion and glucagon gene transcription (Asplin et al., 1981; Maruyama et al., 1984; Philippe, 1989; Weir et al., 1976; Zhang et al., 2012). Data have shown that the diminished insulin release during hyperglycemia associated with diabetes paradoxically stimulates the release of glucagon (Dinneen et al., 1995; Reaven et al., 1987; Yoon et al., 2003). It has also been shown that chronic high glucose induces glucotoxicity increasing glucagon secretion by reducing the insulin-mediated activation of phosphatidylinositol 3-kinase (PI3K)-AKT activity in rat islets and glucagon-secreting cell line (Shen et al., 2012). Studies utilizing *in vitro* approaches have shown that insulin receptors are very abundant on pancreatic α-cells and activate the PI3K/AKT pathway leading to inhibition of glucagon gene transcription and secretion (Schinner et al., 2005; Shen et al., 2012; Xu et al., 2006). Insulin has been shown to induce the AKT-dependent $GABA_A$ receptor translocation to the plasma membrane (which can be activated by GABA (co-released with insulin) and PI3K-dependent opening of K_{ATP} channels, culminating in hyperpolarizing the plasma

membrane and inhibiting glucagon secretion (Xu et al., 2006). Although, the precise mechanisms responsible for changes in the α-cell function in diabetes remain unclear, a recent study by Kawamori and colleagues showed that inhibiting insulin signaling in the pancreatic α-cells of mice through genetic ablation of insulin receptors in α-cells leads to altered glucose metabolism including mild glucose intolerance, hyperglycemia, and mild hyperglucagonemia (Kawamori and Kulkarni, 2009).

GABA (γ-Aminobutyric acid) is produced from the excitatory amino acid glutamate and co-released with insulin from the pancreatic β-cells by high glucose and glutamate stimulation. GABA can diffuse within the islet interstitium to activate $GABA_A$ receptors present on the cell-surface of α-cells (Wendt et al., 2004). This nonpeptidal neurotransmitter has been shown to act as a suppressor of amino acid-stimulated glucagon release in the mouse and isolated α-cells via $GABA_A$ receptors (Gilon et al., 1991). Data have suggested that glucose-stimulated insulin release and the subsequent activation of the Insulin Receptor-PI3K-AKT pathway induce the activation and translocation of $GABA_A$ receptors to the plasma membrane (Xu et al., 2006). The GABA co-released with insulin from the β-cells can activate the newly translocated cell-surface $GABA_A$ receptors and increase Cl^- inhibitory currents, subsequently hyperpolarizing the plasma membrane (Wendt et al., 2004). The hyperpolarization of the membrane closes the voltage-dependent Ca^{2+} channels, which lowers the free cytoplasmic Ca^{2+} levels and reduces glucagon exocytosis (Rorsman et al., 1989; Wendt et al., 2004).

Paracrine Regulation by Somatostatin

Somatostatin, secreted by the islet δ-cells, has been long accepted as a glucagon-suppressing peptide. Exogenous somatostatin inhibits glucagon release in isolated α-cells, as wells as in healthy and diabetic patients (Chen et al., 2011; Gerich et al., 1974). In addition, islets isolated from somatostatin-deficient mice have reduced glucose-suppression of glucagon release (Hauge-Evans et al., 2009). Somatostatin-suppressed glucagon secretion is regulated though the somatostatin receptor type 2 (SS2R) and genetic disruption of the receptor leads to an increased glucagon secretion (Yue et al., 2013).

Autocrine Regulation: Glucagon and Glutamate

Perfusion experiments in the human and rat pancreas have shown that glucagon suppresses insulin and somatostatin release (Brunicardi et al., 2001; Stagner et al., 1989). Glucagon receptor knock out mice exhibit α-cell hyperplasia and hyperglucagonemia, which has been suggested to be due to a lack of autocrine signals of glucagon on the α-cell (Gromada et al., 2007). Contrary to this theory, a recent study has shown that transplantation of wild type islets into mice with liver-specific deletion of the glucagon receptor also develop α-cell hyperplasia (Longuet et al., 2013). These data suggest that a circulating factor generated after the disruption of glucagon signaling in the liver can increase α-cell proliferation independent of direct pancreatic input.

Glutamate is a major excitatory neurotransmitter in the central nervous system, which has also been implicated in the regulation of glucagon release. An elegant study published by Cabrera and colleagues described the positive autocrine signal of glutamate in the human, monkey and mouse islets (Cabrera et al., 2008). The authors proposed a mechanistic model where glutamate co-released with glucagon potentiates glucagon secretion through acting on the ionotropic glutamate receptors on the α-cell membrane and creating a positive autocrine loop (Cabrera et al., 2008).

Regulation of α-cell mass

Although the mechanisms of modulating α-cell mass are not fully understood, several hypotheses have been developed based on animal models with increase in α-cell mass. Mice fed with high protein diet or high fat diet exhibit increased α-cell hyperplasia and hypertrophy suggesting that nutrient environment and/or insulin resistance could regulate α-cell mass expansion (Ellingsgaard et al., 2008; Morley et al., 1982). Studies using liver-specific glucagon receptor knock out mice suggest that a circulating factor generated after the disruption of glucagon signaling in the liver can increase α-cell proliferation independent of direct pancreatic input (Gromada et al., 2007; Longuet et al., 2013). Metabolomic profile in glucagon receptor knock out mice suggest that significant increase in circulating amino acids and their derivatives could be responsible for induction of α-cell mass in these mice (Yang et al., 2011). These studies support the

concept that α-cell mass is a dynamic process and responds to extracellular signals including nutrients (amino acids, glucose), growth factors (insulin) and potentially uncharacterized factors from the liver.

Physiological actions of glucagon at target tissues

Glucagon exerts its physiological action on target tissues *via* the G-protein coupled glucagon receptor. The principle target tissues for glucagon signaling are liver and adipose tissue. However, the glucagon receptor is found on multiple other tissues including intestine, kidney and brain (Jiang and Zhang, 2003).

In the liver, glucagon counteracts the anabolic properties of insulin by promoting gluconeogenesis and glycogenolysis and inhibiting glycolysis resulting in a net increase in hepatic glucose production. The hepatocyte is exposed to high levels of glucagon released by the pancreas *via* the portal vein. The mechanistic actions of glucagon on the hepatocyte are mediated by glucagon's binding and activation of the G-protein coupled glucagon receptors on the cell membrane. The subsequent activation of adenylate cyclase leads to the increase in intracellular cyclic adenosine monophosphate (cAMP) levels and the activation of protein kinase A (PKA) (Jiang and Zhang, 2003). The second messenger cAMP can activate cyclic nucleotide-gated ion channels, Exchange Proteins Activated by cAMP (EPAC) and Protein Kinase A (PKA). Activated PKA leads to glycogen breakdown (glycogenolysis) by the activation of the PKA-glycogen phosphorylase kinase-glycogen phosphorylate cascade and increased expression of glucose-6-phosphatase (*G6Pase*), which converts glucose-6-phosphate to glucose (Jiang and Zhang, 2003). Glucagon's activation of the liver's glucagon receptor leading to hepatic glucose output has been shown to act through the gluconeogenic process is also promoted by the activity of additional transcription factors. The activated CREB binds to the promoter region of the transcriptional coactivator *PGC-1* gene, increasing its transcription. PGC-1 and the nuclear transcription factor Hepatocyte Nuclear Factor-4 (HNF-4) further promote gluconeogenesis by increasing the transcription of *PEPCK* gene and therefore PEPCK activity (Jiang and Zhang, 2003).

Glucagon signaling in adipose tissue is relevant during periods of starvation and stress and in particular when insulin is suppressed. In the adipocyte, glucagon binds to the glucagon receptor to activate the cAMP-PKA pathway, leading to the phosphorylation and activation of hormone-sensitive lipase and the subsequent breakdown of triglycerides (lipolysis) and release of diacylglycerol and free fatty acids into the circulation. The liver can further utilize glycerol and free fatty acids for gluconeogenesis or re-esterification of free fatty acids to form ketone bodies.

Glucagon's physiological effects on the heart and kidney have also been described, although glucagon's actions in these tissues are less understood mechanistically compared to those in the liver and adipose tissue. Glucagon stimulates Ca^{2+} currents *via* increased cAMP thus increasing heart contractility (Gonzalez-Munoz et al., 2008; Mery et al., 1990). Glucagon increases glucose utilization and lipid oxidation in the heart, but decreases cardiomyocyte survival (Campbell and Drucker, 2015). Glucagon has been described as a vasodilator, which lowers blood pressure by decreasing the vascular resistance in the liver and spleen. Glucagon has diuretic effects on the kidney, increasing glomerular filtration and electrolyte/water excretion (Farah, 1983).

Glucagon receptors are expressed in the brain and data has suggested that circulating glucagon can pass the blood-brain barrier to modulate its effects in the central nervous system (CNS). Glucagon is expressed in the brainstem and hypothalamus, but glucagon receptors are widely expressed in the CNS. Glucagon infused in the CNS has shown to cause a transient drop in blood glucose, followed by hyperglycemia (LaPierre et al., 2014). The initial drop in blood glucose was abolished in vagotomized dogs and in pancreatectomized dogs, demonstrating that the parasympathetic system and the pancreas are both essential in the central regulation of blood glucose by glucagon (LaPierre et al., 2014). Glucagon infused in the central nervous system has also shown anorexigenic effects in rats, chicks and sheep. In addition, intravenous infusion of glucagon has been shown to suppress appetite in humans; however, the direct link between glucagon and central food intake regulation in humans is unclear. Although the mechanisms of glucagon's activity on the brain remain largely unclear, the involvement

of the hypothalamic corticotropin-releasing factor (CRF) and the activation of the hypothalamic-pituitary-adrenal (HPA) axis are implicated in modulating glucagon's suppression of food intake (Filippi et al., 2013).

The role of glucagon in diabetes

Type 1 (T1D) and Type 2 (T2D) Diabetes are characterized by uncontrolled hyperglycemia associated with progressive decrease in insulin. Glucagon, insulin's counterregulatory hormone, plays a major role in maintaining glucose homeostasis by promoting glucose production *via* hepatic glycogenolysis and gluconeogenesis. Paradoxically, glucagon levels are elevated in insulin-resistant non-diabetic, T1D, and T2D patients, leading to enhanced hepatic glucose output and thereby exacerbating hyperglycemia (Dinneen et al., 1995; Mezza et al., 2014; Orci et al., 1976; Rahier et al., 1983; Sherwin et al., 1976; Yoon et al., 2003). Increase in glucagon levels in T1D and T2D patients can be explained in part by increase in α-cell mass, but the mechanisms for the increase in α-cell mass in diabetes remain unclear (Orci et al., 1976; Rahier et al., 1983; Yoon et al., 2003).

A major complication in the management of T1D diabetes or advanced T2D is the failure to secrete glucagon in response to hypoglycemia. This results in recurrent hypoglycemia, referred as Hypoglycemia-Associated Autonomic Failure (HAAF), and presents a major limiting factor for optimal glucose control in insulin-dependent diabetic patients (Cryer, 2002; Gerich et al., 1973; Segel et al., 2002). Unfortunately, as T1D and advanced T2D progresses insulin administration becomes increasing necessary and the glucagon response to hypoglycemia could become greatly attenuated.

Insulin Receptor/mTOR signaling and its role in metabolic tissues

The AKT/mTOR signaling pathway

The mammalian/mechanistic target of rapamycin (mTOR) couples the growth of the cell to its nutritional status (Efeyan et al., 2012; Murakami et al., 2004). The mammalian TOR is associated with two distinct complexes (mTORC1 and 2) that differ in upstream inputs and downstream targets (Dowling et al., 2010; Laplante and Sabatini, 2012; Lee et al., 2007; Shimobayashi and Hall, 2014; Soulard et al., 2009). mTORC1 constitutes the rapamycin sensitive arm of mTOR signaling and contains at least 3 distinct proteins: Raptor, mLST8 and PRAS40 (Dowling et al., 2010; Laplante and Sabatini, 2012; Lee et al., 2007; Shimobayashi and Hall, 2014; Soulard et al., 2009). mTORC1 activity is regulated by growth factors, amino acids, energy state, stress and oxygen levels of the cell. mTORC1 activity is negatively regulated by Tuberous Sclerosis Complex (TSC1/2), which functions as a GTPase-activating protein for the Ras homolog enriched in brain GTPase, Rheb (Figure 3). TSC1/2 negatively regulates mTORC1 by keeping Rheb in its inactive GDP-bound state (Inoki et al., 2003). Activation of the Insulin Receptor/IRS1/2 by growth factors leads to phosphorylation and activation of AKT (Protein Kinase B). Upon phosphorylation and inactivation by AKT, TSC1/2 releases its inhibition on Rheb, allowing Rheb's direct activation of mTORC1 (Dan et al., 2002; Inoki et al., 2002; Inoki et al., 2003; Manning et al., 2002). AKT can also directly activate mTORC1, by phosphorylating, inhibiting and allowing the release of PRAS40 from mTORC1. TSC2 exists in a complex with TSC1, but the major function of TSC1 in mTORC1 signaling is to stabilize TSC2 and prevent its ubiquitin-mediated degradation. In contrast, phosphorylation and activation of TSC2 by AMPK and GSK3β inhibits mTOR signaling (Inoki et al., 2006; Inoki et al., 2003). Amino acid-activation of mTORC1 is activated by the subcellular localization of mTOR and Raptor by Rag GTPases, Ragulator complex (LAMTOR1-3) and vacuolar H^+-ATPase (v-ATPase) to the lysosomes and late endosomes (Bar-Peled et al., 2012; Sancak et al., 2010; Sancak and Sabatini, 2009). The Ragulator complex is a pentameric protein complex, consisting of five subunits, p18 (LAMTOR1), p14, MP1, HBXIP, and C7orf59 (Sancak et al., 2010; Sancak et al., 2008). Rapamycin directly inhibits mTORC1 by forming a complex with FK506-binding protein

(FKBP12) (Brown et al., 1994).

mTORC1 controls growth (cell size) and proliferation (cell number) by modulating mRNA translation through phosphorylation of 4E-BP1, 2, and 3 and the ribosomal protein S6 kinases (S6K1 and 2) (Figure 3) (Dowling et al., 2010; Laplante and Sabatini, 2012; Lee et al., 2007; Shimobayashi and Hall, 2014; Soulard et al., 2009). Phosphorylation of the 4E-BPs triggers their release from eiF4E and initiates cap-dependent translation. Thus, activated mTORC1 downstream substrates promote mRNA translation initiation, and progression and control of the rate of protein synthesis.

mTORC1 inhibits autophagy by phosphorylation and activation of the kinase ULK1/2 and subcellular localization of transcription factor EB, TFEB (Figure 3). mTORC1/Raptor directly interact with ULK complexes by phosphorylating and inhibiting their kinase activity to suppress autophagy (Hosokawa et al., 2009; Jung et al., 2009). In turn, the inhibition of mTORC1 activity, such as starvation, suppresses the phosphorylation and therefore inactivates ULK complexes to increase autophagy (Hosokawa et al., 2009). mTORC1-dependent ULK1 phosphorylation induces the dissociation of AMPK from the ULK1 complex, thereby attenuating AMPK-dependent ULK1 phosphorylation and activation (Kim et al., 2011). Nutrient depletion triggers the shuttling of TFEB from cytosol to nucleus, where TFEB initiates transcription of autophagy-mediated genes. Interestingly, it has been also reported that ULK-silenced cells have increased S6K1 activity and that ULK negatively regulates mTORC1 activity to promote increase in cell size (Jung et al., 2009).

mTOR Complex 2 (mTORC2) is insensitive to rapamycin and contains Rictor, mLst/GbL, and mTOR (Dowling et al., 2010; Laplante and Sabatini, 2012; Lee et al., 2007; Shimobayashi and Hall, 2014; Soulard et al., 2009). mTOR Complex 2 phosphorylates AKT on Ser473, suggesting that this pathway indirectly could be linked to proliferation (Sarbassov et al., 2005).

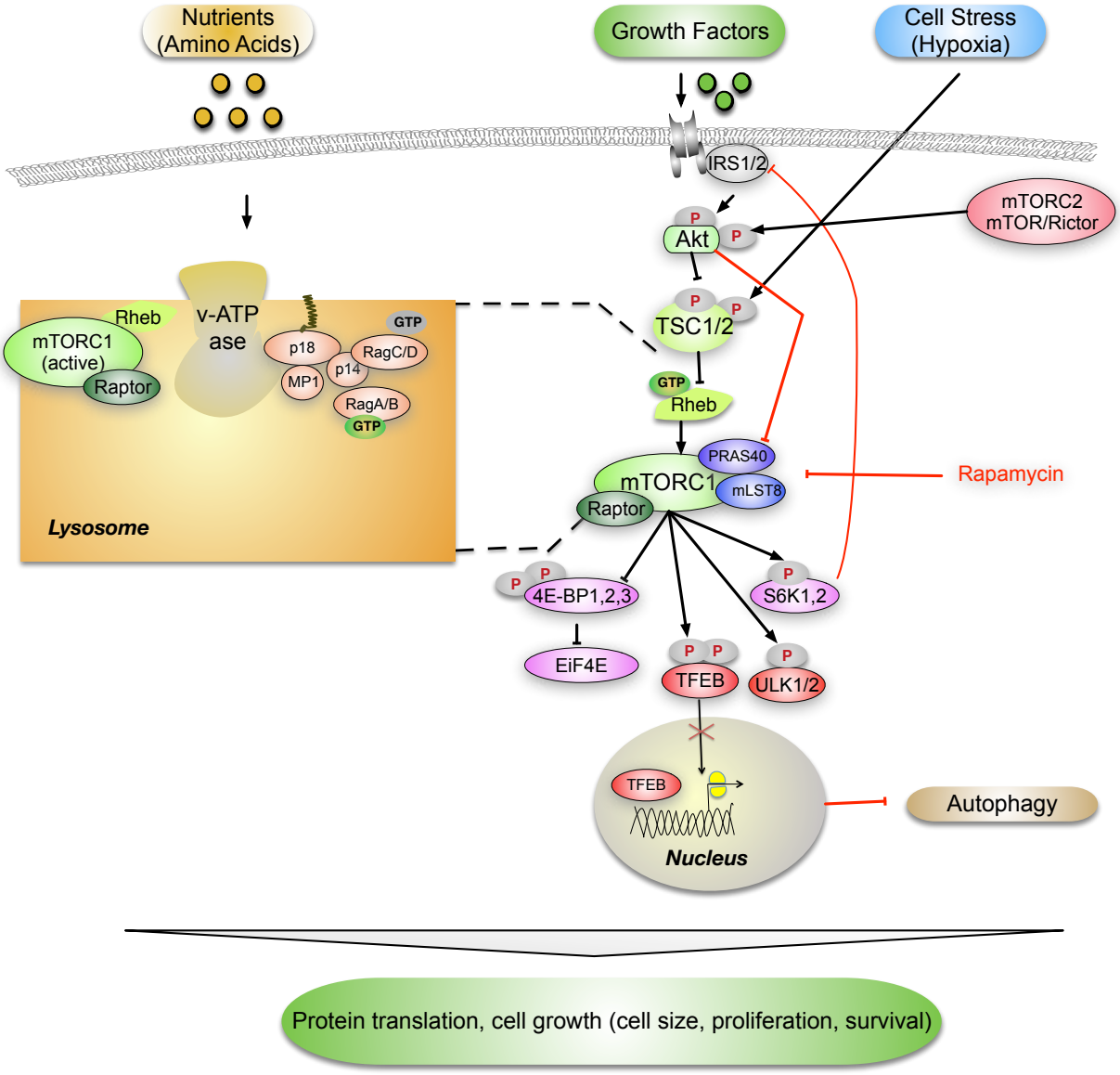

Figure 3. Diagram of the mTOR signaling pathway The mammalian target of rapamycin (mTOR) is essential for cell growth and proliferation. mTOR activity is regulated by growth factors and nutrients, as well as the redox state of the cells. The mammalian TOR is associated with two distinct complexes (mTORC1 and 2). Activation of the Insulin Receptor/IRS1/2 by growth factors, leads to phosphorylation and activation of AKT (Protein Kinase B). mTORC1 activity is negatively regulated by Tuberous Sclerosis Complex (TSC1/2). TSC2 phosphorylation and inactivation by AKT releases the inhibition of small G-protein Rheb, leading to activation of mTORC1. Amino acid-activation of mTORC1 is activated by the subcellular localization of mTOR and Raptor by Rag GTPases, Ragulator complex (LAMTOR1-3) and vacuolar H^+-ATPase (v-ATPase) to the lysosomes and late endosomes. mTORC1 is rapamycin sensitive and controls cell growth (cell size) and proliferation (cell number) by modulating mRNA translation through phosphorylation and inhibition of 4E-BPs and the phosphorylation

and activation of ribosomal protein S6 kinases. mTORC1 inhibits autophagy by phosphorylation and activation of ULK1/2 and TFEB. mTORC2 is insensitive to rapamycin and can phosphorylates and activate AKT.

The role of mTOR Complex 1 in metabolic cells

The excess nutrient intake associated with obesity increases the activity of mTORC1/S6K signaling. The chronic activation of the pathway and specifically, the S6K arm of the mTORC1 activation, leads to a negative feedback inhibition of IRS/IRS2 and AKT signaling and insulin resistance (Figure 3) (Khamzina et al., 2005; Shigeyama et al., 2008; Um et al., 2004). Therefore, the regulation of mTORC1 activity plays a major role in insulin-sensitive tissues, however mTORC1 does have tissue-specific roles. Raptor, regulatory associated protein of mTOR, plays an essential role in the nutrient-dependent regulation of mTORC1 and the regulation of cell size by mTORC1 activity (Kim et al., 2002). The conditional deletion of *raptor* in adipocytes improves glucose tolerance, insulin sensitivity and resistance to high fat feeding (Polak et al., 2008). In turn, deletion of *raptor* in muscle results in mice that are glucose intolerant and have decreased mitochondrial biogenesis and associated proteins (Bentzinger et al., 2008). In the liver, loss of mTORC1 signaling by conditional deletion of *raptor* has major implications to the liver's adaptation to fasting by a defect in ketogenesis (Sengupta et al., 2010). Overall, the role of mTORC1 signaling is tissue-specific and additional studies are needed to understand the contribution of this pathway in pancreatic endocrine cells, which play a major role in the maintenance of normoglycemia.

Insulin receptor signaling regulates α-cell mass and glucagon secretion

Insulin has been shown to be one of the most potent regulators of glucagon synthesis and secretion (Franklin et al., 2005; Ishihara et al., 2003; Kawamori et al., 2009; Philippe, 1989; Schinner et al., 2005; Xu et al., 2006). Mice with loss of the insulin receptor in α-cells have increased fed glucagon levels demonstrating that insulin receptor signaling regulates insulin-mediated suppression of glucagon secretion at the fed state (Kawamori et al., 2009). These findings can be translated to explain the

increased glucagon levels associated with insulin resistance and T2D. Moreover, mice with pancreatic deletion of the Insulin Receptor Substrate 2 (IRS2) have a decreased α-cell mass and glucagon levels, implicating the Insulin-Receptor signaling pathway in promoting α-cell mass and glucagon content (Cantley et al., 2007).

The role of mTOR Complex 1 in the regulation of α-cell mass and glucagon secretion

mTOR Complex 1/Raptor (mTORC1) emerge as prime candidates in the regulation of α-cell mass and glucagon secretion, as mTORC1/Raptor integrates signals from growth factors and nutrients to regulate cell growth, survival and function of insulin-sensitive metabolic tissues (Bentzinger et al., 2008; Cota et al., 2006; Polak et al., 2008; Sengupta et al., 2010). Alpha cell proliferation is reduced by treatment with the mTOR Complex 1/Raptor (mTORC1) inhibitor, rapamycin (Liu et al., 2011; Solloway et al., 2015), suggesting that downstream of the insulin receptor, Tuberous Sclerosis Complex (TSC1/2) and mTORC1 could be important candidates to mediate the effects of insulin on α-cell mass and glucagon secretion. Most recently, studies using glucagon receptor deficient mice report increased α-cell proliferation (Gromada et al., 2007; Longuet et al., 2013) and this was associated with a significant increase of circulating amino acids (known activators of mTORC1) suggesting that certain amino acids could induce α-cell mass in this mouse model (Solloway et al., 2015; Yang et al., 2011). These findings support the concept that α-cell mass and glucagon secretion are sensitive to extracellular signals including nutrients (amino acids, glucose) and growth factors (insulin) and that the mTORC1 pathway may be involved in this process. However, how nutrients or downstream targets of the insulin receptor signaling regulate α-cell mass and glucagon secretion *in vivo* is currently unknown.

CHAPTER 1

Experimental Methods

Animals

Mice were housed in pathogen-free environment and maintained on 12-hour light/dark cycle at the University of Michigan Brehm Center Animal Facility. All protocols are approved by the University of Michigan Animal Care and Use Committee and are in accordance to NIH guidelines. We utilized the *Cre/lox P* system to generate mice with loss of *raptor* expression in α-cells. The Glucagon-Cre mice (generous gift from Dr. G. Gittes at the University of Pittsburg)(Shiota et al., 2013), expressing *Cre* recombinase driven by the glucagon promoter were crossed with $Raptor^{flox/flox}$ (generous gift by Dr. M. Hall and Dr. M. Rüegg at the University of Basel, Switzerland) (Polak et al., 2008).

We generated three experimental groups for all described experiments in Chapter 1: controls ($Raptor^{flox/flox}$, $Raptor^{flox/+}$ and Glucagon-Cre), $\alpha Raptor^{KO}$ (Glucagon-Cre; $Raptor^{flox/flox}$) and $\alpha Raptor^{HET}$ (Glucagon-Cre; $Raptor^{flox/+}$). All animals were *C57BL/6* background. The animals were born in expected Mendelian ratios and expected lifespans.

We generated three experimental groups for all described experiments in Chapter 2: controls ($TSC2^{flox/flox}$, $TSC2^{flox/+}$, Glucagon-Cre), $\alpha TSC2^{KO}$ (Glucagon-Cre; $TSC2^{flox/flox}$) and $\alpha TSC2^{HET}$ (Glucagon-Cre; $TSC2^{flox/+}$). These mice had mixed background between *C57BL/6* and *129X1*. All animals were born in expected Mendelian ratios, but had a reduced lifespan due to decreased body weight and observed seizure episodes of unknown origin (but not due to hypoglycemia).

Reporter transgenic animals CAG-tdTomato, Ins1-EGFP and CAG-YFP were purchased from Jackson Labs and generously provided to us by Drs. Martin Myers and Peter Arvan (University of Michigan). Reporter transgenic mice, GFP-LC3#53 were obtained from RIKEN with the permission of the depositor, Dr. Noboru Mizushima (Mizushima et al., 2004). All metabolic (2 or 8 months) and *ex vivo* islet secretion (2 months) studies were performed with aged-matched male mice. Islet morphometric analysis utilized age-matched cohorts with male and female mice.

Metabolic Studies

Body weight and random blood glucose was monitored monthly for total of 4 months. Fed (9 AM) and fasting (12 hours; 9 PM) glucose, insulin and glucagon levels were evaluated in 2 and 8-month old males. Blood was obtained from the tail vein and blood glucose was measured with Accu-Chek blood glucose meter. Glucagon and insulin levels were measured with ELISAs (Mercodia and Alpco, respectively). IPGTT (2 g/kg), ITT (1 U/kg) and 2 deoxy-D-glucose (2g/kg) were performed by intraperitoneal (IP) injections of respective agents in 4-6 hour fasted male mice. Hepatic glucose production was measured by IP injection of pyruvate (2g/kg) in 16-hour fasted male mice. Active GLP-1 levels were measured by oral administration of glucose (2g/kg) and plasma levels of active GLP-1 were measured with STELLUX Chemiluminescent Assay (Alpco). Prior to measuring active GLP-1 levels, DPP-IV Inhibitor (Millipore) was added to plasma (20 µL per 1 mL of plasma) before storing the samples in -80°C. Food intake and activity levels were recorded for the duration of 3 days using CLAMS metabolic chamber (Columbus Instruments).

Preparation and Treatment with Agents

Rapamycin

Rapamycin (LC Laboratories) was dissolved in 100% ethanol and stored at -20°C. The stock solution was further diluted in an aqueous solution of 5.2% Tween 80 and 5.2% PEG 400 with a final concentration of ethanol of 2% (Mori et al., 2009a; Mori et al., 2009b). Wild-type mice were injected with Rapamycin (2 mg/kg) every other day for 9

days. ITT was performed on day 8 between injections. Necropsy was performed on day 9 after last injection.

Chloroquine

αRaptor^{KO} mice were treated with chloroquine diphosphate (Sigma, St. Louis, MO) in 0.9% saline administered at 7 mg/kg body weight. The mice were treated starting at 2 weeks of age and were treated twice weekly for the duration of 2 weeks.

Streptozotocin

Mice were treated with Streptozotocin (150 mg/kg; Sigma) by a single intraperitoneal injection at 2 months of age (Zhang et al., 2012). The mice were fasted for 6 hours and Streptozotocin was injected in the late afternoon on day 0. Morning (fed) glucose levels were monitored for a week post-STZ treatment. Fed insulin and glucagon levels were measured at 0 and 8 days post-STZ treatment. Pancreata was collected for immunohistochemical analysis of α and β-cell mass on day 8.

Total Pancreatic Glucagon Extraction

Pancreata was dissected, cleaned in cold PBS and blotted on filter paper before weighting. The pancreata was placed in 3 mL ice-cold acid ethanol in polypropylene falcon tubes and homogenized using a tissue polytron for 2 minutes. Acid ethanol was prepared by adding 1 mL of 12N hydrochloric acid to 110 mL of 95% ethanol. After homogenizing the tubes were closed and placed in rotating rack at 4°C for 72 hours. The tubes were centrifuged at 2500 rpm for 30 minutes and the supernatant was placed in a new tube. Glucagon was measured using the supernatant at 1:10 dilution using Glucagon Elisa (R&D Duoset). The glucagon values were divided by the pancreas mass and final supernatant volume to calculate the final pancreatic glucagon content.

Liver Glycogen Content

Liver was dissected and immediately frozen in liquid nitrogen. Liver glycogen content was measured with Glycogen Content Kit (Sigma-Aldrich) using ~5 mg of liver sample and following the manufacturer's instructions.

Free Fatty Acids (NEFA) Measurement

Plasma free fatty acids (NEFA) were measured using NEFA-HR(2) Microtiter Procedure Kit (Wako Diagnostics) and following the manufacturer's instructions.

Islet Studies

Islet Isolation Procedure

Islet isolation was accomplished by collagenase digestion as described previously (Bernal-Mizrachi et al., 2010; Bernal-Mizrachi et al., 2004). Briefly, 1 mg/mL of collagenase (Roche) was dissolved in Hank's Buffer. The junction of the common bile duct to the duodenum was closed using a clamp. Approximately 5 mL of collagenase solution was injected slowly into the common bile duct of each mouse. Glucagon secretion *ex vivo* was assessed using isolated islets by static incubation. After injecting the collagenase solution, the pancreas was dissected and placed in a tube and incubated in water bath at 37°C for 12-16 minutes for further digestion. The digested pancreas was washed multiple times with Hanks's Buffer supplemented with 10% FBS and passed through a strainer to eliminate undigested parts. Finally, the digested pancreas was passed through 70μm filter to collect islets. The islets collected in the filter were washed onto a 100 mm cell culture plate (untreated) and incubated overnight in a cell culture incubator at 37°C.

Islet Secretion Studies

After overnight culture in RPMI containing 5 mM glucose, islets were pre-cultured in Krebs-Ringer (KRBB) medium containing 6 mM glucose and 0.2% BSA for 1 hour. Groups of 15 islets/mouse were placed in 8 μm cell culture inserts (Millicell), pre-incubated in HG KRBB (6 mM glucose) for 1-2 hours and incubated subsequently for 1 hour in each of the following conditions: LG KRBB (1 mM glucose; with a brief wash with LG between HG KRBB and LG KRBB) and LG KRBB + Arginine (20 mM) or KCl (30 mM). Experiments measuring glucagon response to increasing dose concentrations of diazoxide and tolbutamide had incubation time of 30 minutes per condition. Experiment assessing short-term rapamycin treatment on glucagon release was performed using wild-type islets and following the same experimental design with the

addition of +/- rapamycin (30 nM) at increasing concentrations for glucose (1, 6, 12, 24 mM) for 30 minutes per condition. Assessment of glucagon content of the islets was preformed by extraction in 0.5 mL acid-alcohol per 15 islets/insert after each assay. All assays represent results from 2-3 independent experiments. Secreted glucagon levels and islet glucagon content were measured with an ELISA (Glucagon Duoset Elisa from R&D Systems). All data is represented as secreted glucagon in the culture medium normalized to islet glucagon content for each insert of islets and presented as fold change compared to control.

Fluorescent-Activated Cell Sorting (FACS)

Control (Glucagon-Cre) and αRaptor^{HET} mice were crossed to reporter mice Ins1-EGFP and CAG-tdTomato. The islets from 2 month-old Glucagon-Cre$^{Ins1GFP;\ tdTomato}$ and αRaptor$^{HET;Ins1\text{-}EGFP;tdTomato}$ were isolated and incubated overnight in RPMI containing 5 mM glucose. The islets were dispersed into a single-cell suspension and filtered. Sorting was performed on FACS Aria III (BD Biosciences) at the University of Michigan and Moflo Astrios EQ (Beckman Coulter) at the University of Miami. Dead cells were excluded with 4′6-diamidino-2-phenylindole (Sigma) or Ghost Dye Red 780 (Tonbo). Cells expressing CAG-tdTomato (glucagon and insulin) and cells expressing Ins1-EGFP (all insulin) were sorted in separate collection tubes, representing Tomato Gate and GFP Gate, respectively. Hormone content in each gate was analyzed in 4 Control animals by ELISAs for glucagon (Duoset, R&D Systems) and insulin (Alpco) and normalized to the number of cells sorted. Glucagon data is presented as fold change from glucagon content in Tomato Gate. Insulin data is presented as fold change from insulin content in GFP Gate.

Flow Cytometry

Islets were isolated and incubated overnight in RPMI containing 5 mM glucose. The islets were dispersed into a single-cell suspension with trypsin-EDTA and fixed with BD Pharmingen Transcription Factor Phospho Buffer Set (BD Biosciences). The fixed cells were incubated with conjugated antibodies overnight, at 4°C and gentle rotation. Dead cells were excluded by Ghost Dye Red 780 (Tonbo). Glucagon, foxA2, pS6 (Ser240)

expression was analyzed by mean fluorescent intensity (MFI) per glucagon-positive cells using BD LSR II (BD Biosciences). The size of live glucagon positive cells was analyzed by forward scatter area (FSC-A) and glucagon mean fluorescent intensity (MFI).

Immunofluorescence and Cell Morphometry

Pancreata were fixed in 3.7% formaldehyde, embedded in paraffin and sectioned (5 μm). Fluorescent images were acquired using a microscope (Leica DM5500B) and a motorized stage using a camera (Leica DFC360FX) (Leica Microsystems). Cell mass was determined in 5 stained sections (5 μm) separated by 200 μm as described (Bernal-Mizrachi et al., 2004; Bernal-Mizrachi et al., 2001). The area of insulin, glucagon, somatostatin and pancreatic polypeptide and the area of each section were quantified with Image Pro Software (version 7; Media Cybernetics). The ratio of the five hormone stained area to the total pancreatic section area for each mouse were averaged and multiplied by the pancreas weight.

Dispersed cell stainings were performed by gently dispersing isolated islets with trypsin-EDTA (0.25% trypsin, 1 mM EDTA). The cells were cytofuged using StatSpin Cytofuge 2 (Beckman Coulter) on slides pre-coated with poly-L-lysine. The cells were immediately fixed with 3.7% formaldehyde for 20 minutes and incubated with TBS-Triton (0.1%) for 10 minutes at room temperature. For FoxA2 stains, the cells were additionally permeabilized with cold methanol at 4°C for 10 minutes (after fixation with formaldehyde). Analysis for nuclear FoxA2 and DAPI signal intensity was done on 16-bit images acquired at using a microscope (Leica DM5500B) and a motorized stage using a camera (Leica DFC360FX) (Leica Microsystems). FoxA2 and DAPI levels were determined my measuring pixel intensity using Adobe Photoshop (Adobe Systems).

Islet cell size was calculated by immunostaining dispersed islets from 1-month old mice for glucagon and DAPI and measuring the area of glucagon positive cells using NIH Image J Software (v1/49d available free at http://rsb.info.nih.gov/ij/index.html).

Assessment of *Cre*-mediated recombination was measured by counting the number of Glucagon+/Reporter+ cells in dispersed islets from Glucagon-Cre^{YFP} and Glucagon-Cre^{tdTomato} mice (2 months-old). Assessment of autophagy was assessed in Control and αRaptor^{KO} mice bred to GFP-LC3 mice (Mizushima et al., 2004). Islets from 1 month-old Control$^{GFP-LC3}$ and αRaptor$^{KO;GFP-LC3}$ mice were isolated, dispersed and cytofuged on slides and stained for glucagon, GFP and DAPI.

Assessment of cell death was measured by Immunofluorescent-based apoptosis TUNEL assay (Millipore) in 3-5 stained sections (5 μm) separated by 200 μm and co-stained for glucagon and DAPI. Assessment of cell proliferation was measured by staining and counting ki67^{+}/glucagon^{+} cells (Sigma) in 3-5 stained sections (5 μm) separated by 200 μm and co-stained for glucagon and DAPI.

All antibodies used are summarized in Table 1.

K_{ATP} Channel Activity

Islets from Glucagon-Cre^{tdTomato} and αRaptor$^{HET;tdTomato}$ mice, expressing a fluorescent reporter in α-cells mice, were dispersed to single cells and plated overnight on 35-mm dishes as described previously (Dai et al., 2011). Cells were patch-clamped in the whole-cell voltage-clamp configuration in a heated bath at 32-35^{o}C using a HEKA EPC10 amplifier and PatchMaster Software (Heka Electronik, Germany) and patch pipettes with resistances of 5 ~ 6 MOhm after fire polishing. Whole-cell currents of K_{ATP} channel are recorded in response to voltage steps going to −60 and −80 mV from a holding potential of −70 mV. For the K_{ATP} current measurement, the bath solution contained: 138 mM NaCl, 5.6 mM KCl, 1.2 mM $MgCl_2$, 2.6 mM $CaCl_2$, 5 mM HEPES, 1 mM glucose (pH 7.4). The pipette solution for these experiments contained: 125 mM KCl, 30 mM KOH, 1 mM $MgCl_2$, 10 mM EGTA, 5 mM HEPES, 0.3 mM Mg-ATP and 0.3 mM K-ADP (pH 7.15).

Following the experiments, α-cells were positively identified by immunostaining for glucagon (guinea pig anti-glucagon, 1:5,000; Linco, St Charles, MO, USA), and

appropriate secondary antibody (Alexa Fluor 594 goat anti-guinea pig 1:200; Invitrogen, Eugene, OR, USA). Data were analyzed using FitMaster (Heka Electronik) and Prism (v6).

Single Cell Analysis by Fluidigm

Islets from Control (Raptor f/f $^{Ins1\text{-}GFP;tdTomato}$ and Ins1-GFP;tdTomato (n=6) and αRaptor$^{KO;Ins1\text{-}EGFP;tdTomato}$ (n=3) were isolated, dispersed and sorted to enrich an α-cell population and sorted based on viability. The cells were sorted into complete islet medium (RPMI; 10%FBS; 5mM Glucose). The viability (87-97%) and concentration (250-300 cells/μL) of cells were measured by Countess Automated Cell Counter and mixed with C1 Cell Suspension Reagent (Fluidigm) in 3:2 ratio. The cells were captured into a small (5-10μm) or middle (10-17 μm)-sized IFC before undergoing cell lysis, reverse transcription and cDNA amplification in the C1 Single-Cell Auto Prep instrument. Capture sites containing a single cell were identified by careful examination of the IFC using an Olympus CK2 inverted microscope. Quantitative RT-PCR of 96 Delta Gene Assays was performed by BiomarkHD (Fluidigm) using pre-amplified cDNA from single cells, positive (bulk cell) and negative (no template) controls from each IFC capture. Glucagon cells were identified as single cells with detectable levels of glucagon gene expression in the Biomark HD data (Control n=10, αRaptor^{KO} n=19 cells). Delta Gene Assays were validated for single cell gene expression analysis on Biomark HD using mouse pancreatic total islet mRNA serially diluted over 12 two-fold dilutions (512pg to 0.25pg) and 7 replicates.

Quantitative Real-Time PCR

For mRNA expression, total RNA was extracted from islets, αTC-1 cells and liver samples using the RNeasy isolation kit (Qiagen). Gene expression was performed by quantitative real time RT-PCR using Power SYBR Green PCR Mix (Applied Biosystems) using StepOnePlus detection system (Applied Biosystems) with a standard protocol including a melting curve. Relative abundance for each transcript was calculated by a standard curve of cycle thresholds and normalized to 18S (αTC-1 cells

and liver) and β-actin (islets). Primers were purchased from IDT Technologies, with the exception of Arx1, MafB and Nkx2.2 purchased from Operon.

All primer sequences are available in Table 2.

Single Cell RT-PCR

The following methods were adapted and modified from Liss *et al.* and Shiota *et al*. (Liss et al., 1999; Shiota et al., 2005). Red-fluorescent, dispersed islet cells from 1 month-old Control^{tdTomato} and αRaptor$^{KO;tdTomato}$ were individually picked under an inverted phase-contrast microscope (Leica DMI 3000B). Each cell was collected with a pipette adjusted to 1.5 µL in individual tube with 3.5 µL water and 5 µL of a mix containing: 1 µL 10X RT Buffer (Applied Biosystems), 0.5 µL RNAse inhibitor (10 Units; Applied Biosystems) and 0.5 µL dithiothreitol (10 mM; DTT). The tubes were immediately frozen on dry ice. The first strand of cDNA was performed by using High-Capacity Reverse Transcription cDNA Kit and following the manufacturer's directions (Applied Biosystems). Each cell was treated as separate reaction yielding a final volume of 20 µL. Reverse Transcription (RT) reaction was carried for 60 minutes at 42°C, followed by incubation at 75°C for 15 minutes. All cells underwent PCR amplification for glucagon and 18S. Only glucagon-positive cells were further analyzed.

Single Cell-Nested PCR for *SUR1* and *raptor*

SUR1: The first round of PCR contained 8 µL of RT reaction, outside primers for SUR1 (0.5 µM), $MgCl_2$ (2 mM), dNTPs (0.4 mM) and 2 Units Platinium Taq (Invitrogen), in a total volume of 20 µL. The first PCR was performed under the following conditions: 3 minutes at 94°C, 35 cycles (94°C for 30 seconds, 58°C for 60 seconds, 72°C for 3 minutes), final elongation at 72°C for 7 minutes using MasterCycler proS (Eppendorf). The second round of PCR for SUR1 was performed using 1 µL of first-PCR product and 19 µL of a mix containing Power SYBR Green PCR Mix (Applied Biosystems), inside primers and water, and was performed using StepOnePlus detection system (Applied Biosystems). The final product for SUR1 was visualized in an ethidium bromide-stained agorose gel (2%) by electrophoresis. The results were analyzed by the presence or

absence of a positive band. Positive (whole islets) and negative (water) controls were used in every experiment. Primers were purchased from IDT Technologies.

Raptor: The first round of PCR was contained 4 µL of RT reaction, outside primers for *raptor* (0.6 µM), $MgCl_2$ (2 mM), dNTPs (0.4 mM) and 2 Units Platinium Taq (Invitrogen), in a total volume of 20 µL. The first PCR was performed under the following conditions: 4 minutes at 94°C, 35 cycles (94°C for 30 seconds, 55°C for 30 seconds, 72°C for 30 seconds), final elongation at 7°C for 4 minutes using MasterCycler proS (Eppendorf). The second PCR product for *raptor* was performed using 2 µL of the first PCR product and inside primers under the same conditions.

All primer sequences are available in Table 2.

Cell Culture Studies

The glucagon-secreting cell line, αTC-1 cells clone #6, was purchased from ATCC and maintained according to company's instructions. For rapamycin experiments, the cells were cultured in 12-well plates and incubated in complete media +/- rapamycin (30nM) for 48 hours.

Western Blotting

αTC-1 cells and primary cells were collected and lysed in lysis buffer (125 mM Tris, pH7; 2% SDS, 1 mM DTT) containing a phosphatase (Roche Diagnostics) and protease (Sigma) inhibitor cocktails. Cell lysates were boiled for 10 minutes, loaded and electrophoresed on 12% SDS-PAGE and transferred to polyvinylidene fluoride membranes. All antibodies used are listed in Supplemental Table 1. Images were acquired using Western Bright Sirius kit (BioExpress). Band densitometry was determined by measuring pixel intensity using NIH Image J software (v1/49d available free at http://rsb.info.nih.gov/ij/index.html) and normalized to actin in the same membrane.

Electron Microscopy

Islets were isolated and fixed with 2% glutaraldehyde overnight at 4°C, dehydrated and embedded in Epon by the Microscopy & Image Analysis Laboratory Core (MiCORES). Ultrathin sections were stained with uranyl acetate and lead citrate. Images were recorded digitally using electron microscope (JEM-1400 Plus).

Statistical Analysis

Data are presented as means ± S.E.M. The statistical significance of differences between the various conditions/animal groups was determined by nonparametric *U* test (Mann-Whitney) using Prism version 6.0d (GraphPad Software). Results are shown as significant when *P* value was ≤0.05. Analysis of Fluidigm single-cell data identified 55 gene assays (Supplemental Table 3) that qualified for statistical analysis by t-test (≥3 data points/group). Principle Component Analysis (PCA) was performed using gene expression from 55 genes to evaluate whether the groups were separated distinctively. Heat map represents mean Ct of differentially expressed genes (p>0.05) from t-test analysis. We applied a second method of statistical analysis to the dataset using R based MAST (Model-based Analysis of Single-cell Transcriptomics) package (Finak et al., 2015). . Additional gene (*GCG)* was identified as significantly different between the groups using MAST analysis.

Table 1. List of Antibodies

Antibody	Specie	Source	Application
Glucagon	Mouse	Abcam	IFC
Glucagon	Rabbit	Chemicon	IFC
Glucagon-BV421	Human/Mouse	BD Biosciences	FC
Insulin	Guinea Pig	Dako	IFC
Insulin-APC	Human/Mouse/Bovine	R&D	FC
GFP	Chicken	Abcam	IFC
pS6 (S235)	Rabbit	Cell Signaling	IFC
pS6 (S240)	Rabbit	Cell Signaling	IFC
pS6 (S240)-PE	Mouse	BD Biosciences	FC
FoxA2	Rabbit	Cell Signaling	IFC
FoxA2	Mouse	Abcam	WB
FoxA2-Dylight488 (conjugated in house)	Mouse	Abcam	FC
KIR6.2	Rabbit	Alamo Labs	WB
SUR1	Rabbit	Show-Ling Shyng	WB
Somatostatin	Rabbit	Santa Cruz	IFC
Pancreatic Polypeptide	Guinea Pig	Millipore	IFC
Actin	Mouse	Sigma	WB
Ghost Dye Red 780		Tonbo	FC
Ki67	rabbit	Sigma	IFC

WB = Western Blot

IFC = Immunofluorescent Chemistry

FC=Flow Cytometry

Table 2. Primer Sequences

αTC-1 Cells and Primary Islet Cells

Gene	Forward	Reverse
FoxA2	CAGCTACTACGCGGAGCC	GCTCATTCCAGCGCCCAC
SUR1	CTGGTGGCCATCGACACAA	TGTACAGGAGCCAGCAGAAT
KIR6.2	GCTGCATCTTCATGAAAACG	TTGGAGTCGATGACGTGGTA
MafB	GAACGAGAAGACGCAGCTCT	CGAGTTTCTCGCACTTGACCT
Nkx2.2	TCGCTCTCCCCTTTGAACTTT	GTTAACGTTGGGATGGTTTGG
Pou3f4	TTCCTCAAGTGTCCCAAGCC	TAA ACCTCGTGTGGCTGCTG
FoxP1	CGAATGTTTGCTTACTTCCGA	GCCAGGCTGTGA AAGCATATGTGA
FoxP2	GCCAGGCTGTGAAAGCATATGTGA	CATTTGCACTCGACATTGGGCAGT
FoxP4	GTCAGCCTGCAGCCCAAGCCAAGCCTC	GGAGCTGTCTCTCCGAGATGTGAGCAC
18S	GCAATTATTCCCCATGAACG	GGGACTTAATCAACGCAAGC

Single Cell Analysis

Gene	Forward	Reverse
SUR1 (inside)	CTGGTG GCCATCGACACAA	TGTACAGGAGCCAGCAGAAT
SUR1 (outside)	GTCTACTTCCAACCTGTCAA T	ACCCTCGAGCAGAAGATGTT
Raptor (inside; exon 6)	CCTCTGTCCATATACGACCT	CTCTGCAGTGCAAACTGT
Raptor (outside; exons 5&7)	CCTACTGTGGATGAAGTCAA G	CACTCCCATCAAGATTGCTC

Liver Analysis

Gene	Forward	Reverse
GCGR	ACGGTACAGCCAGAAGAT	CTACCAGCAACCAGCAATAG
PEPCK	ATCATCTTTGGTGGCCGTAG	ATCTTGCCCTTGTGTTCTG
G6Pase	CCGGTGTTTGAACGTCATCT	CAATGCCTGACAAGACTCCA
Gck	CTGTTAGCAGGATGGCAGCT	TTT CCTGGAGAGATGCTGTGG
FAS	AGAAGCCATGTGGGGAAGAT	AGCAGGGACAGGACAAGACAA

Table 3. Fluidigm Gene Targets Included in Analysis

CCNB1	NOTCH1	ABCC8	CCND1	FOXO1	LAMP1	PAX6
EIF4E	SNAP25	HSP90AB1	CCND2	FOXP1	LAMTOR2	PCSK2
CHRM3	ULK2	CACNA1S	CDKN1A	FOXP4	LAMTOR3	PTF1A
NEUROG3	MAFB	XBP1	CDKN1B	GCG	MAFA	RFX6
LAMTOR1	FOXA2	ARX	CPE	GIPR	NKX6-1	TM4SF4
NKX2-2	POU3F4	CACNA1A	CRYBA2	GLP1R	NOTCH2	UCP2
ULK1	KCNJ11	CASP3	DDIT3	HSPA5	OGT	VAMP2
GATA4	RBPJ	CCNA2	ERN1	IRS2	PAX4	

CHAPTER 2

Nutrient signaling maintains alpha cell mass and promotes K_{ATP} channel-dependent regulation of glucagon secretion

Introduction

Type 1 (T1D) and Type 2 (T2D) Diabetes are characterized by uncontrolled hyperglycemia associated with the progressive decrease in insulin. Glucagon, insulin's counterregulatory hormone, plays a major role in maintaining glucose homeostasis by promoting glucose production *via* hepatic glycogenolysis and gluconeogenesis. Paradoxically, glucagon levels are elevated in insulin-resistant non-diabetic, T1D and T2D patients, leading to enhanced hepatic glucose output and thereby exacerbating hyperglycemia (Dinneen et al., 1995; Mezza et al., 2014; Sherwin et al., 1976). On the contrary, On the contrary and much less understood is the failure of α-cells to secrete glucagon in response to hypoglycemia. This presents a major limiting factor for optimal glucose control in insulin-dependent T1D diabetes or advanced T2D patients (Cryer, 2002; Gerich et al., 1973; Segel et al., 2002). Thus, a better understanding of the molecular mechanisms governing glucagon levels could have major implications in understanding abnormal responses to hypoglycemia in diabetes and provide novel avenues for diabetes management.

Mice with loss of the insulin receptor in α-cells have increased fed glucagon levels suggesting insulin signaling mediates the suppression of glucagon secretion in the fed state (Kawamori et al., 2009). In addition, mice with pancreatic deletion of the Insulin Receptor Substrate 2 (IRS2) exhibit decreased α-cell mass and lower glucagon protein

and RNA levels, implicating IRS signaling in the control of α-cell mass and glucagon expression (Cantley et al., 2007). Insulin inhibits glucagon gene transcription and secretion and promotes α-cell proliferation by activation of IRS2/PI3K/Akt signaling (Schinner et al., 2005; Xu et al., 2006). Alpha cell proliferation is reduced by treatment with the mTOR Complex 1 (mTORC1) inhibitor, rapamycin (Liu et al., 2011; Solloway et al., 2015), suggesting that downstream of the insulin receptor, mTORC1 mediates the effects of insulin on α-cell mass and glucagon secretion.

Arginine, alanine and glutamine potentiate glucagon secretion and this effect is suppressed by high glucose in an insulin-independent manner (Pipeleers et al., 1985). Most recently, studies using glucagon receptor deficient mice report increased α-cell proliferation associated with a significant increase of circulating amino acids, known activators of mTORC1, suggesting that certain amino acids could induce α-cell mass in this mouse model (Longuet et al., 2013; Solloway et al., 2015; Yang et al., 2011). These findings support the concept that α-cell mass and glucagon secretion are sensitive to extracellular signals including nutrients (amino acids, glucose) and growth factors (insulin) and that the mTORC1 pathway may be involved as a downstream regulator of one or both of these processes. However, how downstream targets of nutrient or insulin receptor signaling regulate α-cell mass and glucagon secretion *in vivo* is unknown.

To investigate the importance of endogenous mTORC1 function on α-cell mass and glucagon secretion, we generated mice with a conditional deletion of *raptor* in α-cells. Our data uncovered a novel role of mTORC1 in maintenance of postnatal α-cell mass and identify a previously unknown function of this pathway on glucagon secretion during fasting and hypoglycemia by modulation of K_{ATP} channel subunit expression (*SUR1* and *KIR6.2*) and channel activity. We also discovered that mTORC1 positively regulates *KIR6.2* and *SUR1* expression by regulation of *FoxA2* levels, a critical transcription factor dysregulated in diabetes. This work provides new insights into how nutrient-dependent glucagon secretion and α-cell mass are regulated and suggests that pharmacologic inhibition of this pathway using immunosuppressant medications, such as everolimus or rapamycin, could alter glucagon levels and glucose homeostasis.

Results

Lack of mTORC1 signaling after deletion of *raptor* in α-cells

Alpha cell-specific deletion of *raptor* was achieved by crossing Glucagon-Cre and Raptor$^{flox/flox}$ mice (αRaptor^{KO}) (Polak et al., 2008; Shiota et al., 2013). Single α-cells cells were isolated from control and αRaptor^{KO} mice. Single cell RT-PCR followed by nested PCR was performed for *raptor* in single α-cells from control and αRaptor^{KO} mice. Tissue-specific and single cell mRNA expression showed a lack of *raptor* expression exclusively in α-cells from αRaptor^{KO} mice (Figure 4A). Expression of raptor was preserved in the liver, hypothalamus, total pancreas and kidney in control and αRaptor^{KO} mice (Figure 4A). Loss of mTORC1 signaling was confirmed by lack of phospho-S6 (Serine240/44) immunofluorescent staining only in glucagon-positive cells from 1 month-old αRaptor^{KO} mice (Figure 4B). Phospho-S6 (Serine240) staining by flow cytometry of dispersed islets showed that phospho-S6 levels were nearly lost in glucagon-positive cells, but preserved in the insulin-positive cells from 1 month-old αRaptor^{KO} mice (Figure 4C,D). Recombination efficiency of Glucagon-Cre assessed by crossing these mice to reporter mice showed that Cre-mediated recombination was achieved in the majority of α-cells (84.2% +/- 6.4, n=4). These data demonstrate that we have successfully generated a mouse model with conditional deletion of *raptor* and loss of mTORC1 signaling in α-cells.

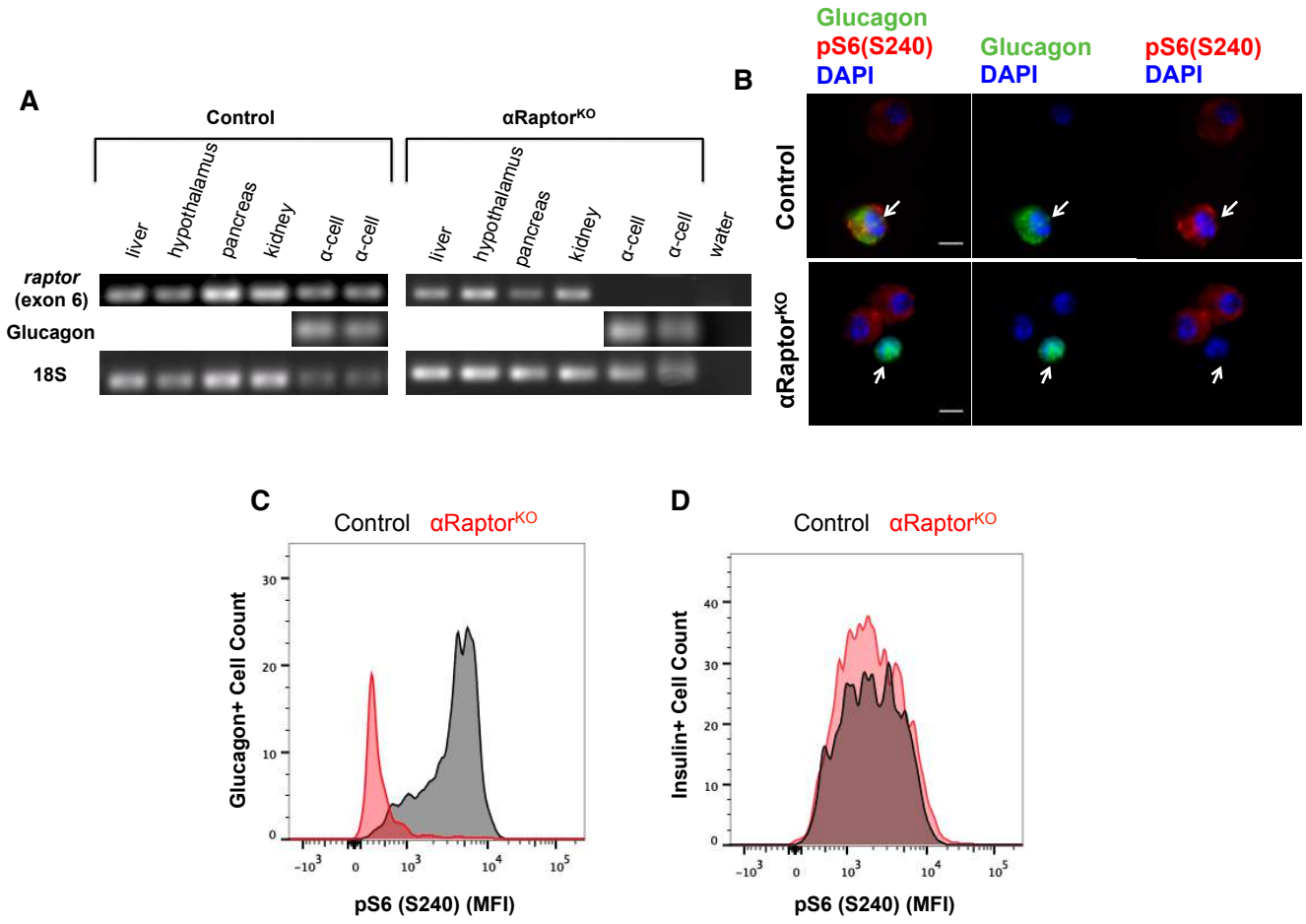

Figure 4. Loss of *raptor* and mTORC1 activity in α-cells of αRaptor^{KO} mice. A. Single α-cells cells were isolated from control and αRaptor^{KO} mice. Single cell RT-PCR followed by nested PCR was performed for *raptor* in single α-cells from control and αRaptor^{KO} mice. Tissue-specific and single cell analysis show lack of *raptor* expression exclusively in α-cells from αRaptor^{KO} mice. **B.** Immunofluorescent staining showing positive mTORC1 activity shown by pS6 (S240) stain in the control and lack of mTORC1 activity in the glucagon positive-cells of the αRaptor^{KO} mice in dispersed islets from 1 month-old mice (scale 10 μm). **C.** Flow cytometry analysis showing loss of mTORC1 activity by pS6 (S240) in glucagon positive-cells of the αRaptor^{KO} mice (n=3-4). **D**. Flow cytometry analysis showing preserved mTORC1 activity by pS6 (S240) in insulin positive-cells of the αRaptor^{KO} mice (n=3-4). Data are shown as means ± S.E.M. *p≤0.05; Nonparametric *U* test (Mann Whitney).

Low fed and fasting glucagon levels in mice with loss of mTORC1 signaling in α-cells

Body weight and random fed blood glucose were not different between control mice and mice with homozygous (αRaptor^{KO}) and heterozygous (αRaptor^{HET}) deletion of *raptor* (Figure 5A,B). Glucose tolerance at 2 and 8 months of age was not different between the three groups (Figure 5C,G). Assessment of the adaptation to the fasting state showed that control mice exhibited a decrease in glucose levels after 12 hours of fasting (Figure 5D,H). Compared to controls, 2 month-old αRaptor^{HET} mice had lower blood glucose after 6 hours of fasting, but this difference disappeared after 12 hours (Figure 5D). In contrast, αRaptor^{KO} mice were able to maintain blood glucose levels during the first 12 hours of fasting (Figure 5D). Glucose levels during fasting were similar among all the groups at 8 months (Figure 5H). Glucagon levels in the fed state were reduced in αRaptor^{KO} mice at 2 and 8-months of age (Figure 5E,I). Interestingly, αRaptor^{HET} mice exhibited fed glucagon levels that were reduced, but not to the level observed in the αRaptor^{KO} at 2 and 8 months (Figure 5E,I). Glucagon secretion is induced in states of decreasing blood glucose, as seen in 2 and 8 month-old control mice in response to fasting (Figure 5E). Compared to controls, glucagon levels decreased after 12-hour fasting in young and old αRaptor^{KO} and αRaptor^{HET} mice suggesting that the adaptation of glucagon secretion to fasting was compromised in these mice (Figure 5E,I). No differences were observed in fed or fasting insulin levels between controls, αRaptor^{KO} and αRaptor^{HET} mice at 2 and 8 months (Figure 5F,J).

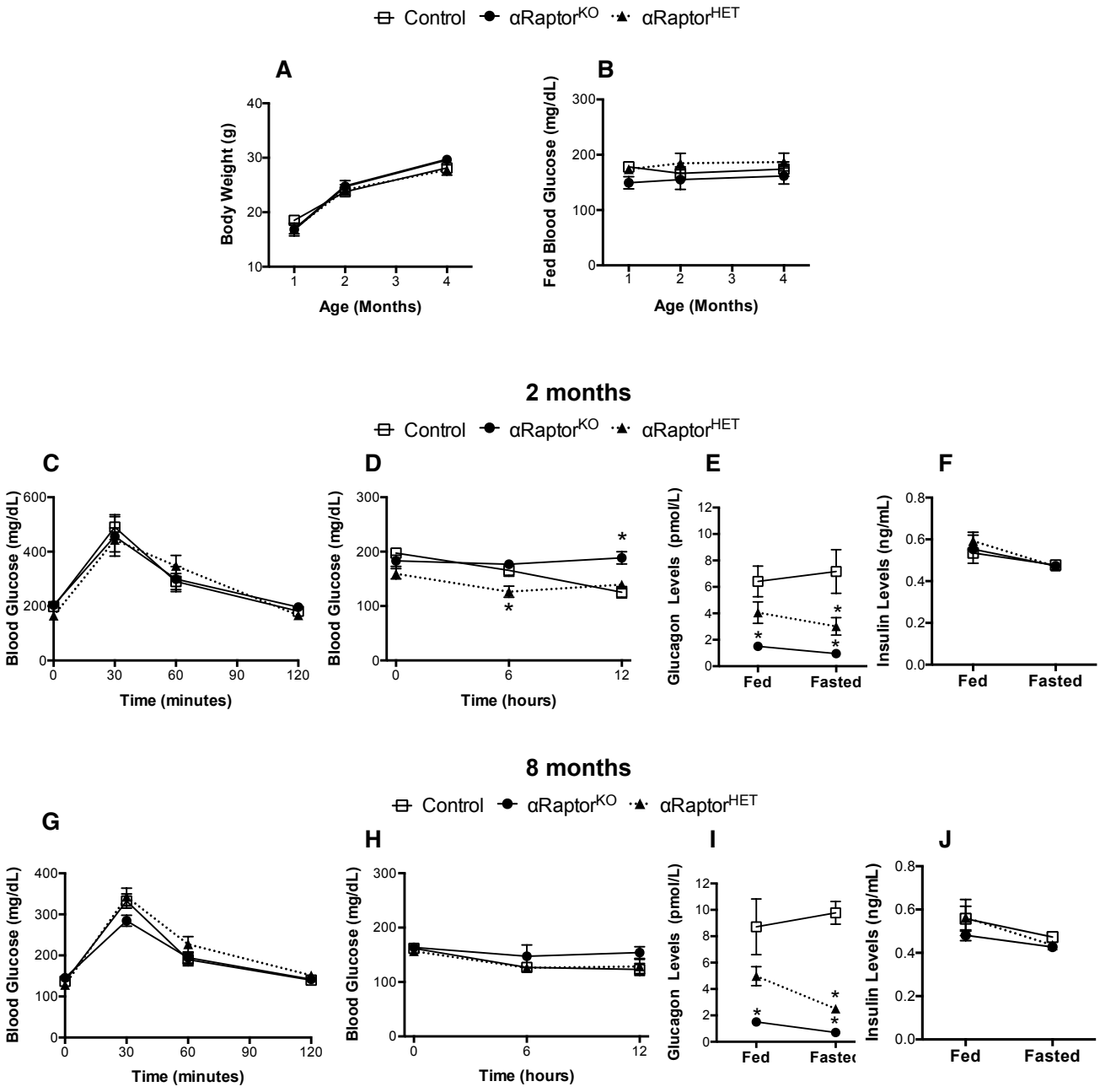

Figure 5. Mice with loss of mTORC1 signaling in α-cells exhibit low fed and fasting glucagon levels. A. Body weight and **B.** Random-fed blood glucose of control, αRaptor^{KO} and αRaptor^{HET} mice (n=8-9). Intraperitoneal glucose tolerance tests, IPGTT (2g/kg) of **C.** 2 months (n=3-4) and **G.** 8 months-old mice (n=5-8). Fasting blood glucose of **D.** 2 months (n=7-9) and **H.** 8 months-old mice (n=3-4). Fed and fasted glucagon levels of **E.** 2 months (n=5-6) and **I.** 8 months-old mice (n=5-6). Fed and fasted insulin levels of **F.** 2 months (n=3-4) and **J.** 8 months-old mice (n=3-4). Data are shown as means ± S.E.M. *p≤0.05; Nonparametric *U* test (Mann Whitney).

The adaptation of fasting during physiological conditions involves multiple metabolic adjustments to maintain glucose levels. We showed that fasting glucose levels in 2 month-old αRaptor^{KO} mice were maintained at 12 hours, but returned to the levels of controls at 24 hours (Figure 6A). The lack of drop in glucose levels after 12 hours of fasting in αRaptor^{KO} mice was interesting as these mice exhibited very low glucagon levels. Assessment of liver weight and glycogen content showed that both were reduced after 12 hours of fasting, but fasting glycogen levels were higher in αRaptor^{KO} mice (Figure 6B,C). This suggested that gluconeogenesis could be upregulated in αRaptor^{KO} mice. Consistent with this, glucose levels after pyruvate tolerance testing were higher in αRaptor^{KO} mice suggesting that hepatic gluconeogenesis was increased (Figure 6D). The results of these studies suggest that αRaptor^{KO} mice were more resistant to a decrease in glucose during the first 12 hours of fasting by an increase in gluconeogenic pathways, but these mechanisms were not sufficient to maintain glucose after prolonged fasting (24 hours).

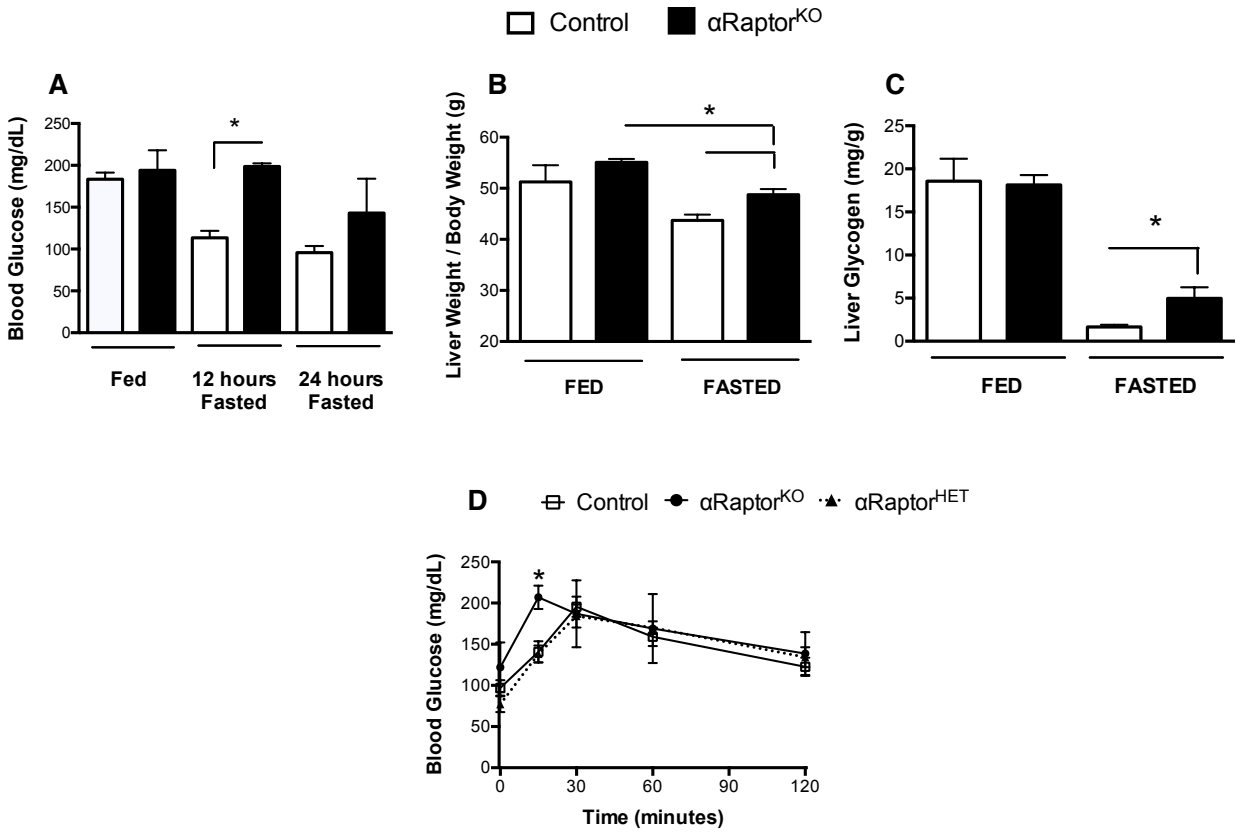

Figure 6. αRaptor^{KO} mice have increased gluconeogenesis. A. Fasting blood glucose (n=3-4). **B.** Fed and fasted liver weight (n=3-4) and **C.** Liver glycogen content (n=3-6) in 8 months-old control and αRaptor^{KO} mice. **D.** Pyruvate tolerance test (2 g/kg) in 2-months old mice (n=3-6). Data are shown as means ± S.E.M. *p≤0.05; Nonparametric *U* test (Mann Whitney).

mTORC1 signaling is necessary for the maintenance of postnatal α-cells

Morphometric analysis at postnatal day 1 demonstrated that αRaptor^{KO} mice were born with normal α-cell mass (Figure 7B). At 2 weeks of age, αRaptor^{KO} mice exhibited normal α-cell mass, lower levels of proliferation and no changes in apoptosis (Figure 7C and Figure 8A,B). αRaptor^{KO} mice displayed a loss of α-cells as evidenced by a reduction in α-cell mass and pancreatic glucagon content at 2 and 8 months (Figure 7D-G). In contrast, β, δ (somatostatin) and PP (pancreatic polypeptide)-cell mass at 2 months mass was not altered in newborn and 2-month old αRaptor^{KO} mice (Figure 7H,I and Figure 8C-E). There was no difference in α-cell mass and pancreatic glucagon content in αRaptor^{HET} mice compared to controls at 2 months of age (Figure 7D,E).

However, by 8 months αRaptor^{HET} mice showed a reduction in α-cell mass and pancreatic glucagon content (Figure 7F,G). A decrease in the number of α-cells, but not the cell size or cellular glucagon content analyzed by flow cytometry in dispersed islets from αRaptor^{HET} mice, was responsible for the reduction in the α-cell mass of older αRaptor^{HET} mice (Figure 8F-H). Interestingly, β-cell mass was increased in 8 month-old αRaptor^{KO} mice with an intermediate increase in the 8 month-old αRaptor^{HET} mice (Figure 7J). In addition, pancreas weight was increased in 2 month-old αRaptor^{KO} mice (Figure 7K).

Morphologic evaluation by electron microscopy in 1 month-old αRaptor^{KO} showed a reduction in α-cell size (Figure 7L). Reduced cell size was confirmed by independent cell size measurements by immunohistochemistry using dispersed islets from 1 month-old control and αRaptor^{KO} (Figure 7M). In addition, the number of glucagon granules appeared reduced in α-cells from αRaptor^{KO} mice and was independently validated by reduced intracellular glucagon levels using flow cytometry (Figure 7N). To investigate the mechanisms of loss of α-cells in αRaptor^{KO} mice, we examined the role of decreased mTORC1 signaling in autophagy-mediated cell death (Egan et al., 2011; Kim et al., 2011; Sanchez et al., 2012). To test this, we crossed αRaptor^{KO} mice to an *in vivo* reporter of autophagy (GFP-LC3 mice) (Mizushima et al., 2004). Our results showed that at 1 month, αRaptor^{KO} mice have increased GFP-LC3 punctate in α-cells, suggesting that the loss in α-cell mass was mediated by autophagy (Figure 7O). Inhibition of autophagy by treatment of 2 week-old αRaptor^{KO} mice with chloroquine for 2 weeks showed that α-cell mass in αRaptor^{KO} mice treated with chloroquine was slightly improved (Figure 7P). These results are consistent with a role of autophagy in the loss of α-cell mass in αRaptor^{KO} mice.

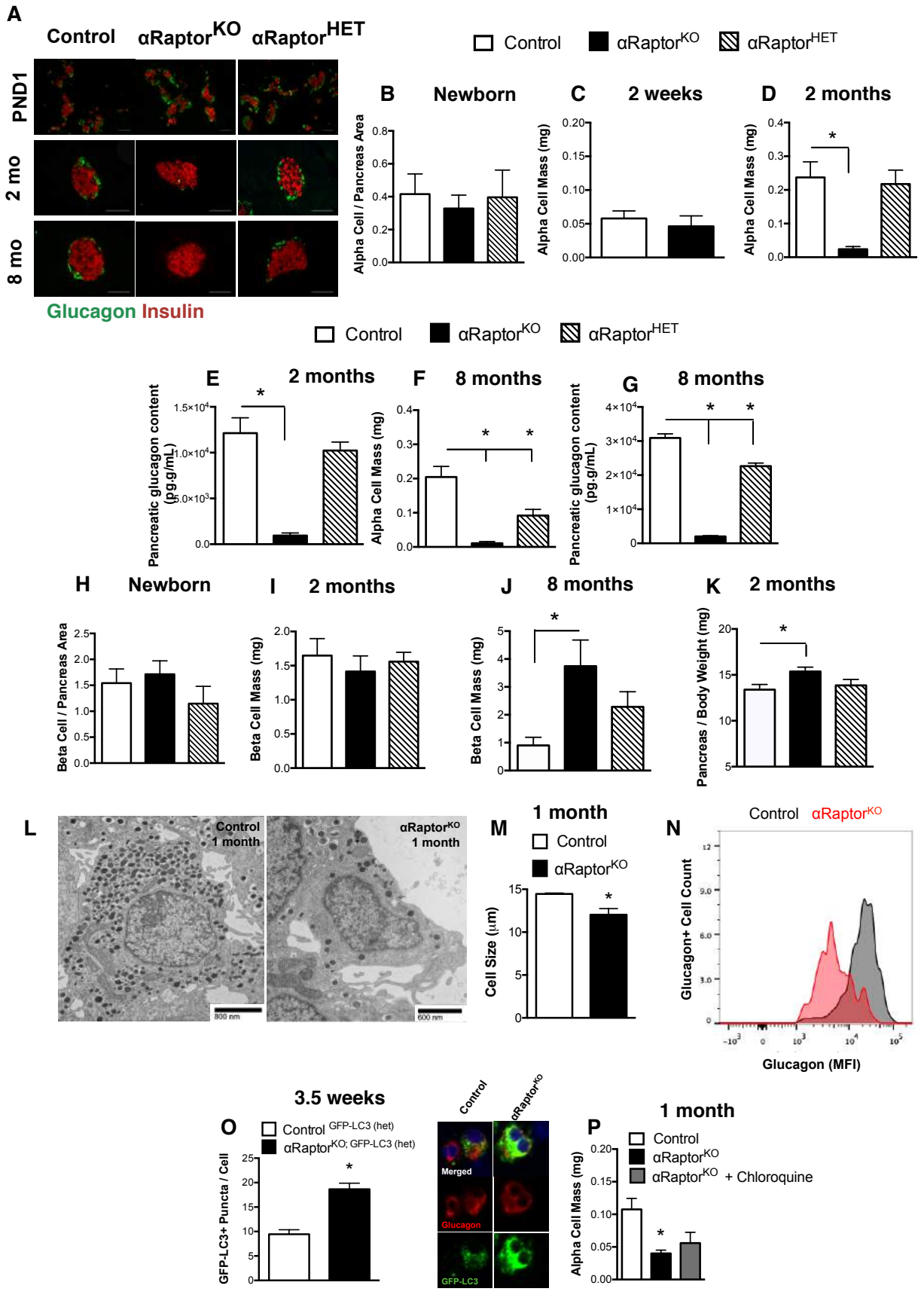
A
Control
αRaptorKO
αRaptorHET
PND1
2 mo
8 mo
Glucagon Insulin
Control
αRaptorKO
αRaptorHET
B Newborn
Alpha Cell / Pancreas Area
C 2 weeks
Alpha Cell Mass (mg)
D 2 months
Alpha Cell Mass (mg)
E 2 months
Pancreatic glucagon content (pg.g/mL)
F 8 months
Alpha Cell Mass (mg)
G 8 months
Pancreatic glucagon content (pg.g/mL)
H Newborn
Beta Cell / Pancreas Area
I 2 months
Beta Cell Mass (mg)
J 8 months
Beta Cell Mass (mg)
K 2 months
Pancreas / Body Weight (mg)
L
Control 1 month
αRaptorKO 1 month
800 nm
600 nm
M 1 month
Control
αRaptorKO
Cell Size (μm)
N
Control
αRaptorKO
Glucagon+ Cell Count
Glucagon (MFI)
3.5 weeks
O
Control GFP-LC3 (het)
αRaptorKO; GFP-LC3 (het)
GFP-LC3+ Puncta / Cell
Control
αRaptorKO
Merged
Glucagon
GFP-LC3
1 month
P
Control
αRaptorKO
αRaptorKO + Chloroquine
Alpha Cell Mass (mg)

Figure 7. mTORC1 signaling is necessary in the maintenance, and not development of α-cells. A. Immunofluorescent images (scale 50 μm) and **B.** Quantification of α-cell fraction at postnatal day-1 (newborn). Quantification of α-cell mass at **C.** 2 weeks (n=4). Quantification of **D.** α-cell mass (n=4-5) and **E.** Pancreatic glucagon content (n=4-6) in 2 month-old mice. Quantification of **F.** α-cell mass (n=3-4) and **G.** Pancreatic glucagon content (n=3-4) in 8 month-old mice. **H.** Quantification of β-cell fraction at postnatal day-1 (newborn), **I.** β-cell mass in 2 month-old mice (n=4-5) and **J.** β-cell mass in 8 month-old mice (n=3-4). **K.** Pancreas weight normalized to total body weight in 2 month-old mice (n=5-6). **L.**Electron microscopy images from 1 month-old Control and αRaptor^{KO} mice. **M.** Analysis α-cell size of control and αRaptor^{KO} mice at 1 month of age by immunohistochemistry using dispersed islets (n= 3-4) and **N.** Flow cytometry analysis of cell glucagon content of control and αRaptor^{KO} mice at 1 month (n=3-4). **O.** GFP-LC3 puncta in α-cells and representative immunofluorescent images (n=50-51 cells) in 3.5 week-old mice. **P.** Quantifications of α-cell mass at 1 month of age +/- chloroquine treatment in αRaptor^{KO} mice from 2-4 weeks of age (n=3-4)**.** Data are shown as means ± S.E.M. *p≤0.05; Nonparametric *U* test (Mann Whitney).

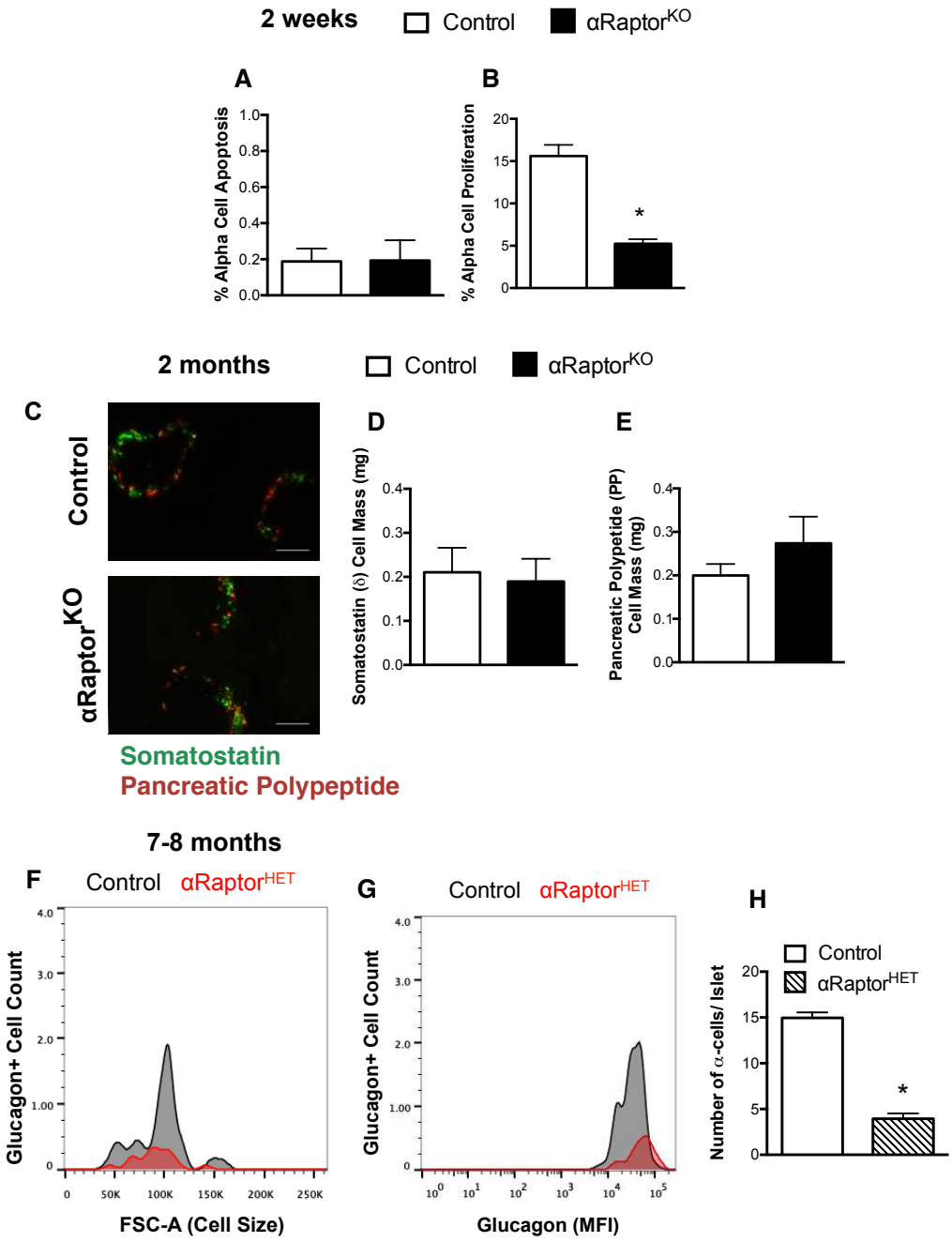

Figure 8. Loss of mTORC1 signaling in α-cells leads to decreased cell number and proliferation in αRaptor^{KO} and older αRaptor^{HET} mice. A. Quantifications of α-cell apoptosis and **B.** Proliferation at 2 weeks of age (n=4). **C.** Immunofluorescent images (scale 50 μm) and quantification of **D.** δ (somatostatin) and **E.** PP (pancreatic polypeptide) cell mass in 2 month-old mice (n=3-4). **E.** Flow cytometry analysis of α-cell size and **F.** Glucagon content in older αRaptor^{HET} mice (n=3). **G.** Quantifications of number of α-cells/islet of older control and αRaptor^{HET} mice by immunohistochemistry using pancreatic sections (n=4). Data are shown as means ± S.E.M. *p≤0.05; Nonparametric *U* test (Mann Whitney).

αRaptor^{KO} mice have increased active GLP-1 levels from intestinal origin

Interestingly, β-cell mass was increased in 8 month-old αRaptor^{KO} mice with an intermediate increase in the 8 month-old αRaptor^{HET} mice (Figure 7J). Analysis of incretin levels showed an increase in fed circulating active GLP-1 levels in αRaptor^{KO} mice at 2 months of age, associated with an improved oral glucose tolerance and increased active GLP-1 levels at zero and 10 minutes post oral glucose administration (Figure 9A-C). At 8 months of age, fed circulating GLP-1 levels in αRaptor^{KO} were further increased, with an intermediate rise in fed active GLP-1 levels in the αRaptor^{HET} mice (Figure 9E). However, analysis of pancreatic active GLP-1 levels at 2 and 8 months of age showed a reduction in αRaptor^{KO} mice, suggesting that the increased circulating active GLP-1 in these mice is not of pancreatic origin (Figure 9D,F). We measured active GLP-1 levels in intestinal extracts from 2-month old mice, and our data showed that αRaptor^{KO} mice have increased active GLP-1 levels (Figure 9G). Therefore, we concluded that the increase in circulating active GLP-1 levels αRaptor^{KO} mice is of intestinal origin.

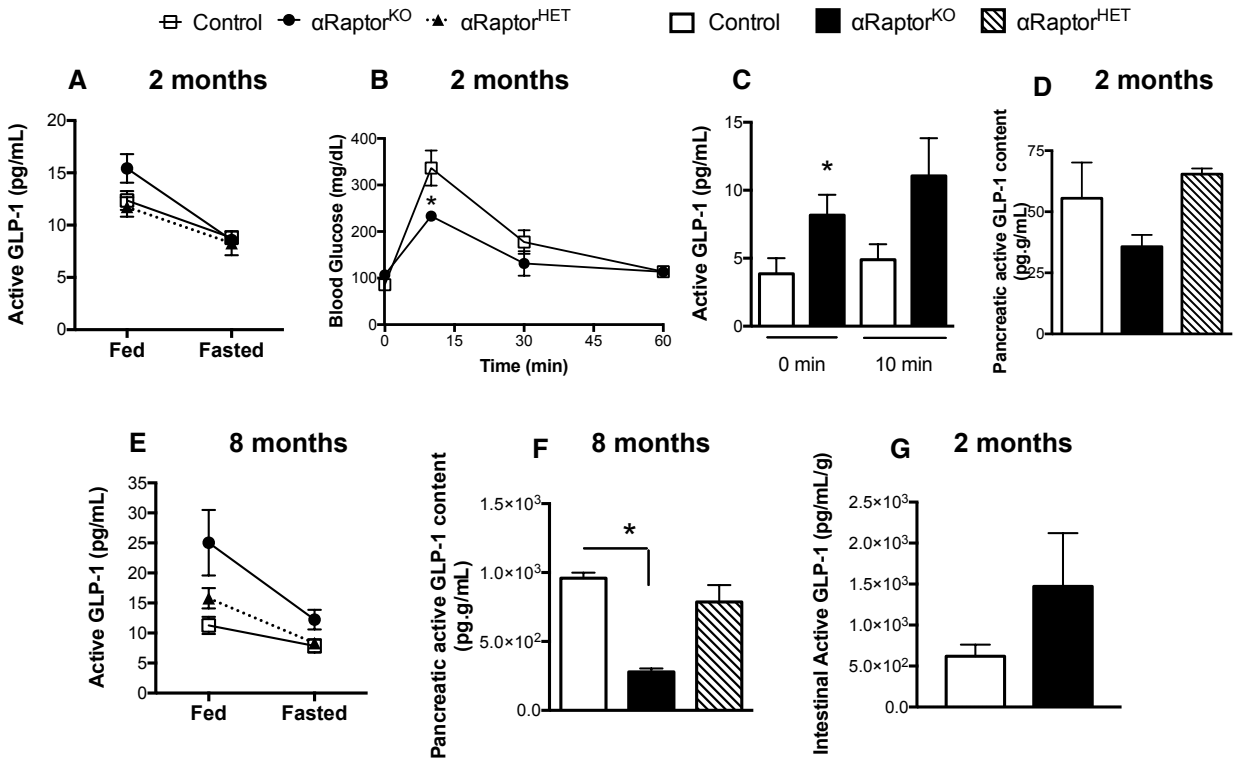

Figure 9. Improved oral glucose tolerance and increased active GLP-1 levels in αRaptor^{KO} mice. A. Fed and fasted active GLP-1 levels in 2 month-old mice (n=4). **B.** Blood glucose response to oral glucose tolerance test (2g/kg.bw) and **C.** Circulating active GLP-1 levels at zero and 10 minutes post oral glucose administration (n=6-7). **D.** Total pancreatic active GLP-1 levels in 2 month-old mice (n=4-5). **E.** Fed and fasted active GLP-1 levels in 8 month-old mice (n=3-4). **F.** Total pancreatic active GLP-1 levels in 8 month-old mice (n=3-4). **G.** Total intestinal active GLP-1 levels in 2 month-old mice (n=2-3). Data are shown as means ± S.E.M. *p≤0.05; Nonparametric *U* test (Mann Whitney).

Glucagon secretion in response to fasting, hypoglycemia and neuroglycopenia is impaired in αRaptor^{HET} mice

The reduction in glucagon levels in αRaptor^{KO} could be explained in part by a marked reduction in α-cell mass. However, lower fasting glucagon levels with normal α-cell mass in 2-month-old αRaptor^{HET} mice suggested a defect in glucagon secretion. We investigated mTORC1 activity in α-cells from mice that were fasted for 6 hours and refed for 2 hours and mice fasted for 6 hours followed by administration of exogenous insulin (1 Unit/kg). Our data showed that mTORC1 is not active in α-cells in the fed pancreas; however, insulin-induced hypoglycemia significantly increased mTORC1

activity in α-cells (Figure 10A,B). To further investigate the role of mTORC1 on glucagon secretion, we subjected these mice to different stimulatory conditions *in vivo*. Examination of glucagon secretion by insulin-induced hypoglycemia in 2 month-old mice showed that insulin induced similar decreases in blood glucose in αRaptor^{KO}, αRaptor^{HET} and control mice (Figure 10C). However, glucagon secretion after insulin-induced hypoglycemia was compromised in αRaptor^{KO} mice, explained by the severe loss of α-cell mass (Figure 10D). In contrast, αRaptor^{HET} mice were able to respond, but showed reduced glucagon secretion after 30 minutes of insulin injection (Figure 10D). Next, we examined glucagon secretion under neuroglycopenic conditions induced by 2-deoxy-D-glucose (2DG) injection, a non-metabolizable glucose analog that inhibits phosphorylation of glucose by hexokinase. 2DG-induced neuroglycopenia triggers counterregulatory responses including glucagon secretion by activation of the autonomic nervous system (Karlsson and Ahren, 1987; Marty et al., 2005). As expected, control mice exhibited increased glucose levels at 60 and 120 minutes after 2DG glucose injection (Figure 10E). Glucose levels were higher at 120 minutes after 2DG injection in αRaptor^{KO} mice compared to those of control mice, explained by increased gluconeogenic mechanisms in these mice (Figure 10E). αRaptor^{HET} mice displayed higher glucose levels at 30 minutes after 2DG glucose injection, but glucose levels were not different than controls after 60 minutes (Figure 10E). Assessment of glucagon secretion after 2DG injection showed that αRaptor^{KO} failed to respond to neuroglycopenia, also likely due to the severe loss of α-cell mass. (Figure 10F). Although αRaptor^{HET} mice had a higher response in blood glucose output at 30 minutes, these mice displayed impaired glucagon responses compared to the controls (Figure 10F).

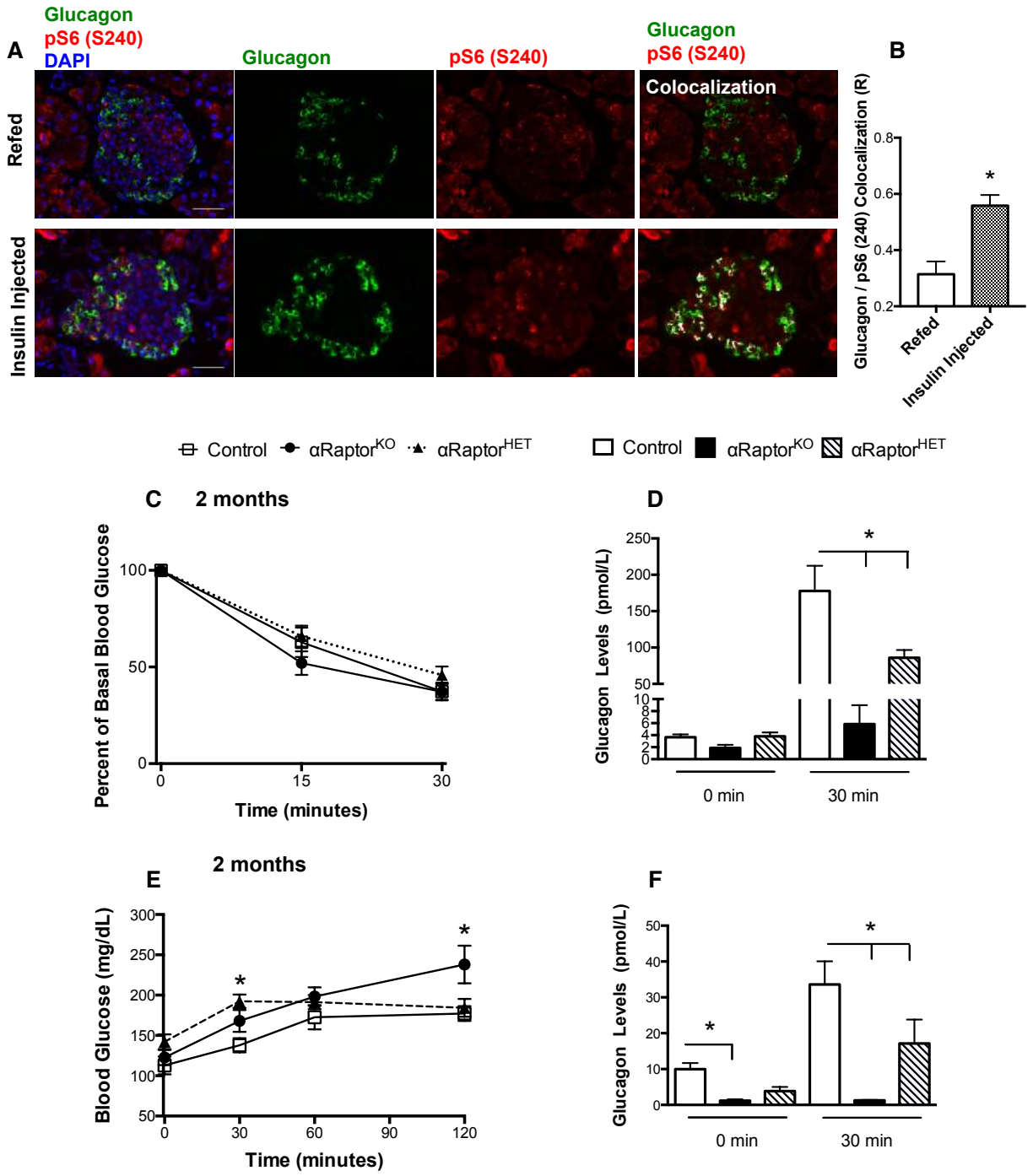

Figure 10. αRaptor^{HET} mice have decreased glucagon response to hypoglycemia and neuroglycopenia. A. Immunofluorescent images (scale 50 μm) of glucagon (green) and pS6 (S240; red) and **B.** Glucagon and pS6 colocalization (white) quantification by Pearson's Correlation Coefficient (R) in α-cells from mice fasted for 6 hours and refed for 2 hours or after administering exogenous insulin (1 Unit/kg). **C.** Blood glucose response and **D.** Glucagon response to Insulin Tolerance Test, ITT (1 U/kg.bw) at 2 months (n=5-6). **E.** Blood glucose response and **F.** Glucagon response to

2-deoxy-D-glucose (2 g/kg) at 2 months (n=4-5). Data are shown as means ± S.E.M. *p≤0.05; Nonparametric *U* test (Mann Whitney).

Streptozotocin (STZ)-induced diabetes leads to increase in mTORC1 signaling in α-cells

In order to assess the role of mTORC1 on α-cell mass expansion we assessed the responses to Streptozotocin (STZ)-induced diabetes (Plesner et al., 2014; Zhang et al., 2012). mTORC1 signaling assessed by phospho–S6 (Serine 235/236) staining was enhanced in α-cells from control mice treated with STZ (Figure 11A) and therefore, we hypothesized that the α-cell mass expansion in this model is mTORC1-dependent. We administered a single, high-dose STZ (150 mg/kg) to controls, αRaptor^{KO} and αRaptor^{HET} mice. Insulin levels were greatly reduced a week after STZ injection (Figure 11B). All groups had a rapid increase in fed blood glucose levels and by 6 days post-injection the control mice had above-detectable fed blood glucose (Figure 11C). Compared to controls, αRaptor^{KO} mice restored their blood glucose to normal as early as 6 hours under fasting (Figure 11D). Examination of glucagon levels after STZ-treatment showed a significant increase in control mice (Figure 11E). A trend to a decreased glucagon levels was observed in αRaptor^{HET} mice post-STZ treatment (Figure 11E) and αRaptor^{KO} mice had no response in glucagon levels as a result of STZ (Figure 11E). As expected, controls showed increased α-cell mass after STZ injection (Figure 11F). The expansion of α-cell mass was partially reduced in αRaptor^{HET} mice and no response to STZ was observed in α-cell mass of αRaptor^{KO} mice (Figure 11F,G).

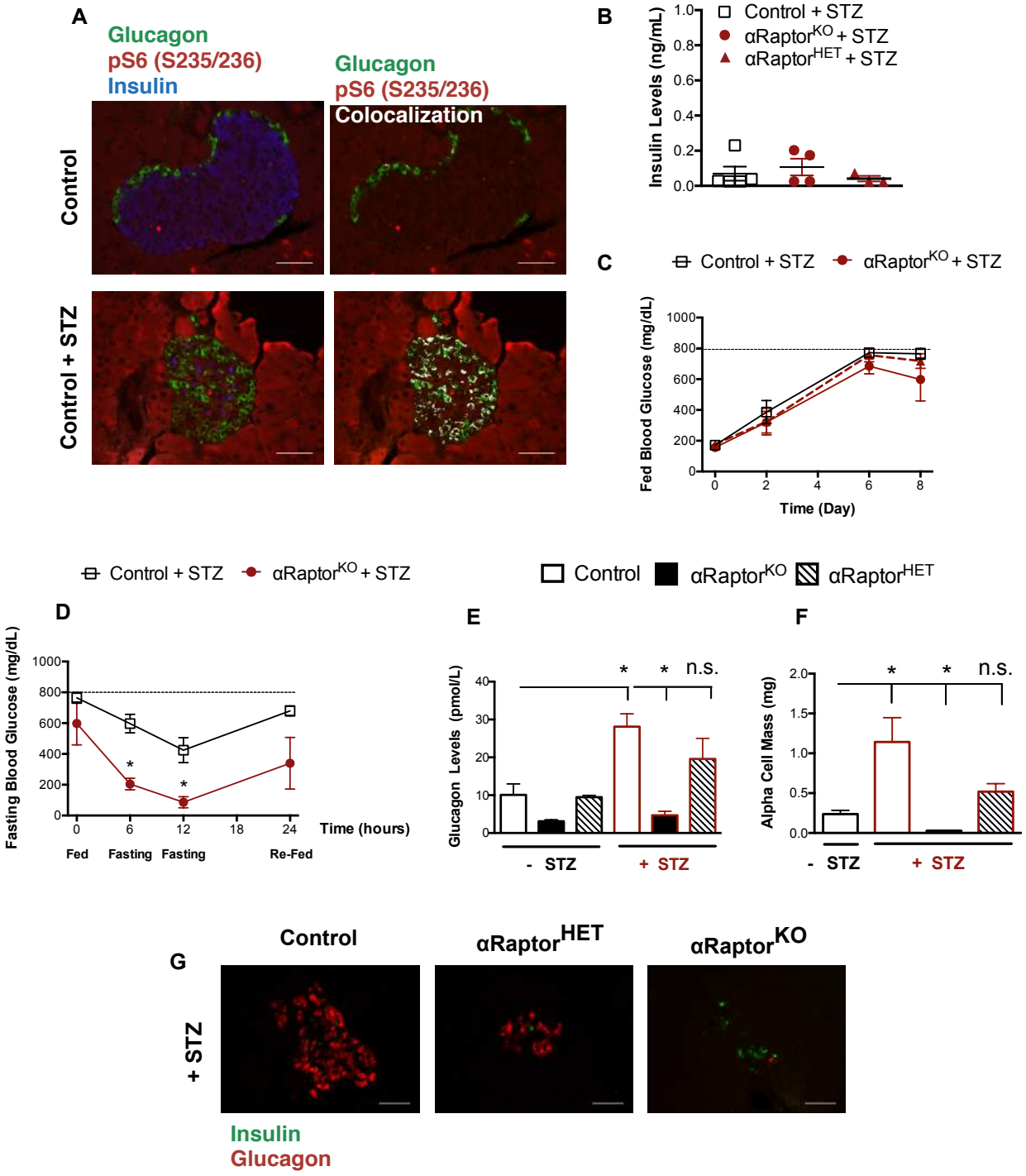

Figure 11. Streptozotocin (STZ)-induced diabetes leads to increase in mTORC1 signaling in α-cells. A. Imminofluorescent images representing glucagon (green), insulin (blue), pS6 (S235/36; red) and glucagon+pS6 colocalization (white) in control and control mice treated with STZ (150 mg/kg) (scale 50 μm). **B.** Circulating insulin levels 8-days post single IP dose of 150 mg/kg STZ (n=3-5). **C.** Fed blood glucose from day 0 to day 8 post STZ (n=3-5). **D.** Fasting and re-fed blood glucose on day 8 post

STZ (n=4-5). **E.** Glucagon levels before and 8-days post STZ (n=3-5). **F.** Alpha cell mass of mice treated with STZ (150 mg/kg) for 8 days (n=3-5); data is represented as fold change from α-cell mass in non-treated mice. **G.** Imminofluorescent images representing insulin (green) and glucagon (red) in pancreas sections from control, $\alpha Raptor^{KO}$ and $\alpha Raptor^{HET}$ mice treated with STZ (scale 50 μm). Data are shown as means ± S.E.M. *p≤0.05; Nonparametric *U* test (Mann Whitney).

Rapamycin treatment *in vivo* reduces glucagon secretory response to hypoglycemia

In order to assess the role of mTORC1 signaling inhibition on glucagon secretion using a more clinically relevant model, we assessed the effects of systemic administration of rapamycin on glucagon secretion. Rapamycin (2 g/kg) was administered in wild type male mice by intraperitoneal injection every other day for total of five injections (Figure 12A). Body weight and fed blood glucose were not affected in all the groups at the end of rapamycin treatment (Figure 12B,C). After insulin injection, rapamycin-treated mice achieved similar drop in blood glucose levels during the first 60 minutes and lower glucose levels were observed at 120 minutes post insulin injection, suggesting an impairment in glucose counterregulation (Figure 12D). Evaluation of glucagon secretion showed that although rapamycin-treated mice had comparable baseline glucagon levels to those of control mice, the glucagon secretory response to hypoglycemia was blunted (Figure 12E). Glucagon content in isolated islets was also reduced in rapamycin-treated mice (Figure 12F). To determine if rapamycin treatment acutely alters glucagon secretion independently of glucagon content we assessed glucagon secretion in isolated control islets after short exposure to rapamycin (30 minutes at each glucose condition, for total of 2 hours). As expected, glucagon secretion decreased with increase in glucose concentrations (Figure 12G). However, 30 minutes of rapamycin treatment decreased glucagon secretion at 1mM glucose and had no additional effect under increasing glucose conditions, confirming *in vivo* data that rapamycin inhibits glucagon secretion in response to hypoglycemia (Figure 12G). The reduction in glucagon secretion induced by acute treatment with rapamycin was not explained by alterations in glucagon content suggesting that short-term rapamycin treatment can

affect glucagon secretion during states of low-glucose independently of alterations in glucagon content (Figure 12H).

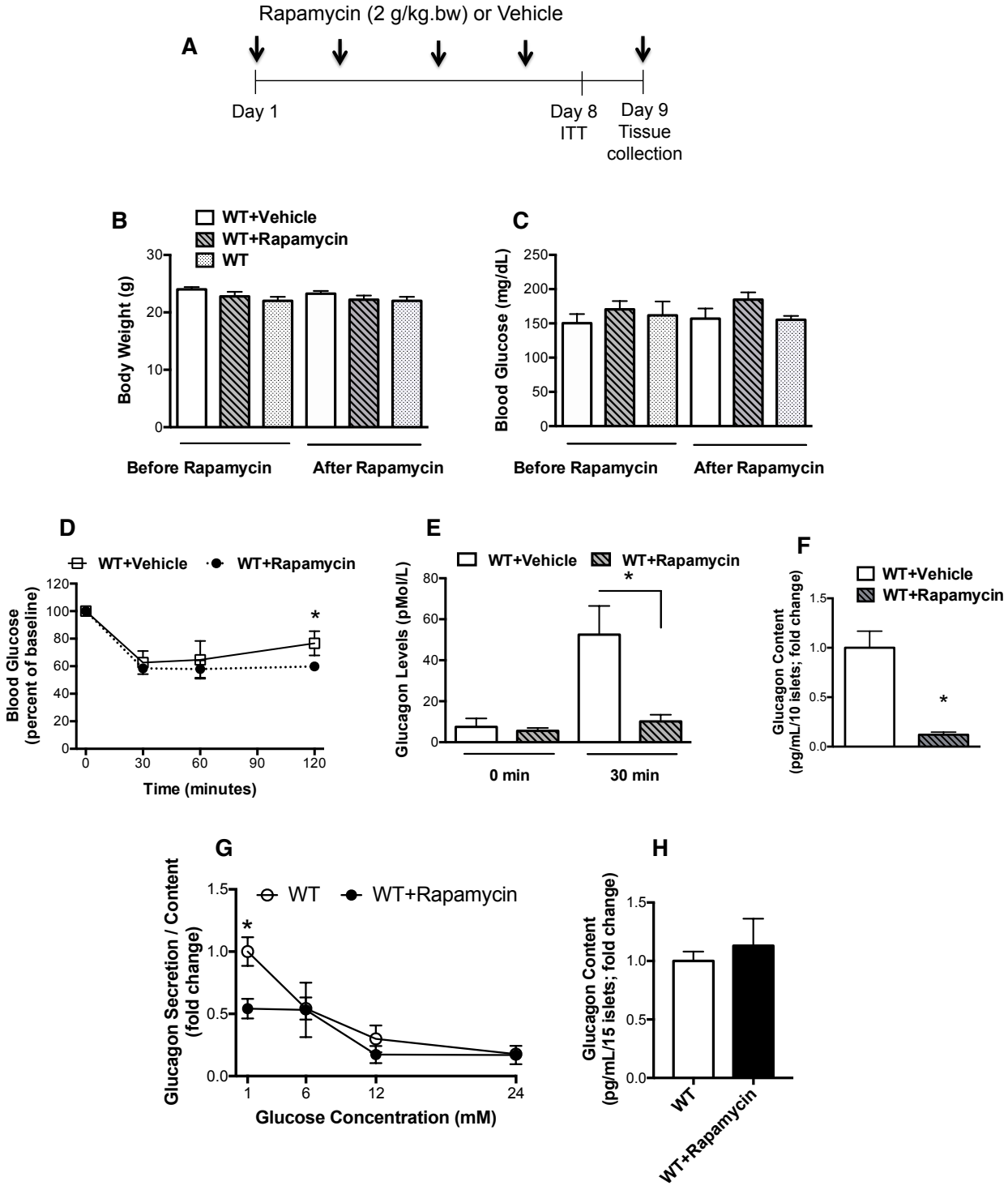

Figure 12. Rapamycin treatment *in vivo* recapitulates decreased glucagon secretory response to hypoglycemia and leads to decreased islet glucagon content. A. Experimental design for administering rapamycin to wild type, 2 month-old male mice. Arrows indicate intraperitoneal administration of rapamycin (2g/kg) every other day for 9 days. **B.** Body weight and **C.** Blood glucose levels on day 8 (n=4-5). **D.** Insulin Tolerance Test, ITT (1 U/kg) and **E.** Glucagon response at day 8 (n=4-5). **F.** Islet

glucagon content (n=4; presented as fold change from WT+Vehicle). **G.** Glucagon secretion and **H.** Islet glucagon content from isolated control islets treated with +/- rapamycin (30nM; n= 3-4 mice/treatment). Data are presented as fold change from control at 1 mM Glucose. Data are shown as means ± S.E.M. *p≤0.05; Nonparametric *U* test (Mann Whitney).

Glucagon secretory responses induced by pharmacologic manipulation of K_{ATP} channels in αRaptor^{HET} islets is abnormal

In vivo data showed that αRaptor^{HET} mice exhibited impaired glucagon secretion in response to fasting and hypoglycemia. To uncover the mechanisms responsible, we examined the secretory responses of isolated islets. Glucagon secretion in response to depolarization induced by a strongly depolarizing concentration of potassium chloride (KCl; 30 mM) was similar between control and αRaptor^{HET} islets (Figure 13A). Next, we examined the glucagon response to arginine, a secretagogue that induces glucagon secretion in part by modulating K_{ATP} channels (Shiota et al., 2005). Glucagon secretion induced by arginine was blunted in αRaptor^{HET} islets (Figure 13B). Taken together these data suggested that the defect in glucagon secretion in αRaptor^{HET} mice resided in steps prior to cell depolarization and possibly at the level of the K_{ATP} channel. We further evaluated glucagon secretion during pharmacological modulation of K_{ATP} channel activity with increasing concentrations of tolbutamide (K_{ATP} channel antagonist) and diazoxide (K_{ATP} channel agonist). Under low glucose conditions, when a relatively larger fraction of K_{ATP} channels are open, tolbutamide treatment of control islets induces glucagon secretion up to concentrations of 10μM, whereas glucagon secretion was inhibited at higher concentrations as previously described (MacDonald et al., 2007; Rorsman et al., 2008; Walker et al., 2011). In contrast, tolbutamide treatment of αRaptor^{HET} islets failed to induce glucagon secretion and suppressed glucagon release at lower concentrations of tolbutamide (Figure 13C). Next we tested the effects of diazoxide-mediated opening of K_{ATP} channels at high glucose, where most K_{ATP} channels should be closed. Increasing concentrations of diazoxide (0–10 μM) relieved the suppression of glucagon secretion in control islets (Figure 13D). In contrast, islets from αRaptor^{HET} mice were unresponsive to diazoxide and this agent failed to induce glucagon secretion (Figure 13D). Conversely, under low-glucose (1 mM) conditions

when at least some K_{ATP} channels are open, diazoxide further induced glucagon secretion at 1 mM followed by a dose-dependent suppression at 10 and 100 mM in control islets (Figure 13E). Under this condition, αRaptor^{HET} islets still failed to respond to diazoxide (Figure 13D,E). Taken together, these studies suggest that K_{ATP} channel function is altered in α-cells with reduced mTORC1 signaling.

mTORC1 regulates glucagon secretion by modulating K_{ATP} channel activity and expression

Next, we tested whether the changes in glucagon secretion obtained by pharmacologic manipulation of K_{ATP} channels in αRaptor^{HET} mice resulted from alterations in K_{ATP} channel activity. Whole-cell patch clamp was performed on α-cells at low glucose from Glucagon-Cre^{tdTomato} and αRaptor$^{HET;tdTomato}$ mice expressing a fluorescent reporter in α-cells. Following establishment of the whole-cell patch-clamp, and subsequent washout of intracellular ATP, K_{ATP} channel current was significantly reduced in αRaptor^{HET} α-cells compared to controls (Figure 13F, G). To test the hypothesis that these results could be explained by alterations in K_{ATP} subunit expression, we measured the expression of K_{ATP} channels subunits *KIR6.2* and sulfonylurea receptor subunit 1 (*SUR1*) in α-cells. We isolated an enriched population of α-cells by FACS sorted dispersed islets from αRaptor^{HET} and control mice crossed to Ins1-EGFP and CAG-tdTomato reporter mice (approximately 60-70% glucagon). Our data showed that the enriched α-cell population from αRaptor^{HET} exhibited a decrease in *SUR1* and *KIR6.2* mRNA expression (Figure 13H) and a lower protein level of SUR1 (Figure 13I). We were unable to assess KIR6.2 levels due to a lack of antibody detection. Single cell mRNA expression for *SUR1* in α-cells showed that young αRaptor$^{KO;tdTomato}$ mice had less positive α-cells for *SUR1* (Figure 13J). Unfortunately, we were unable to detect mRNA expression of *KIR6.2* in single cells using this methodology. Lastly, we measured mRNA and protein in αTC-1 cells, a glucagon-expressing cell line, treated with rapamycin (30 nM) for 48 hours. These studies showed that inhibiting mTORC1 signaling leads to decreased KIR6.2 and SUR1 protein and RNA expression (Figure 13K,L). Overall, our data showed that mTORC1 regulates the expression and activity of K_{ATP} channels in α-cells.

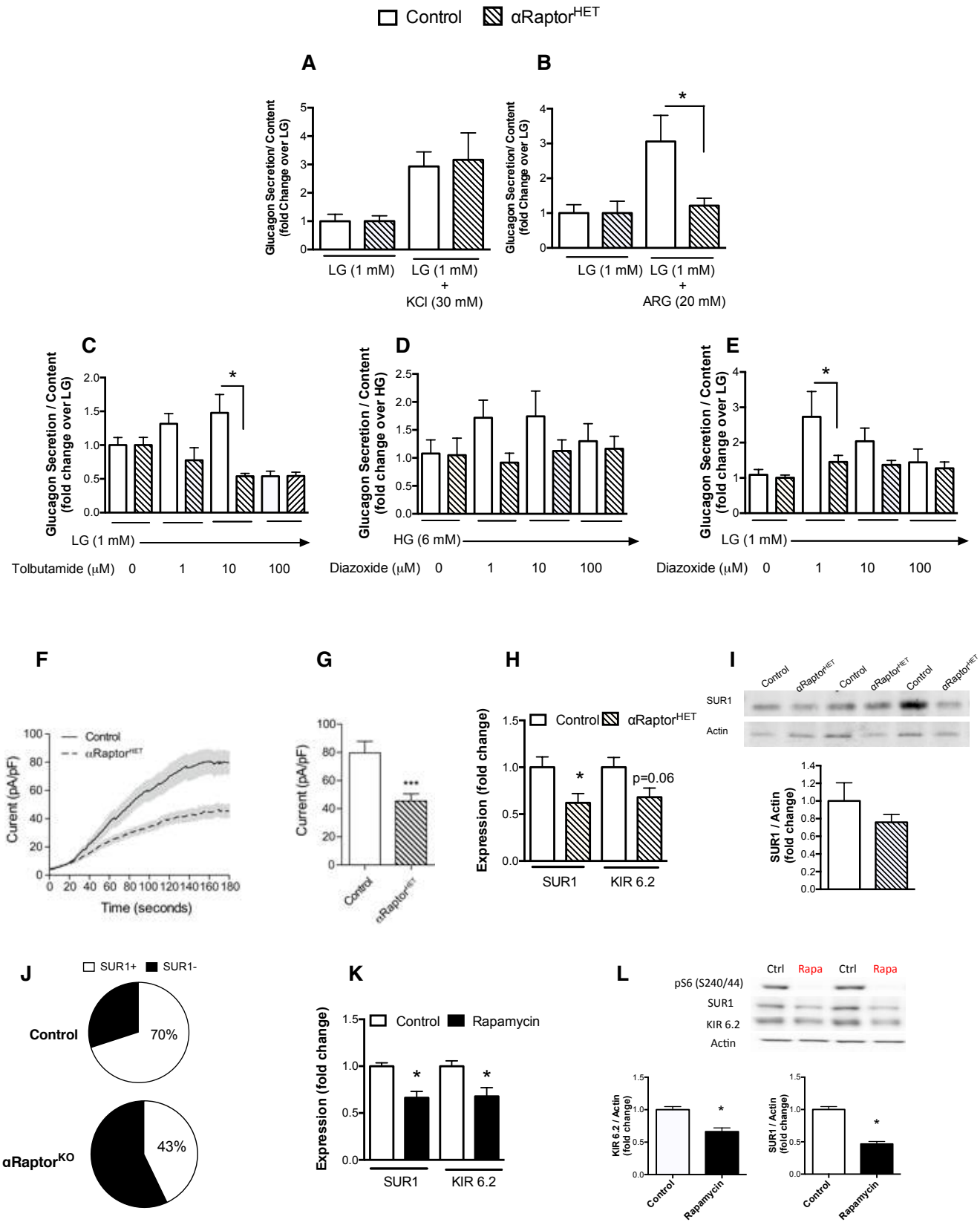
Control
αRaptorHET
A
B
Glucagon Secretion/ Content (fold Change over LG)
LG (1 mM)
LG (1 mM) + KCl (30 mM)
LG (1 mM) + ARG (20 mM)
C
D
E
Glucagon Secretion / Content (fold change over LG)
Glucagon Secretion / Content (fold change over HG)
LG (1 mM)
HG (6 mM)
Tolbutamide (μM) 0 1 10 100
Diazoxide (μM) 0 1 10 100
F
G
H
I
Current (pA/pF)
Time (seconds)
Expression (fold change)
SUR1
KIR 6.2
p=0.06
Actin
SUR1 / Actin (fold change)
J
SUR1+
SUR1-
70%
43%
K
Rapamycin
L
Ctrl
Rapa
pS6 (S240/44)
KIR 6.2 / Actin (fold change)
Control
Rapamycin

Figure 13. mTORC1 regulates glucagon response by alterations in K_{ATP} channel expression and activity. Glucagon response from isolated islets to **A.** KCl (30 mM) (n=8 mice) and **B.** Arginine (20 mM) (n=5-7 mice) under low-glucose Krebs Buffer (LG 1 mM). Glucagon response from isolated islets to increasing concentrations of **C.** Tolbutamide (0-100 μM) under low-glucose conditions (1 mM; n=3-4 mice); **D.** Diazoxide (0-100 μM) under high-glucose conditions (6 mM; n=5-7 mice); and **E.** Diazoxide (0-100 μM) under low-glucose conditions (1 mM; n=5-6 mice). **F.** K_{ATP} channel activity during washout of intracellular ATP and **G.** Current amplitude quantification at 180 seconds in α-cells from control and αRaptor^{HET} mice (n=30-41 cells from 3-4 mice). **H.** RNA expression of *SUR1* and *KIR6.2* (n=6) and **I.** protein expression of SUR1 (n=3) in enriched α-cell population from control and αRaptor^{HET} mice. **J.** Single-cell analysis of *SUR1* expression frequency in α-cells from 1 month-old control and αRaptor^{KO} mice (n=20-21 cells from 3-4 mice). **K.** RNA expression and **L.** Protein levels of SUR1 and KIR6.2 from αTC-1 cells treated +/- rapamycin (30 nM) for 48 hours (n=7-8). Data are presented as fold change from control and shown as means ± S.E.M. *p≤0.05; Nonparametric *U* test (Mann Whitney).

mTORC1 regulates K_{ATP} channel expression *via* the regulation of FoxA2 expression

To validate the expression studies and further explore the mechanisms linking mTORC1 to regulation of α-cell function and mass, we assessed expression of critical α-cell genes using Fluidigm C1 platform for RNA expression of single pancreatic islet cells (Table 3 in Experimental Methods for complete list of genes included in analysis). Single-cell gene analysis validated the decrease in *SUR1* and *KIR6.2* expression in αRaptor^{KO} and further showed reduced glucagon gene expression in these mice (Figure 14A,B). Autophagy-associated genes *ULK1* and *ULK2* were decreased in αRaptor^{KO} confirming a known role of this pathway in autophagy. Importantly, gene expression of key transcription factors involved in α-cell development and maintenance, such as *FoxA2*, *Neurogen3*, *Gata4*, *MafB*, *Pou3f4*, *Notch1*, *RBPJ* and *Nkx2.2*, were lower in αRaptor^{KO} compared to control α-cells (Figure 14A,B). Decreased expression of *CCNB1* (Cyclin B) and *EIF4E* suggest that these genes could be involved on the alteration of α-cell proliferation in αRaptor^{KO}. Single-cell gene analysis also identified targets involved in exocytosis and glucagon secretion, such as *SNAP25* (Synaptosomal-associated protein 25), *CACNA1S* (L-type voltage-dependent calcium channel) and *CHRM3* (muscarinic acetylcholine M3 receptor). Endoplasmic-reticulum stress-associated

genes, *XBP1* and *HSP90AB1*, were also decreased in αRaptor^{KO}. Reduced *FoxA2*, *MafB*, *Nkx2.2*, *Pou3f4* mRNA expression was also decreased in αTC-1 cells treated with rapamycin (30 nM) for 48 hours, validating the results obtained by the single cell analysis (Figure 14C).

The reduction in *Foxa2* expression in α-cells from αRaptor^{KO} was particularly interesting, as *FoxA2* has been shown to directly regulate glucagon, *SUR1* and *KIR6.2* gene expression in α-cells (Gao et al., 2007; Heddad Masson et al., 2014; Lantz et al., 2004; Lee et al., 2005; Philippe et al., 1994; Wang et al., 2002). Therefore, we hypothesized that mTORC1 modulates glucagon and K_{ATP} channel subunit expression through modulation of *FoxA2* expression. Flow cytometry analysis confirmed that FoxA2 protein levels were also reduced in α-cells from αRaptor^{KO} mice (1 month old) (Figure 14D,E). In addition, nuclear FoxA2 levels were decreased, as measured by the ratio of signal intensity of nuclear FoxA2 over DAPI in the α-cells from αRaptor^{KO} mice (Figure 14F,G).

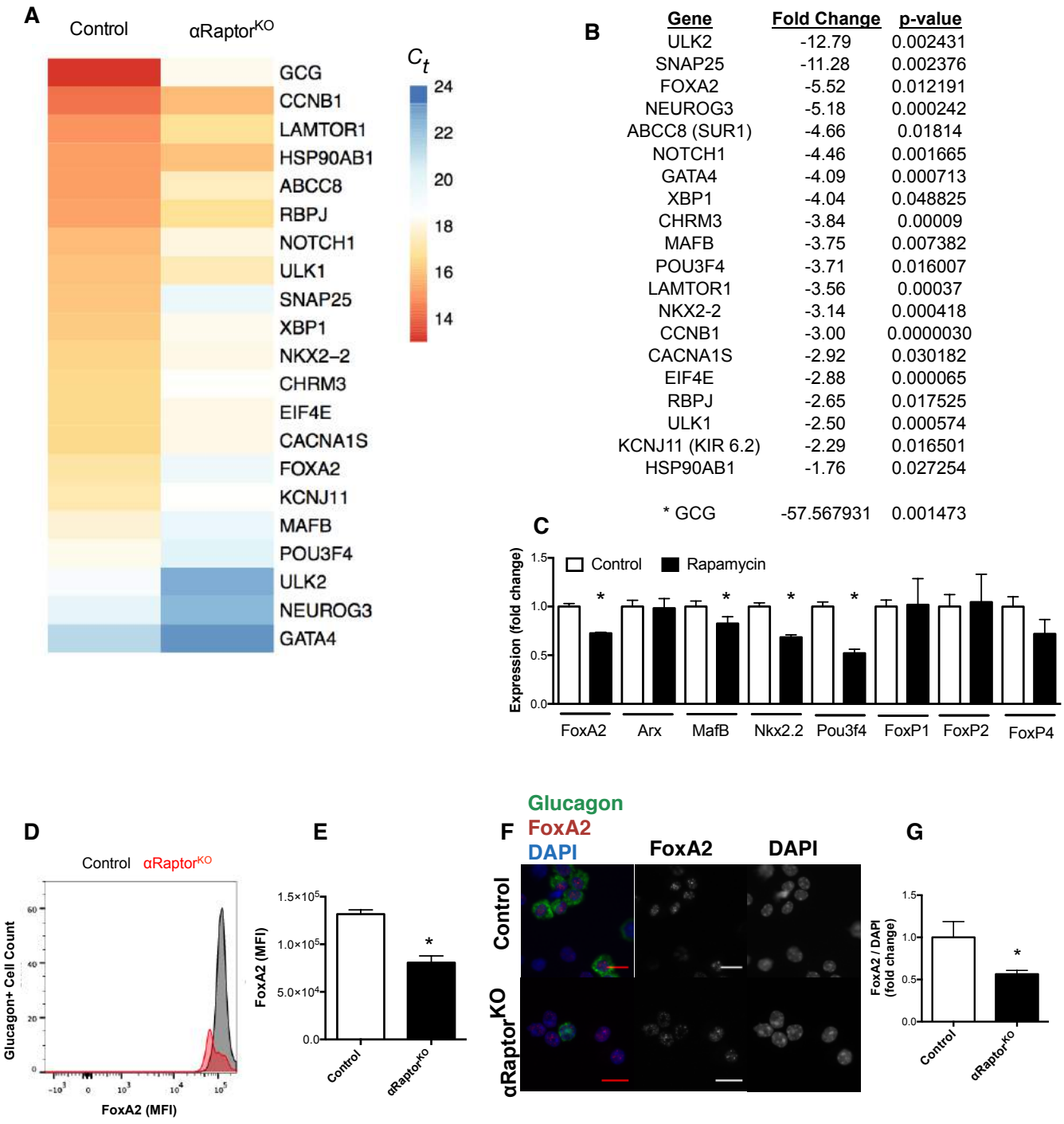

Figure 14. mTORC1 regulates the expression of genes involved in glucagon synthesis and regulation of glucagon secretion. A. Heat map represents mean Ct of differentially expressed genes (p>0.05) from Fluidigm single-cell analysis. **B.** Fold change and p-value of differentially expressed genes identified in single-cell by t-test and *MAST analysis. **C.** RNA expression of genes from αTC-1 cells treated +/- rapamycin (30 nM) for 48 hours (n=4-8/group). **D.** Flow cytometry analysis and **E.**

quantification of FoxA2 protein in α-cells from 1 month-old control and αRaptor^{KO} mice (n=3-4). **F.** Immunofluorescent images representing FoxA2 (red), glucagon (green) and DAPI (blue) stain of isolated and dispersed islets from 1 month-old control and αRaptor^{KO} mice (scale 10 μm). **G.** Quantification of the ratio of the signal intensity of nuclear FaxA2 over DAPI in dispersed α-cells from 1 month-old control and αRaptor^{KO} mice (n=4). Data are presented as fold change from control and shown as means ± S.E.M. *p≤0.05; Nonparametric *U* test (Mann Whitney).

Discussion

The current studies provide new insights into the regulation of glucagon secretion and α-cell mass. Our studies were designed to examine signaling events controlling α-cell mass and glucagon secretion by characterizing mice with a conditional deletion of *raptor* in α-cells. This work demonstrated that mTORC1 signaling positively regulates α-cell mass maintenance and glucagon secretion during fasting. Our data also show that mTORC1 is dispensable for α-cell development and plays a role in the maintenance of α-cells after weaning. Importantly, these experiments uncover a novel role of mTORC1 signaling on regulation of glucagon secretion by transcriptional regulation of K_{ATP} channel subunit expression. We also present a novel role of mTORC1 on controlling critical transcription factors in α-cells and identified *FoxA2* as a novel mTORC1 target that mediates transcriptional regulation of K_{ATP} channel subunit and glucagon expression. More importantly, the decrease in glucagon secretion by lack of mTORC1 activity was recapitulated by administration of the clinically-used immunosuppressant and mTORC1 inhibitor, rapamycin. Our data suggest that these mechanisms could negatively regulate glucagon levels *in vivo* and thus inhibiting glucagon responses to hypoglycemia in patients taking these medications.

Morphologic studies showed that the decrease in glucagon levels observed in αRaptor^{KO} mice resulted from a loss of α-cells. Given the importance of mTORC1 signaling in autophagy, we hypothesized that the loss in α-cell mass in the αRaptor^{KO} mice was caused by increased autophagy-mediated failure of proper cell maintenance (Egan et al., 2011; Kim et al., 2011; Sanchez et al., 2012). This hypothesis was confirmed by crossing control and αRaptor^{KO} mice with mice expressing a molecular

marker of autophagy (LC3-GFP) and the partial restoration of α-cell mass at 1 month by 2-week treatment of the autophagy inhibitor, chloroquine. The lack of complete rescue could be explained by the concomitant decrease in α-cell proliferation observed in αRaptor^{KO} mice at 2 weeks of age. In addition to increased autophagy, smaller α-cells also contributed to the decrease in α-cell mass in αRaptor^{KO} mice. Increase in mTORC1 inhibits autophagy by phosphorylating ULK1/2 and the current studies showed that this kinase could also regulate *ULK1/2* mRNA levels. Interestingly, αRaptor^{HET} mice also showed reduction in α-cell mass only at 8 months suggesting that long-term reduction of mTORC1 activity could have an impact on controlling α-cell mass. Together, our data suggest that the loss in α-cell mass is mediated by an increased rate of autophagy in αRaptor^{KO} mice and that mTORC1 is essential for proper α-cell maintenance, α-cell size and glucagon content.

Glucose-dependent regulation of glucagon release is a complex process and much less understood than that of glucose-induced insulin secretion. Glucagon secretion is decreased by high glucose and paracrine factors released from neighboring insulin-secreting β-cells, somatostatin-secreting δ-cells and is also regulated by neural control (Bloom et al., 1978; Franklin et al., 2005; Gerich et al., 1973; Ishihara et al., 2003; Rorsman et al., 1989). αRaptor^{KO} and αRaptor^{HET} mice have abnormal glucagon response to fasting at 2 and 8-months of age. The decrease in glucagon levels could be explained by a marked reduction in α-cell mass observed in αRaptor^{KO} mice. In contrast, αRaptor^{HET} mice exhibited normal α-cell mass at 2 months, but impaired glucagon secretion during fasting, insulin-induced hypoglycemia and neuroglycopenia. These studies are consistent with the concept that mTORC1 is required for increase in glucagon secretion during fasting and hypoglycemia. Interestingly, suppression of glucagon secretion in the fed states appears to not be regulated by Insulin/Insulin Receptor/mTORC1 axis.

The current studies demonstrated that reduction of mTORC1 signaling decreases glucagon secretion during fasting and hypoglycemia. The finding that mTORC1 activity is important for proper potentiation of glucagon secretion during fasting is

counterintuitive, as this complex is mostly inactive during starvation. However, it is possible that the physiological increase in circulating amino acids during fasting could provide stimulatory signals to induce mTORC1 in α-cells. To this end, we have observed that mTORC1 activity is increased in α-cells during hypoglycemia but is inactive in the fed state. Therefore, our observations are consistent with a model in which mTORC1 is active and essential for nutrient-induced glucagon secretion in α-cells in the fasting conditions. The similar glucagon secretory responses to KCl treatment in controls and αRaptor^{HET} islets suggested that the secretory defect occurred prior to cell depolarization (Shiota et al., 2005). In contrast, glucagon responses to arginine or tolbutamide were impaired in αRaptor^{HET}. While tolbutamide and arginine should also depolarize the α-cell, KCl likely provided a much stronger depolarization that supports the sustained activation of L-type Ca^{2+} channels, as opposed to the P/Q-type channels that appear to control glucagon secretion under more physiologic conditions (Rorsman et al., 2014; Zhang et al., 2013). Based on these findings, together with impaired responses to low glucose observed *in vivo,* we hypothesized that the mechanistic defect in the glucagon secretory pathways in αRaptor^{HET} lied at the level of the K_{ATP} channel. Therefore, we assessed glucagon secretion to pharmacologic agents that open or close K_{ATP} channels in a dose-response manner as described (MacDonald et al., 2007). The dose-response alterations to diazoxide and tolbutamide, K_{ATP} channel activity modulators, are consistent with reduced K_{ATP} channels and currents in αRaptor^{HET} α-cells. Titration of K_{ATP} channel activity can enhance action potential firing to the point at which voltage-gated Na^+, Ca^{2+}, and K^+ channels undergo voltage-dependent inactivation (Gopel et al., 2000; Ramracheya et al., 2010; Spigelman et al., 2010) and thus suppress glucagon secretion (as seen with 100 mM tolbutamide in the controls). The lower density of K_{ATP} currents in the αRaptor^{HET} α-cells is therefore consistent with the suppressive effect of tolbutamide on glucagon secretion occurring at lower concentrations, and the lack of effect of diazoxide. The reduction in K_{ATP} channel activity results from reduction of *KIR6.2* and *SUR1* expression in αRaptor^{HET} mice, indicating that mTORC1 signaling controls gene expression of K_{ATP} channel components. These *ex vivo* data were complimented by studies showing that single α-cell expression analysis in αRaptor^{KO} and mTORC1 signaling inhibition by rapamycin in αTC-1 leads to

decreased mRNA and protein expression of K_{ATP} channel subunits, SUR1 and KIR6.2. In addition, expression of several genes involved in secretory machinery were reduced in αRaptor^{KO} mice, identifying novel targets that could be regulated by mTORC1 (*SNAP25*, *CHRM3*, *CACNA1S*) and suggesting that additional mechanisms could also be involved. Taken together, these results uncovered a previously unknown function of mTORC1 signaling on controlling fasting-induced glucagon secretion by modulating expression of K_{ATP} channel subunit expression and K_{ATP} channel activity.

Our data showed that inhibiting mTORC1 signaling in αRaptor^{KO} mice and by rapamycin administration *in vivo* leads to decreased glucagon content and glucagon secretion. Single-cell gene expression analysis further showed that the decreased glucagon content resulted from reduced glucagon (*Gcg*) gene expression in αRaptor^{KO} and key transcription factors important for α-cell development, maintenance and glucagon synthesis including *FoxA2*, *Neoreg3*, *Gata4*, *MafB*, *Pou3f4*, and *Nkx2.2* (Artner et al., 2006; Mastracci et al., 2011; Ritz-Laser et al., 2005; Wang et al., 2009). The changes on *FoxA2* were particularly interesting, as this transcription factor has been shown to play a major role in regulating *Gcg*, *SUR1* and *KIR6.2* expression (Heddad Masson et al., 2014; Lantz et al., 2004; Lee et al., 2005; Philippe et al., 1994; Wang et al., 2002). FoxA2 protein levels and nuclear FoxA2 levels were also significantly reduced in α-cells from young αRaptor^{KO} mice. These data describe a novel link between mTORC1 and *FoxA2* gene transcription and provide evidence for the mechanisms responsible for alteration in *Gcg*, *SUR1* and *KIR6.2* expression in αRaptor^{KO} mice. Decreased *Gcg, MafB*, *Pou3f4*, *Nkx2.2, SUR1* and *KIR6.2* also support the decrease in *FoxA2*-dependent transcription, as FoxA2 directly promotes transcription of these genes (Heddad Masson et al., 2014). Overall, our data identified an mTORC1/FoxA2/K_{ATP} axis as a critical component linking nutrient signaling to α-cell function and glucagon synthesis.

In summary, dysregulation of glucagon secretion plays a major pathogenic role in the development of hyperglycemia in T2D and failure to secrete glucagon in T1D or advanced T2D patients results in recurrent hypoglycemia. These studies provide novel

insights into the molecular mechanisms and signaling pathways regulating glucagon secretion and α-cell mass. Our findings identify mTORC1 as a major signaling pathway controlling glucagon secretion under states of low glucose and identify a novel mechanistic link between mTORC1/FoxA2 on transcriptional regulation of K_{ATP} channel subunits and glucagon. These alterations were recapitulated by treatment with the immunosuppressant rapamycin, a known mTORC1 inhibitor used in the clinic. The findings obtained by rapamycin treatment could have major clinical implications in responses to hypoglycemia in post-transplant diabetics and perhaps explain the defects in counterregulation to hypoglycemia in patients after islet transplantation under chronic immunosuppression by rapamycin analogs (Paty et al., 2002; Rickels et al., 2007).

CHAPTER 3

Deletion of Tuberous Sclerosis Complex 2 (TSC2) in alpha cells results in hyperglucagonemia and alpha cell hypertrophy in the absence of diabetes

Introduction

Type 2 Diabetes (T2D) is characterized by defective adaptation of β-cells to insulin resistance. Most of the research effort has focused on elucidating the physiological, molecular, and genetic components that regulate β-cell mass and insulin secretion, presenting diabetes as a unihormonal disorder. Contrary to this current approach, clinical data and animal experiments have shown that increased α-cell mass and glucagon secretion play a role in the pathogenesis of hyperglycemia in diabetes (Dinneen et al., 1995; Mezza et al., 2014; Orci et al., 1976; Rahier et al., 1983; Sherwin et al., 1976; Yoon et al., 2003).

Increase in glucagon levels in T1D and T2D patients can be explained in part by increase in α-cell mass (Orci et al., 1976; Rahier et al., 1983; Yoon et al., 2003). Although the mechanisms leading to the increase in α-cell mass and glucagon levels in diabetic patients are not fully understood, several hypotheses have been developed based on animal models. Mice fed with high protein diet or high fat diet develop α-cell hyperplasia and hypertrophy suggesting that nutrient environment and/or insulin resistance could regulate α-cell mass (Ellingsgaard et al., 2008; Morley et al., 1982). In addition to the changes in α-cell mass, prolonged hyperinsulinemia in early stages of T2D could also induce α-cell insulin-resistance with loss of suppression of glucagon release by insulin (Liu et al., 2011). Studies using liver-specific glucagon receptor knock

out mice suggest that a circulating hepatic factor(s) can increase α-cell proliferation independent of direct pancreatic input (Gromada et al., 2007; Longuet et al., 2013). The metabolomics profile in the glucagon receptor knock out mice showed significant increase of circulating amino acids that could be responsible for the increase in α-cell mass observed in this mouse model (Yang et al., 2011). These studies support the concept that changes in α-cell mass are regulated by extracellular signals including nutrients (amino acids, glucose) and growth factors (insulin) but the intrinsic molecular mechanisms are largely unclear.

Previous data from our lab showed that mTORC1 signaling maintains the α-cell mass and potentiates glucagon secretion during fasting in a K_{ATP} channel-dependent manner. We also showed that complete ablation of β-cells and insulin levels by Streptozotocin (STZ) results in significant increase in α-cell mass and glucagon levels in control mice. The increase in α-cell mass was associated with increased mTORC1/phospho S6 signaling in α-cells of control mice treated with STZ. In the present studies, we tested the hypothesis that a gain in mTORC1 activity potentiates α-cell mass expansion and glucagon secretion as observed in diabetic patients. To test this hypothesis, we increased mTORC1 activity in α-cells by conditional deletion of *TSC2*, a negative mTORC1 regulator, in α-cells ($\alpha TSC2^{KO}$). Our findings showed that $\alpha TSC2^{KO}$ mice exhibited severe hyperglucagonemia as a result of increased α-cell mass. Despite hyperglucagonemia, these mice had normal fed blood glucose levels, but upon fasting their blood glucose was decreased in comparison to controls. Further, $\alpha TSC2^{KO}$ mice had improved glucose tolerance, attributed to decreased hepatic glucose production. Surprisingly, β-cell destruction after Streptozotocin (STZ) treatment showed that these mice exhibited further increase in glucagon levels, but had lower blood glucose levels compared to the hyperglycemic STZ-treated controls. These studies demonstrated that activation of mTORC1 signaling in α-cells is sufficient to induce α-cell mass expansion and hyperglucagonemia and presents a molecular mechanism for increased glucagon levels and α-cell mass in diabetic patients.

Results

Mice with gain of mTORC1 signaling in α-cells have fasting hypoglycemia despite severe hyperglucagonemia

Alpha cell-specific deletion of *TSC2* was achieved by crossing Glucagon-Cre and $TSC2^{flox/flox}$ mice ($\alpha TSC2^{KO}$) (Hernandez et al., 2007; Shiota et al., 2013). Phospho-S6 (Serine240) staining showed that mTORC1 activity was lost in control glucagon-positive cells incubated in Krebs Buffer supplemented with 2 mM glucose for 2 hours. Unlike control cells, phospho-S6 (Serine240) was preserved in the glucagon-positive cells from 2 month-old $\alpha TSC2^{KO}$ mice, despite lack of complete media (Figure 15A). $\alpha TSC2^{KO}$ had decreased body weight from 1-month of age, which persisted until 3 months (Figure 15B). The decrease in body weight was attributed to increased locomotor activity and no changes in food intake of $\alpha TSC2^{KO}$ compared to control mice at 2 months of age (Figure 16A,B). In addition, *Cre*-recombination was detected in brainstem and hypothalamic regions (dorsomedial hypothalamic nucleus, DMH), which could contribute to changes in feeding and activity levels of these mice (Figure 2C). Although $\alpha TSC2^{KO}$ had a tendency of lower random blood glucose, they were hypoglycemic after a 12-hour fasting (Figure 15C,D). Fed and fasting glucagon measurements revealed that $\alpha TSC2^{KO}$ mice have severe hyperglucagonemia (Figure 15E,F). Insulin levels were slightly lower in $\alpha TSC2^{KO}$ mice compared to controls, reflecting potential compensatory decrease in insulin to the lower blood glucose levels of these mice (Figure 15G). Insulin levels after a 12-hour fast were undetectable in all groups. Fed and fasting active GLP-1 levels were not different between $\alpha TSC2^{KO}$ and control mice, suggesting that increased glucagon levels detected in $\alpha TSC2^{KO}$ are not due to aberrant proglucagon processing (Figure 15H,I).

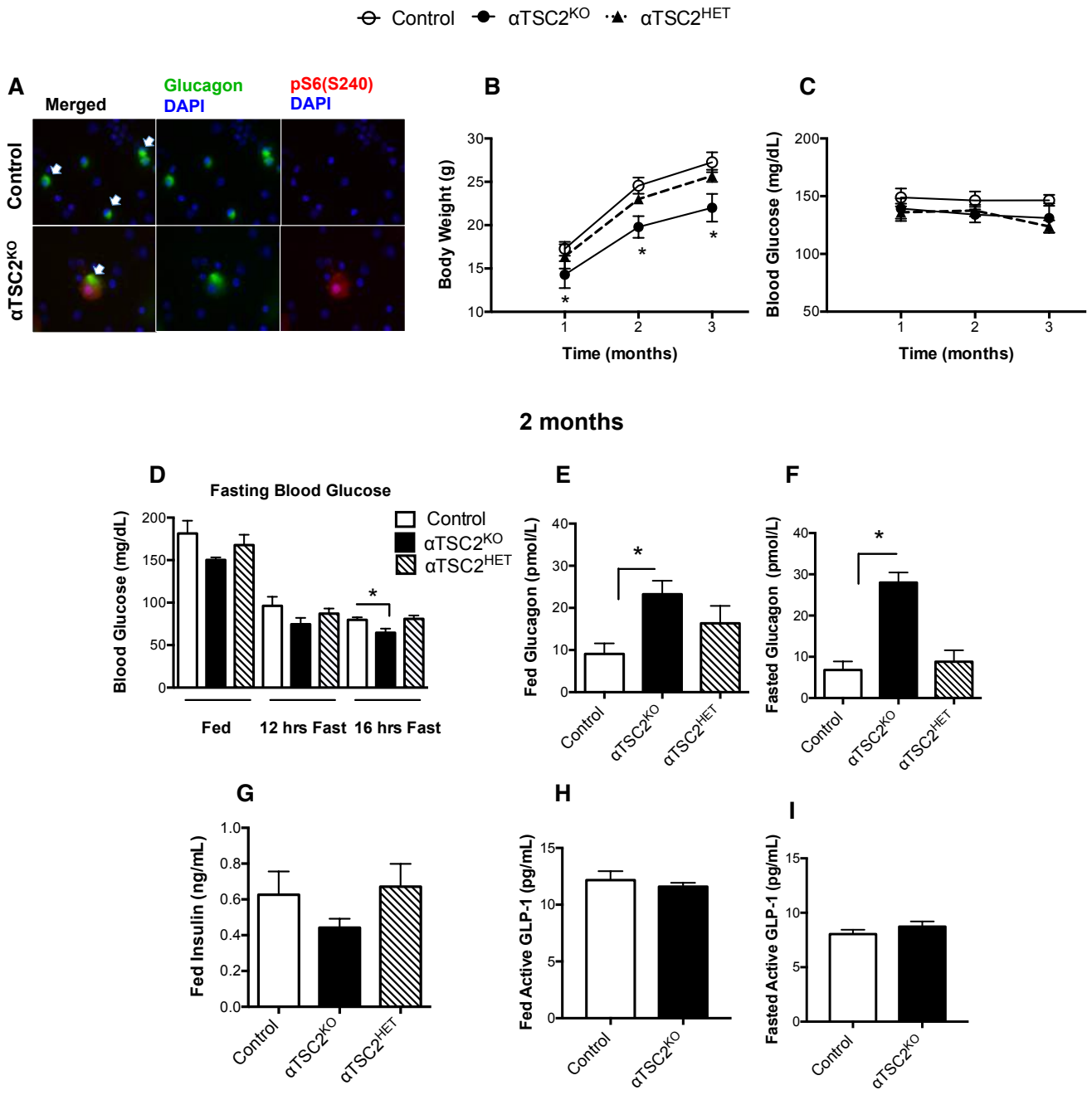

Figure 15. Mice with gain of mTORC1 signaling in α-cells have increased fed and fasting glucagon levels. **A.** Immunofluorescent staining showing lack of positive mTORC1 activity (shown by phospho-S6 S240) stain in the control and the sustained mTORC1 activity in glucagon positive-cells of the αTSC2^{KO} mice in dispersed islets incubated in 2 mM Glucose KRBB for 2 hours. **B.** Body weight and **C.** Random-fed blood glucose of control, αRaptor^{KO} and αRaptor^{HET} mice (n=4-8). **D.** Fasting blood glucose (n=3-7). **E.** Fed glucagon (n=5-7) and **F.** Fasted glucagon levels (n=3-6). **G.** Fed insulin levels (n=4-5). **H.** Fed active GLP-1 (n=4) and **I.** Fasted active GLP-1 levels (n=3-4). Data are shown as means ± S.E.M. *p≤0.05; Nonparametric *U* test (Mann Whitney)

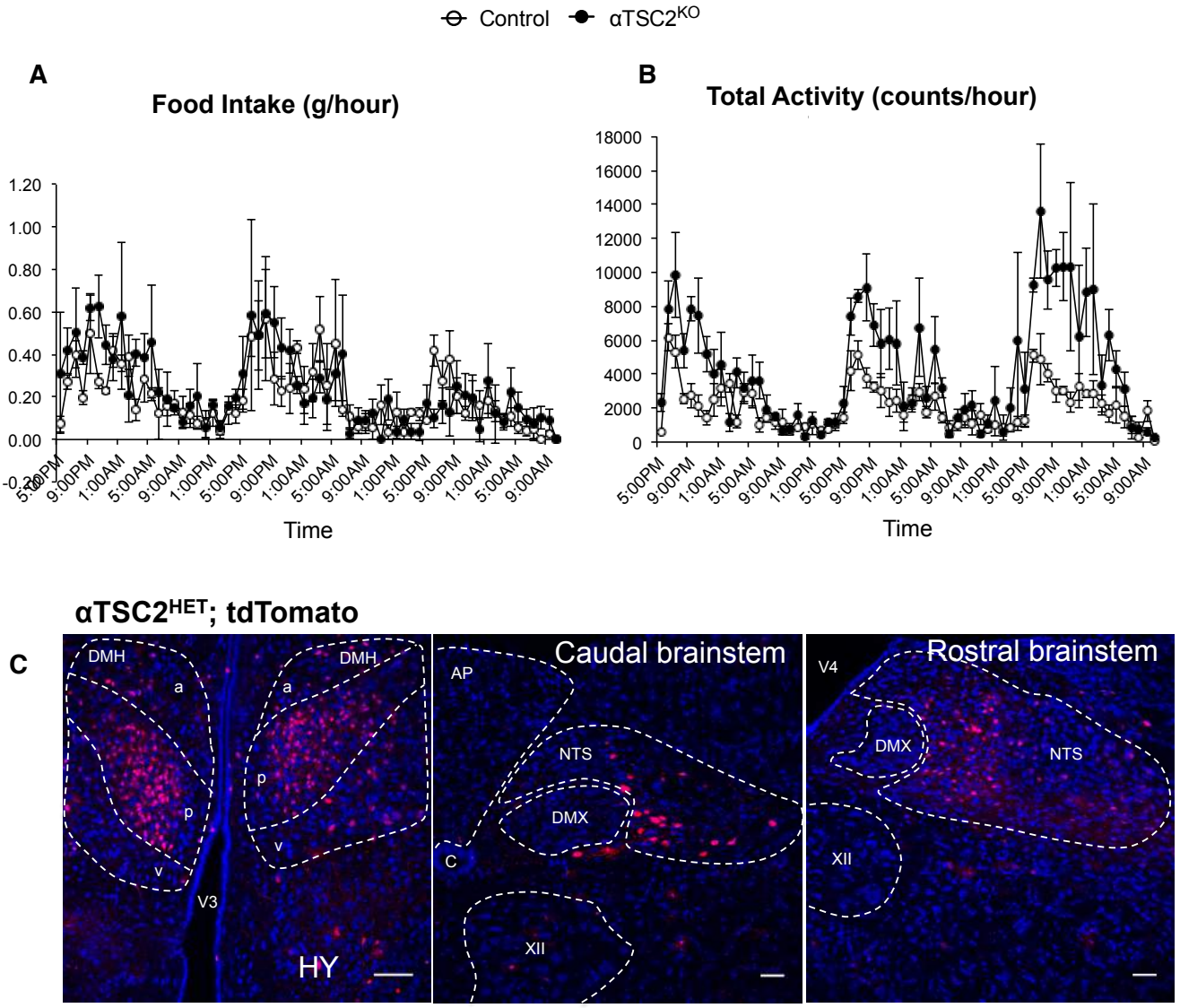

HY – Hypothalamus
DMH – Dorsomedial Nucleus of Hypothalamus (a-anterior, p-posterior, v-ventral)
V3 – Third Ventricle
AP – Area Postrema
NTS – Nucleus of the Solitary Tract
C – Central Canal
DMX – Dorsal Motor Nucleus of Vagus
XII – Hypoglossal Nucleus
V4 – Fourth Ventricle

Figure 16. αTSC2^{KO} mice have lower body weight associated with increase in activity levels. A. Food intake (grams/hour) for 3 days in 2-month old male control and αTSC2^{KO} mice (n=3). **B.** Locomotor activity levels (counts/hour) in for 3 days in 2-month old male control and αTSC2^{KO} mice (n=3). **C.** Immunofluorescent staining showing *Cre*-expressing neurons by positive tdTomato (*Cre*-expression) and Nissl (neuron) stain in αTSC2^{HET} mice (scale 50 μm).

Gain in mTORC1 signaling in α-cells results in α-cell hypertrophy and hyperplasia

Morphometric analysis at postnatal day 1 demonstrated that αTSC2^{KO} mice were born with normal α-cell mass (Figure 17A), reflecting previous data from our lab that mTORC1 signaling is dispensable for α-cell development. Morphologic evaluation by electron microscopy in 1 month-old αTSC2^{KO} showed an increase in α-cell size that was confirmed by cell size measurements at 2 months of age (Figure 17B,F). In addition, the number of glucagon granules appeared to be largely increased and this was confirmed by the increase in total pancreatic glucagon content at 2 months (Figure 17E). αTSC2^{KO} mice also showed an increase in α-cell mass and proliferation, with no changes in apoptosis at 2 months (Figure 17D,G, H). In contrast, β-cell mass at 2 months was not altered in αTSC2^{KO} mice compared to controls (Figure 17I). The pancreas weight normalized to body weight was reduced in αTSC2^{KO} mice compared to controls (Figure 17J). Overall, our data show that gain of mTORC1 signaling in α-cells results in increased α-cell mass, size and proliferation contributing to increased pancreatic glucagon content and severe fed and fasting hyperglucagonemia.

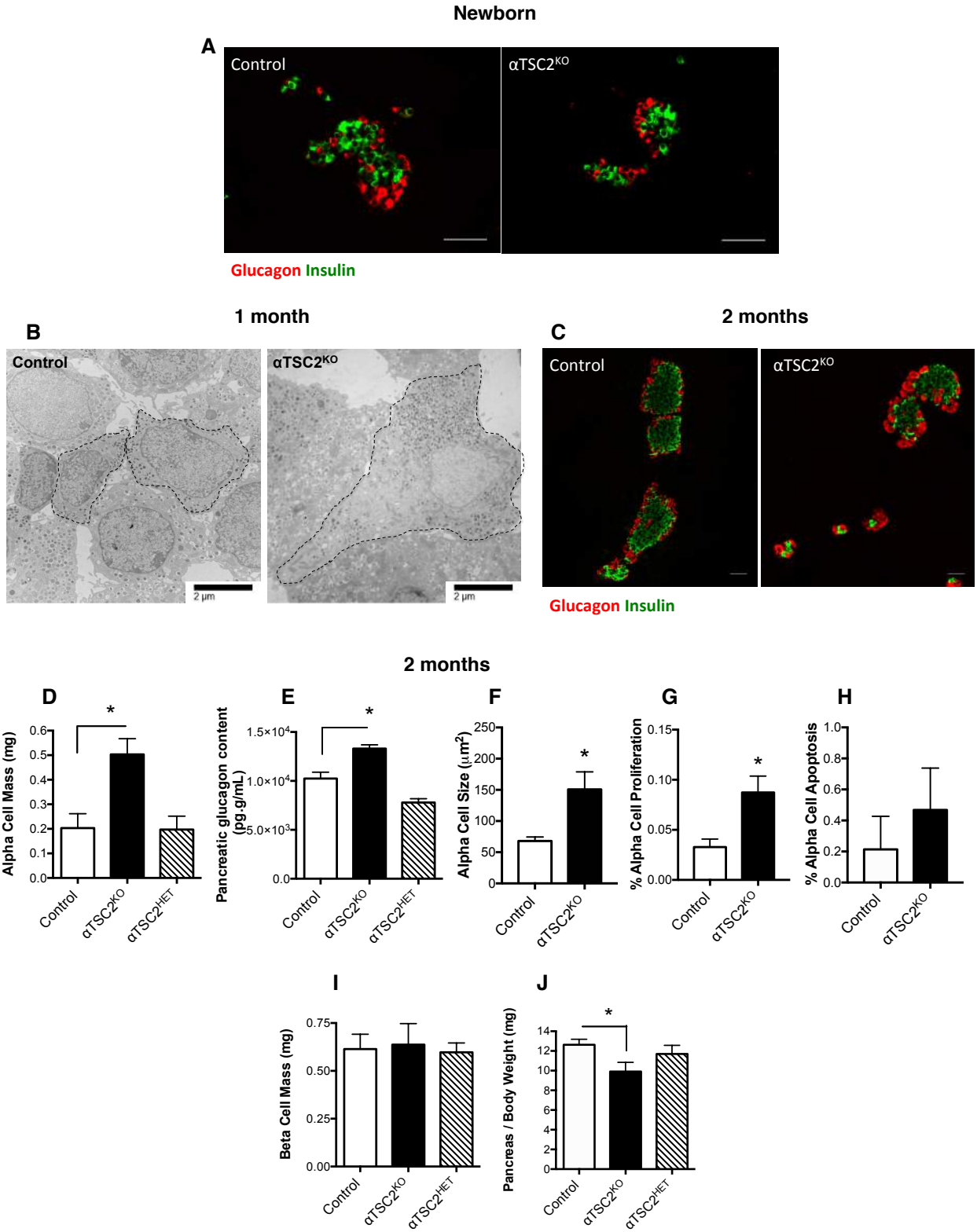
Newborn
A
Control
αTSC2KO
Glucagon Insulin
1 month
B
Control
αTSC2KO
2 µm
2 µm
2 months
C
Control
αTSC2KO
Glucagon Insulin
2 months
D
Alpha Cell Mass (mg)
Control
αTSC2KO
αTSC2HET
E
Pancreatic glucagon content (pg.g/mL)
Control
αTSC2KO
αTSC2HET
F
Alpha Cell Size (µm2)
Control
αTSC2KO
G
% Alpha Cell Proliferation
Control
αTSC2KO
H
% Alpha Cell Apoptosis
Control
αTSC2KO
I
Beta Cell Mass (mg)
Control
αTSC2KO
αTSC2HET
J
Pancreas / Body Weight (mg)
Control
αTSC2KO
αTSC2HET

Figure 17. Gain in mTORC1 signaling in α-cells results in α-cell hypertrophy and hyperplasia. A. Immunofluorescent images of glucagon (red) and insulin (green) in pancreas at postnatal day 1 (scale 50 μm). **B.** Electron microscopy images from 1 month-old control and αTSC2^{KO} mice. **C**. Immunofluorescent images of glucagon (red) and insulin (green) at 2 months (scale 50 μm). **D.** Quantification of α-cell mass at 2 months (n=3-4). **E.** Pancreatic glucagon content at 2 months (n=4). **F.** Quantification of α-cell size (n=4) and **G.** Proliferation by positive ki67 and glucagon co-stain (n=3) and **H.** Apoptosis by positive TUNEL and glucagon co-stain (n=4) in 2 month-old mice. **I.** Quantification of β-cell mass in 2 month-old mice (n=3-4). **J.** Pancreas weight in 2 month-old mice (n=7-10). Data are shown as means ± S.E.M. *p≤0.05; Nonparametric *U* test (Mann Whitney).

αTSC2^{KO} mice have reduced glycemic counterregulation to hypoglycemia despite hyperglucagonemia

To further investigate the role of gain in mTORC1 signaling on glucagon secretion, we subjected these mice to hypoglycemia by administration of insulin. Examination of the glycemic response by insulin-induced hypoglycemia in 2 month-old mice showed that hypoglycemia by exogenous insulin administration induced similar decreases in blood glucose in control and αTSC2^{KO} mice at 30 minutes (Figure 18A). However, αTSC2^{KO} mice had sustained low blood glucose at 120 minutes, suggesting that the compensatory counterregulation of blood glucose to hypoglycemia was compromised in these mice (Figure 18A). Glucagon secretion after insulin-induced hypoglycemia was increased in all mice; however αTSC2^{KO} mice maintained hyperglucagonemia before and after insulin-induced hypoglycemia (Figure 18B).

In vivo data showed that αTSC2^{KO} mice are severely hyperglucagonemic in the fed and fasting state. To uncover the mechanisms responsible, we examined the secretory responses of isolated islets to inhibitory and stimulatory secretagogues. Pancreatic α-cells are exposed to high levels of intra-islet insulin secreted from the β-cells and insulin is a potent inhibitor of glucagon secretion and glucagon gene transcription (Asplin et al., 1981; Maruyama et al., 1984; Philippe, 1989; Weir et al., 1976; Zhang et al., 2012). We measured the effect of exogenous insulin in suppressing glucagon secretion. Administration of insulin decreased glucagon secretion in control, but had no effect in suppressing glucagon in αTSC2^{KO} islets (Figure 18C). Next, we examined the glucagon

response to depolarization induced by a strongly depolarizing concentration of potassium chloride (KCl; 30 mM). Glucagon secretion was increased in αRaptor^{KO} compared to control islets in response to KCl (Figure 18C). Our data showed that the α-cells of αTSC2^{KO} are resistant to insulin-dependent regulation of glucagon secretion, and they are more sensitive to cell depolarization, culminating in increased glucagon levels.

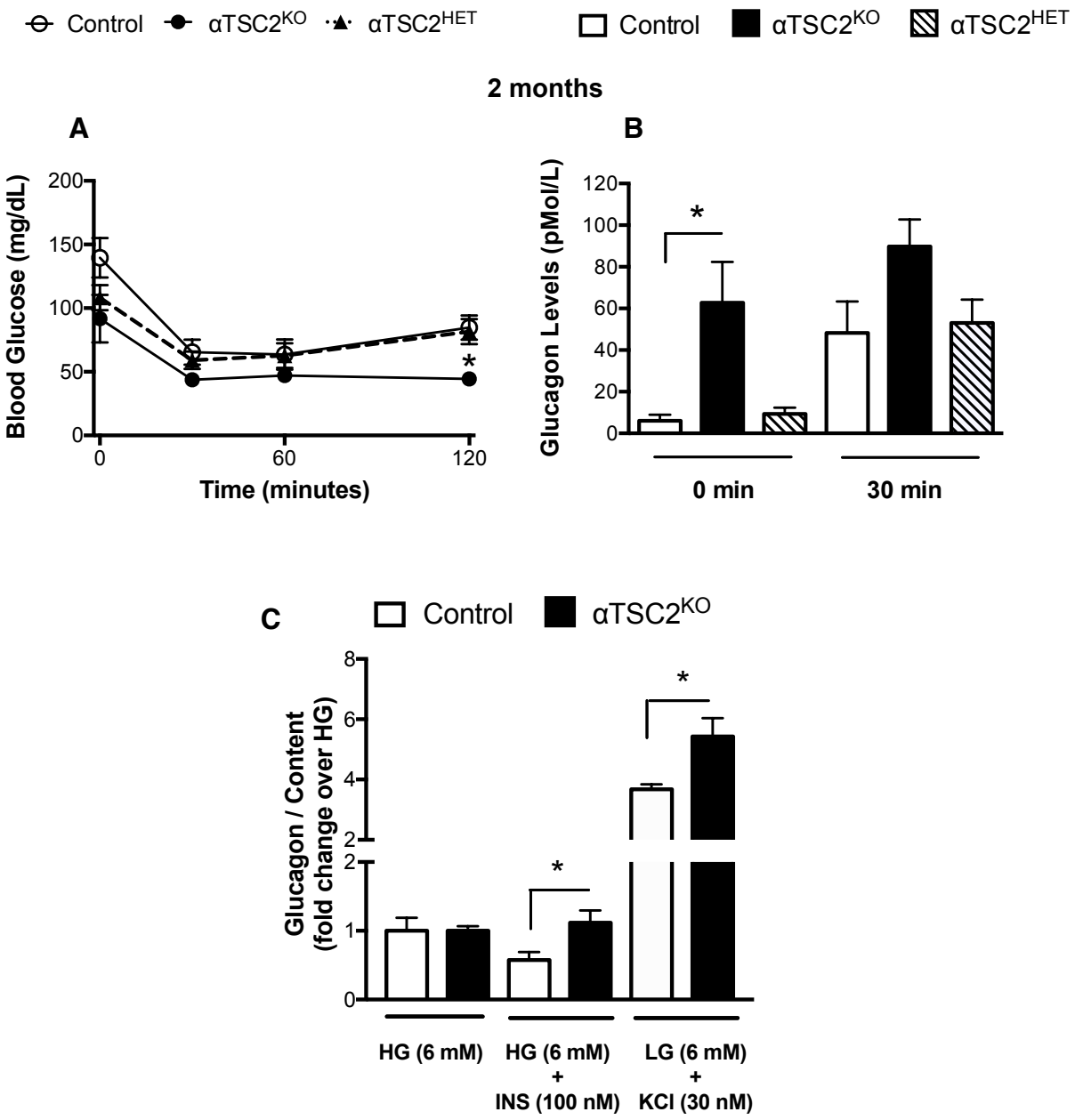

Figure 18. αTSC2^{KO} mice have reduced blood glucose counterregulation in response to hypoglycemia. A. Blood glucose response and **B.** Glucagon response to Insulin Tolerance Test, ITT (0.75 U/kg.bw) at 2 months (n=4-6). **C.** Glucagon response from isolated islets to exogenous insulin (100nM) and KCl (30nM) (HG=6 mM Glucose; LG=1 mM Glucose; n=3-8 mice). Data are shown as means ± S.E.M. *p≤0.05; Nonparametric *U* test (Mann Whitney).

αTSC2^{KO} mice have improved glucose tolerance and decreased gluconeogenesis

Intraperitoneal glucose-tolerance test revealed that αTSC2^{KO} mice have improved glucose clearance at 2 months (Figure 19A). This was accompanied by decreased pyruvate tolerance and hepatic glucose production. These data suggested that αTSC2^{KO} mice have improved glycemic tolerance associated with decreased gluconeogenesis (Figure 19B).

Fed liver glycogen content was not different between αTSC2^{KO} and control mice (Figure 19C). RNA expression of the glucagon receptor (*GCGR*), phosphoenolpyruvate carboxykinase (*PEPCK*) and glucokinase (*Gck*) were decreased in fed liver of αTSC2^{KO} mice compared to controls (Figure 19D,E,G). No changes were observed in the RNA expression of glucose 6-phosphatase (*G6Pase*) and fatty acid synthase (*FAS*) in fed liver (Figure 19F,H). The fasting-induced increase in non-esterified free fatty acids (NEFA) was observed in αTSC2^{KO}, αTSC2^{HET} and control mice; however, αTSC2^{KO} mice had lower fed and slightly lower fasting levels of free fatty acids compared to the controls (Figure 19I). We measured the insulin sensitivity of the liver by administration of insulin *in vivo* (1 Unit/kg). Control and αTSC2^{KO} mice responded similarly to exogenous insulin by a robust increase in AKT (phosphor-Ser473) activation, suggesting that hepatic insulin sensitivity was not increased in αTSC2^{KO} (Figure 19 J).

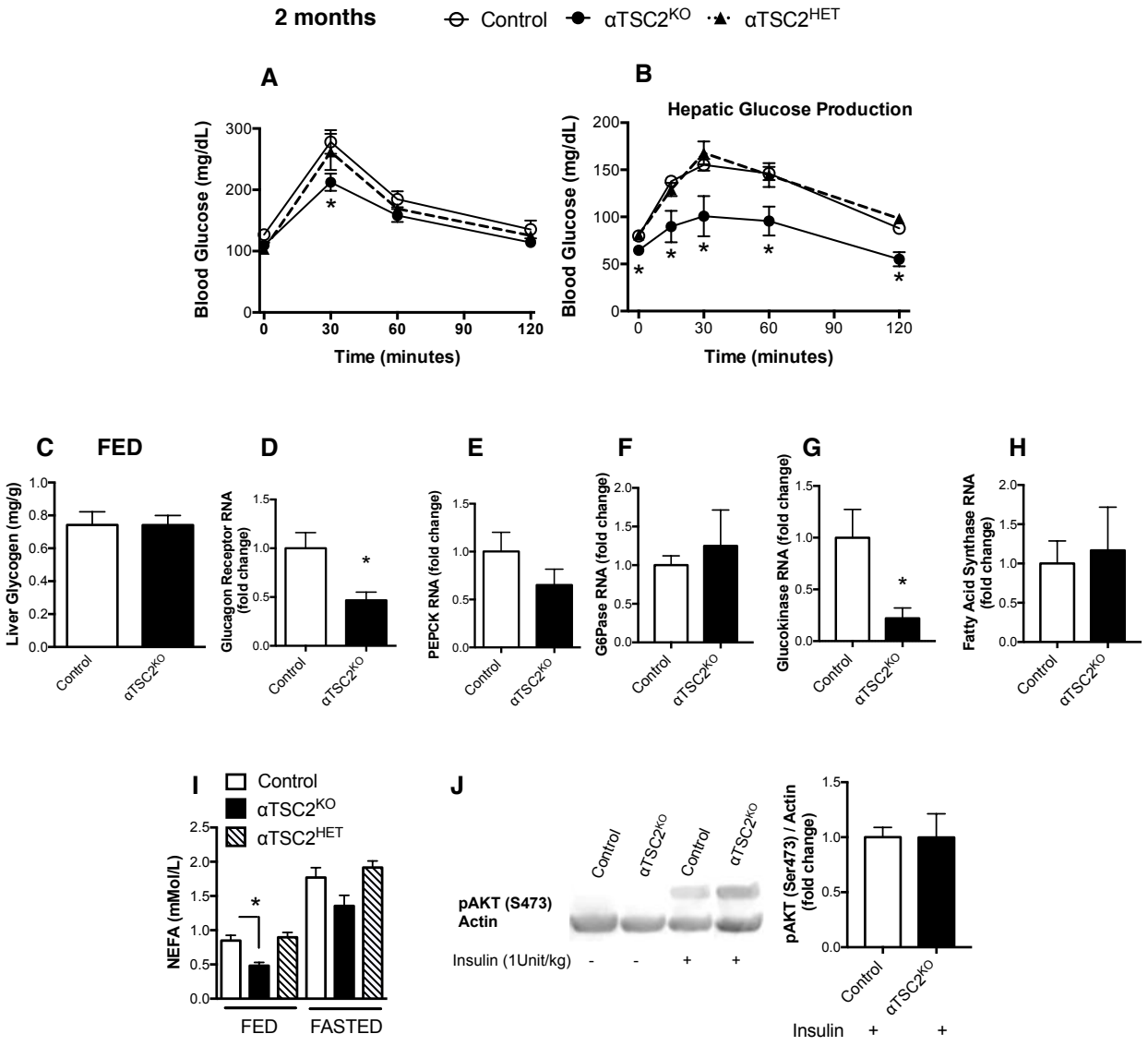

Figure 19. αTSC2^{KO} mice have improved glucose tolerance and decreased gluconeogenesis. A. Glucose tolerance test (2g/kg.bw) in 2-month old mice (n=5-8). **B.** Pyruvate tolerance test (2 g/kg) in 2-months old mice (n=3-6). **C.** Fed liver glycogen content (n=6-8). Fed liver mRNA levels of **D.** Glucagon Receptor, **E.** PEPCK, **F.** G6Pase, **G.** Glucokinase, **H.** Fatty acid synthase (n=5-8). **I.** Fed and fasting NEFA levels at 2 months (n=3-6). **J.** Western blot and quantification showing hepatic insulin sensitivity measured by phospho-AKT (S473) after insulin administration *in vivo* (1 Unit/kg). Data are shown as means ± S.E.M. *p≤0.05; Nonparametric *U* test (Mann Whitney).

Hyperglycemia after STZ-induced diabetes is reduced in αTSC2^{KO} mice

Previous findings have shown that mTORC1 signaling is enhanced in α-cells from control mice treated with Streptozotocin (STZ) (Figure 11A) and therefore we wanted to evaluate if gain in mTORC1 will recapitulate the effect of STZ in α-cell mass expansion and increased glucagon levels. Fed insulin levels were not detectable after a week of a single, high-dose STZ injection (150 mg/kg) and β-cell mass was nearly ablated (Figure 20E). All mice had a rapid increase in fed blood glucose levels, but αTSC2^{KO} mice maintained slightly lower blood glucose compared to controls (Figure 20A). Examination of glucagon levels after STZ showed an increase in glucagon levels of control mice (Figure 20B). αTSC2^{KO} mice remained hyperglucagonemic before and after STZ, although they presented a tendency of increased glucagon levels post-STZ (Figure 20B). Consistent with these findings, αTSC2^{KO} mice maintained higher α-cell mass, size and proliferation compared to controls (Figure 20D,F,G). Liver glycogen content was not different between control and αTSC2^{KO} mice and liver glycogen levels of control and αTSC2^{KO} mice were similarly decreased in response to STZ (Figures 19E and 20I). Hepatic mRNA expression of glucagon receptor (*GCGR*), *PEPCK*, *G6Pase*, glucokinase (*Gck*) and fatty acid synthase (*FAS*) showed a trend of increased expression in αTSC2^{KO} mice compared to controls after STZ (Figure 20 J-N).

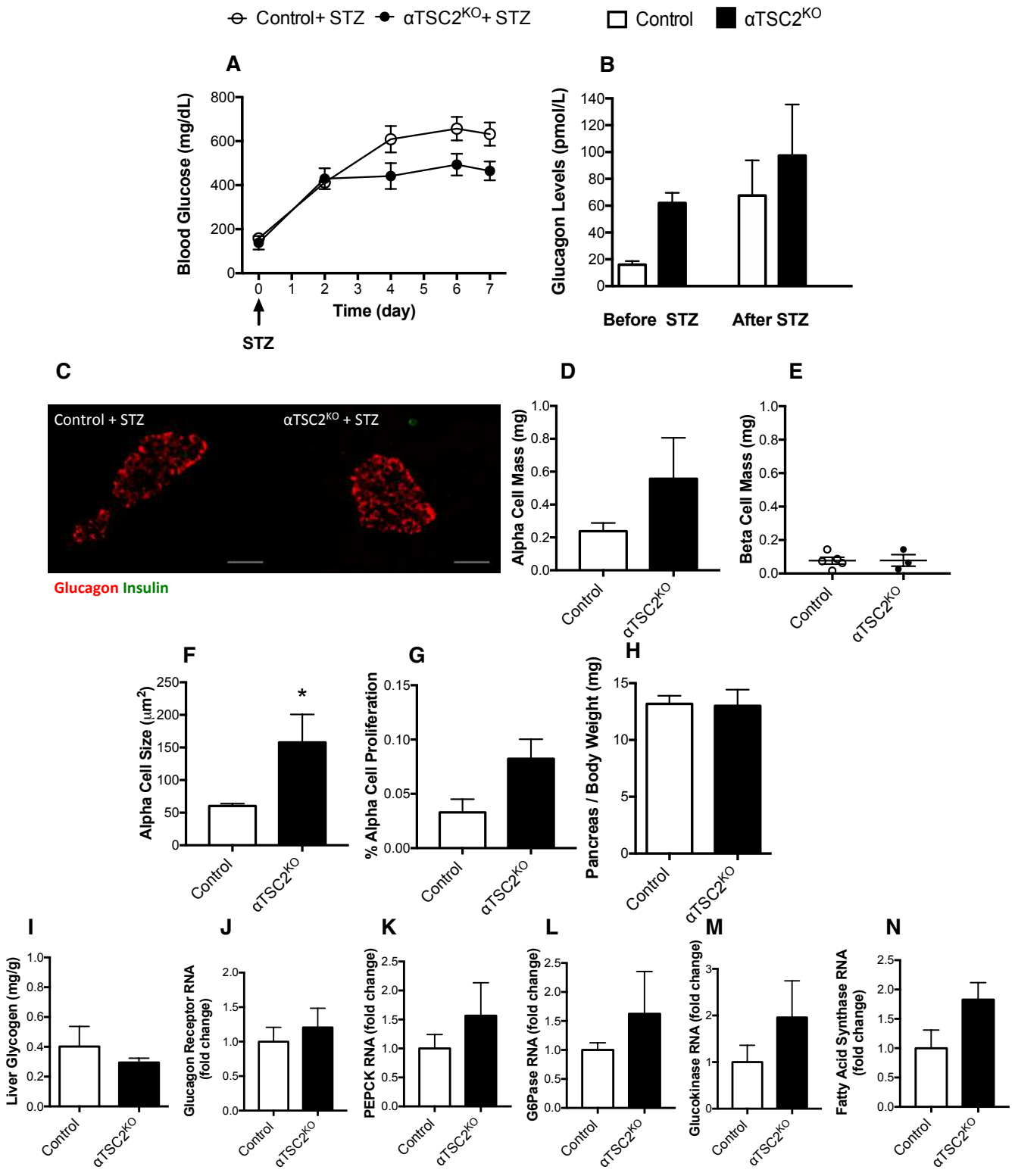

Figure 20. Hyperglycemia after STZ-induced diabetes is reduced in αTSC2^{KO} mice. A. Fed blood glucose from day 0 to day 7 after single IP dose of 150 mg/kg STZ (n=3-5). **B.** Circulating glucagon levels before and 7 after STZ (n=3-5). **C.** Imminofluorescent images representing insulin (green) and glucagon (red) in pancreas

sections from control and αTSC2^{KO} mice treated with STZ (scale 50 μm). **D.** α-cell and **E.** β-mass of mice after STZ (n=3-5). **F.** α-cell size and **G.** Proliferation after STZ (n=3-5). **H.** Pancreas weight of control and αTSC2^{KO} mice treated with STZ (n=3-5). **I.** Liver glycogen content (n=3-5). RNA levels of **J.** Glucagon receptor, **K.** PEPCK, **L.** G6Pase, **M.** Glucokinase, **N.** Fatty acid synthase (n=3-4). Data are shown as means ± S.E.M. *p≤0.05; Nonparametric *U* test (Mann Whitney).

Discussion

Glucagon plays a major role in maintaining glucose homeostasis by promoting glucose production *via* hepatic glycogenolysis and gluconeogenesis. Clinical data has shown that α-cell mass and glucagon levels are elevated in insulin-resistant/non-diabetic, T1D, and T2D patients, leading to enhanced hepatic glucose output and thereby exacerbating the diabetic hyperglycemic state (Dinneen et al., 1995; Mezza et al., 2014; Orci et al., 1976; Rahier et al., 1983; Sherwin et al., 1976; Yoon et al., 2003). The current studies provide new insights into the signaling mechanisms that play a role in potentiating the increase in glucagon secretion and α-cell mass observed in diabetic patients. Our studies were designed to test the hypothesis that gain in mTORC1 activity plays a role in α-cell mass expansion and glucagon secretion as observed in diabetic patients. To test this hypothesis, we increased mTORC1 activity in α-cells by conditional deletion of *TSC2*, a negative mTORC1 regulator (αTSC2^{KO}). Our findings showed that gain in mTORC1 signaling in α-cells of αTSC2^{KO} increased postnatal α-cell mass (hypertrophy and hyperplasia) and pancreatic glucagon content. Fed and fasting glucagon levels were greatly increased in αTSC2^{KO} mice compared to controls. Fed insulin levels were slightly lower in αTSC2^{KO} mice, which could be attributed to compensation in response to the lower blood glucose levels of these mice.

Body weight was significantly reduced in young αTSC2^{KO} mice and persisted through the lifespan of these mice. Recent studies have shown that glucagon increases energy expenditure in humans, similarly to that of cold-activation, but independent of brown adipose fat (Salem et al., 2016). Food intake and locomotor activity measurements revealed that αTSC2^{KO} mice had increased activity compared to controls. However, no changes were detected in food intake. The central nervous system integrates nutrient

signals to the regulation of energy balance by the mediobasal hypothalamus. Studies have shown that mTORC1 activation in the caudomedial nucleus of solitary tract (NTS) in the brainstem decreases food intake and body weight (Blouet et al., 2009; Blouet et al., 2008; Blouet and Schwartz, 2012). Assessment of *Cre*-recombination in CNS revealed that *Cre*-expressing neurons are present in the brainstem and dorsomedial hypothalamic nucleus (DMH), which could contribute to changes in feeding and activity levels. However, increased plasma levels of glucagon could be directly acting in the CNS to decrease body weight in αTSC2^{KO} mice. Importantly, recent study has shown that chronic glucagon receptor signaling agonism is coupled with increased locomotor activity, in agreement with our data showing increased activity levels of αTSC2^{KO} mice (Habegger et al., 2013).

Increased glucagon levels increase gluconeogenesis and glycogenolysis in control mice; however, αTSC2^{KO} mice were hyperglucagonemic, but had reduced fasting blood glucose levels. These data were puzzling and therefore, we examined whether the increased glucagon levels detected in αTSC2^{KO} mice were result of abnormal proglucagon processing. Glucagon is processed from proglucagon in pancreatic α-cells by prohormone convertase (PC2). Mice lacking expression of *PC2* have reduced fasting blood glucose, α-cell hyperplasia and hypertrophy and increased glucose tolerance, all of which we observed in αTSC2^{KO} mice (Blouet and Schwartz, 2012). As a result of abnormal proglucagon processing, GLP-1 levels were also increased in PC2 knock out mice (Blouet and Schwartz, 2012). However, we did not detect any changes in fed or fasting active GLP-1 levels between αTSC2^{KO} and control mice, suggesting lack of abnormal proglucagon processing. Further analysis of PC2 mRNA and protein expression in α-cells from αTSC2^{KO} and control mice is needed to fully exclude the role of abnormal proglucagon processing as result of increased mTORC1 signaling in α-cells.

Despite hyperglucagonemia, αTSC2^{KO} mice had normal fed blood glucose levels, but upon fasting their blood glucose was decreased in comparison to controls. These mice also lacked counter-regulatory increase in blood glucose levels after severe

hypoglycemia. Further, αTSC2^{KO} mice had improved glucose tolerance, attributed to decreased gluconeogenesis and hepatic glucose production. Ample evidence has shown that inhibiting glucagon signaling results in hypoglycemia. Administration of glucagon-neutralizing antibodies and the genetic ablation of the glucagon receptor *in vivo* result in mild hypoglycemia (Blouet et al., 2009; Blouet et al., 2008; LaPierre et al., 2015). Although fed liver glycogen content was not different, the expression analysis of genes involved in gluconeogenesis, glycolysis and fatty acid synthesis revealed that αTSC2^{KO} have reduced hepatic gluconeogenesis. RNA expression of the glucagon receptor in fed liver was reduced in αTSC2^{KO} compared to controls. Phosphoenolpyruvate carboxykinase (*PEPCK*) catalyzes a rate-limiting step in early gluconeogenesis and its mRNA expression is increased in response to glucagon signaling during fasting. Expression of *PEPCK* mRNA was slightly lower in the fed liver of αTSC2^{KO}. Glucokinase is suppressed by glucagon (as part of glucagon's inhibitory role in glycolysis) to decrease glucose entry into glycolysis. Glucokinase mRNA expression was reduced in αTSC2^{KO} mice in cohort with hyperglucagonemia in these mice and proper glucagon inhibition of glucokinase. In addition, lack of changes in *G6Pase* and fatty acid synthase expression suggests that hyperglucagonemia in αTSC2^{KO} mice does not impact glycogenolysis and fatty acid synthesis (Longuet et al., 2008). This is in cohort with data showing that glucagon signaling plays an essential role in fatty acid oxidation, but does not regulate the expression of genes involved in fatty acid synthesis. Free fatty acids rise during fasting as result from hydrolysis of triglycerides within the adipocyte (Karpe et al., 2011) and exogenous administration of glucagon decreases the plasma levels of triglycerides and free fatty acids (Longuet et al., 2008). Fed free fatty acid levels were lower in αTSC2^{KO}, and although they increased with fasting, they remained slightly lower in comparison with controls. In addition, our data suggest that the role of glucagon in inhibiting glucokinase and suppressing glycogenolysis and glucagon's suppression of plasma free fatty acid levels is preserved and consistent with increased levels of fed glucagon in αTSC2^{KO} mice. Hepatic insulin sensitivity was not increased in αTSC2^{KO} and therefore does not contribute to the observed improvement in glucose tolerance. Based on our data, we suggest that chronic hyperglucagonemia in αTSC2^{KO} mice leads to decrease in hepatic

glucagon signaling and gluconeogenesis, contributing to decreased fasting blood glucose and improved glucose tolerance.

Previous data from our lab showed that complete ablation of β-cells and insulin levels by Streptozotocin (STZ) administration results in significant increase in α-cell mass and glucagon levels and the development of severe hyperglycemia in control mice. The increase in α-cell mass was associated with increased mTORC1/phospho-S6 signaling in α-cells of control mice treated with STZ. Surprisingly, β-cell ablation after Streptozotocin (STZ) treatment of αTSC2^{KO} showed that these mice exhibited further increase in glucagon levels, but had lower blood glucose levels compared to the hyperglycemic STZ-treated controls. The mRNA expression levels of glucagon receptor and gene targets involved in gluconeogenesis (*GCGR*, *PEPCK*, *G6Pase*), glycolysis (glucokinase) and fatty acid synthesis (fatty acid synthase) had a trend of increased hepatic expression in αTSC2^{KO} mice compared to controls after STZ.

In summary, our findings showed that gain of mTORC1 signaling in α-cells results in increased α-cell mass (hyperplasia and hypertrophy) and hyperglucagonemia in αTSC2^{KO} mice. Despite hyperglucagonemia, these mice had normal fed blood glucose levels and reduced fasting blood glucose, improved glucose tolerance and decreased hepatic glucose production. Surprisingly, β-cell destruction after Streptozotocin (STZ) treatment showed that these mice exhibited further increase in glucagon levels, but have decreased blood glucose compared to the hyperglycemic STZ-treated controls. These studies demonstrated that activation of mTORC1 signaling in α-cells is sufficient to induce α-cell mass expansion and hyperglucagonemia. However, it remains unclear what downstream molecular mechanisms are responsible for the mTORC1-dependent increase in α-cell size and proliferation and increased glucagon content.

CHAPTER 4

Conclusions and Future Directions

The presented studies revealed a novel role of mTOR complex 1 (mTORC1) as a major regulator of α-cell mass and glucagon secretion. By ablating mTORC1 activity by generating mice deficient of *raptor* exclusively in the α-cell, we revealed that mTORC1 potentiates glucagon secretion in the fasting state by modulation of K_{ATP} channels and glucagon expression. A novel mTORC1/FoxA2 axis provided a link between mTORC1 and transcriptional regulation of key genes responsible for α-cell function (Figure 21). Furthermore, we also found that mTORC1 signaling promotes the maintenance of islet α-cells by an autophagy-mediated process (Figure 21). Streptozotocin-ablation of β-cells ablation revealed that α-cell mass expansion is associated with an increase in mTORC1 activity. In following studies we showed that increased mTORC1 activity in α-cells by deletion of *TSC2*, a negative mTORC1 regulator, resulted in severe hyperglucagonemia as a result of increased α-cell mass. Despite hyperglucagonemia, these mice had fasting hypoglycemia, improved glucose tolerance and decreased gluconeogenesis. However, the molecular mechanisms responsible for mTORC1-dependent increase in α-cell size and proliferation and increased glucagon content remain unclear.

The findings that decrease in mTORC1, as shown by $\alpha Raptor^{KO}$ mice, is important to promote glucagon secretion and plays a role in α-cells during fasting is counterintuitive, as this complex is mostly inactive during starvation. However, it is possible that the physiological increase in circulating amino acids during fasting could provide stimulatory signals to increase mTORC1 in α-cells and consequently, to increase glucagon

secretion. The amino acids glutamine, lysine, leucine, tyrosine and cysteine plasma concentrations increase in fasting and some of these amino acids, particularly glutamine, are potent stimulants for glucagon secretion (Daniel et al., 1977; Marroqui et al., 2014). To this end, we have observed that mTORC1 activity is increased in α-cells during hypoglycemia, but not mTORC1 activity is blunted in α-cells in the fed state. Future studies will evaluate the role of glutamine in mTORC1-dependent activation in α-cells during fasting conditions. Our conclusions are consistent with a model in which mTORC1 is active and essential for nutrient-induced glucagon secretion in α-cells during fasting. Therefore, mice with lack of mTORC1 signaling represent α-cells "stuck" in the fed state and therefore their response to fasting is blunted. Increasing mTORC1 signaling, as in αTSC2^{KO} mice, presents a model of α-cells "stuck" in the fasting state that have a consistent signal to increase glucagon secretion. We also hypothesize that the increase in α-cell mass in αTSC2^{KO} mice is secondary and in response to the increased demand of glucagon secretion due to a constitutively active mTORC1.

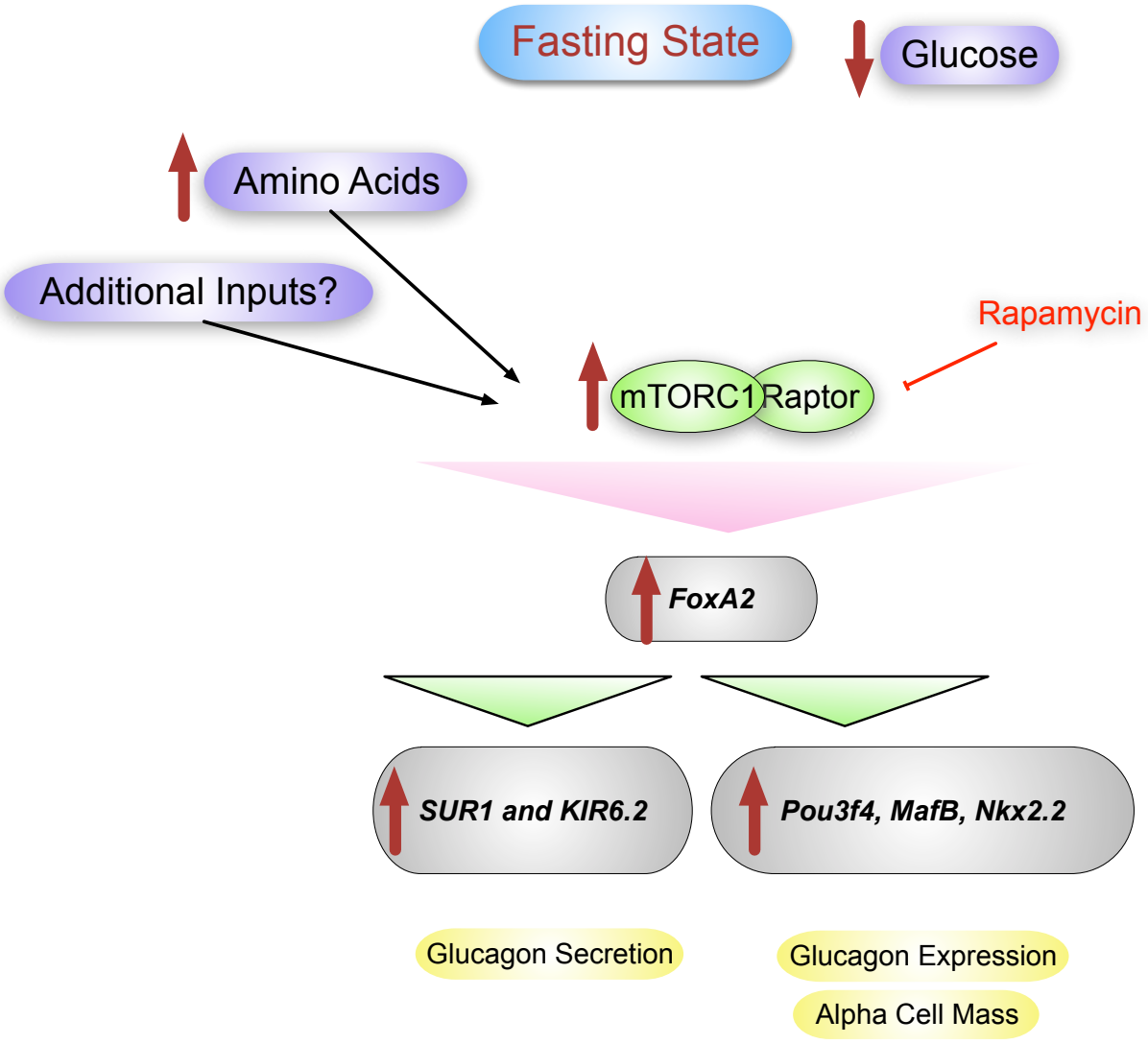

Figure 21. mTOR complex 1 (mTORC1) is a major regulator of α-cell mass and glucagon secretion. Using mice deficient of *raptor* exclusively in α-cells, we revealed that mTORC1 potentiates glucagon secretion in the fasting state by promoting K_{ATP} channels and glucagon expression. A novel mTORC1/FoxA2 axis provided a link between mTORC1 and transcriptional regulation of key genes responsible for α-cell function. Furthermore, we also found that mTORC1 signaling modulates the maintenance of islet α-cells by an autophagy-mediated process.

Chapter 2: Nutrient signaling maintains alpha cell mass and promotes K_{ATP} channel-dependent regulation of glucagon secretion

Despite very low circulating levels of glucagon and low α-cell mass, the αRaptor^{KO} mice had an increased circulating fed active GLP-1 levels. The β-cell mass of these animals were comparable to the controls at 2 months of age; however, by 8 months the β-cell mass was much higher in the αRaptor^{KO} compared to controls. In addition, the pancreas weight (particularly the exocrine pancreas weight) was increased in αRaptor^{KO} mice at 2 months of age. Studies have shown that GLP-1 increases β-cell mass and pancreas weight (Brubaker and Drucker, 2004; Kim et al., 2003; Rolin et al., 2002; Stoffers et al., 2000; Wang et al., 2004). Therefore, the increase in active GLP-1 levels could contribute to the increased pancreas weight at 2 months and increased β-cell mass in older αRaptor^{KO} mice. The presence of intra-islet GLP-1 has been proposed by recent studies (summarized in (Fava et al., 2016). The total pancreatic active GLP-1 content at 2 and 8 months was lower in αRaptor^{KO}, ruling out the possibility that the increased circulating active GLP-1 was of pancreatic origin and a result of abnormal proglucagon processing within the α-cell. However, this data supports that the majority of intra-islet GLP-1 comes from α-cells. We measured active GLP-1 levels in intestinal extracts from 2-month old mice, and our data showed that αRaptor^{KO} mice have increased active GLP-1 levels. Therefore, we concluded that the increase in circulating active GLP-1 levels αRaptor^{KO} mice is of intestinal origin. However, it still remains unknown as to why active GLP-1 levels were increased in an animal model of low α-cell mass and glucagon levels. Future studies will examine the response of plasma, pancreatic and gut active GLP-1 levels using toxin receptor-mediated α-cell knockout model by crossing Glucagon-Cre mice to mice expressing diphtheria toxin (DT) receptor. In addition to increased plasma active GLP-1 levels, increased plasma amino acids could also contribute to the increase in pancreas weight and β-cell mass in αRaptor^{KO} mice. Decreased glucagon availability and decreased hepatic glucagon signaling in αRaptor^{KO} mice could result in increased plasma amino acids which act as potent anabolic agents that could expand pancreas weight and β-cell mass. Future studies will evaluate the plasma amino acid levels in control and αRaptor^{KO} mice.

Contrary to the regulation of glucagon release in high glucose conditions, it has been shown that extrinsic paracrine signals (insulin/GABA, somatostatin) do not play a role in regulating glucagon secretion in low glucose concentration (1-6 mM) (Walker et al., 2011). Mice with genetic ablation of the insulin receptor in α-cells (αIRKO) have increased glucagon levels in the fed state, with no differences detected during fasting. However, data from αIRKO mice also show that inhibiting insulin signaling in the pancreatic α-cells does not prevent an increase in glucagon levels after Streptozotocin (STZ)-induced hypoinsulimic-hyperglycemia. This suggests that insulin is necessary for inhibiting glucagon secretion in hyperglycemia; however, other signaling mechanisms likely contribute to an increase in glucagon levels in STZ-model of diabetes (Kawamori and Kulkarni, 2009). Further, mild hyperglycemia in αIRKO mice can be reversed with phloridzin without restoration of glucagon levels, showing that glucopenia does not contribute to rise in glucagon levels (Kawamori and Kulkarni, 2009). In order to further evaluate whether the role of mTORC1 signaling in α-cells is insulin-dependent, we induced hypoinsulimic-hyperglycemia in αRaptor^{KO} and αRaptor^{HET} mice using STZ. STZ-induced diabetes has been a well-characterized model for the study of α-cell mass expansion and increase in circulating glucagon levels (Plesner et al., 2014; Zhang et al., 2012). Particularly interesting, we found that mTORC1 signaling is enhanced in α-cells from control mice treated with a single, high dose of STZ. Our findings showed that hypoinsulimic-hyperglycemia did not promote an increase in mass and glucagon levels from the remaining α-cells of αRaptor^{KO} mice. Although, this was partly expected because αRaptor^{KO} mice have a substantial loss of α-cell mass, a study had shown that two percent of remaining α-cells (after an extreme loss of α-cell mass) is sufficient to produce enough glucagon and maintain normal glucagonemia (Thorel et al., 2011). The partial inhibition of mTORC1 signaling in αRaptor^{HET} mice was not sufficient to fully rescue the increased cell mass and glucagon levels following STZ. These data show that partial ablation of mTORC1 signaling in αRaptor^{HET} mice inhibits glucagon response during hypoglycemia and neuroglycopenia, but is not sufficient to prevent the rise in glucagon levels in a model of STZ-diabetes. Taken together, further studies utilizing an inducible model of complete mTORC1 inhibition in adult mice, are needed to sufficiently show whether α-cell mass expansion and glucagon increase following STZ treatment

are mTORC1-dependent. Further, future studies will examine the distinct or culminating roles of insulin receptor and mTORC1 signaling in promoting α-cell mass expansion and glucagon increase in the STZ model.

Chapter 3: Deletion of Tuberous Sclerosis Complex 2 (TSC2) in alpha cells results in hyperglucagonemia and alpha cell hypertrophy in the absence of diabetes

Recent studies have shown that glucagon increased energy expenditure in humans, similarly to that of cold-activation but independent of brown adipose fat (Salem et al., 2016). Body weight was significantly reduced in young αTSC2^{KO} mice and persisted through the lifespan of these mice. Food intake and activity measurements revealed that αTSC2^{KO} mice had increased activity compared to controls and no changes were detected in food intake. The central nervous system integrates nutrient signals to the regulation of energy balance by the mediobasal hypothalamus. Studies have shown that mTORC1 activation in the caudomedial nucleus of solitary tract (NTS) in the brainstem decreases food intake and body weight (Blouet et al., 2009; Blouet et al., 2008; Blouet and Schwartz, 2012). Assessment of *Cre*-recombination in CNS revealed that *Cre*-expressing neurons are present in the brainstem and dorsomedial hypothalamic nucleus (DMH), which could contribute to changes in feeding and activity levels. The central nervous system integrates nutrient signals to the regulation of energy balance by the mediobasal hypothalamus. Studies have shown that mTORC1 activation in the caudomedial nucleus of solitary tract (NTS) in the brainstem decreases food intake and body weight (Blouet et al., 2009; Blouet et al., 2008; Blouet and Schwartz, 2012). Based on these data, increased mTORC1 in in the DMH and brainstem could drive the decrease we see in body weight and increased activity levels of αTSC2^{KO} mice. However, increased plasma levels of glucagon could be directly acting in the CNS to decrease body weight in αTSC2^{KO} mice. Importantly, recent study has shown that chronic glucagon receptor signaling agonism is coupled with increased locomotor activity, in agreement with our data showing increased activity levels of αTSC2^{KO} mice (Habegger et al., 2013). Additional studies will dissect the role of 1) *Cre*-expression in brain and 2) the increase in plasma glucagon levels in regulating the decrease in body

weight of αTSC2^{KO} mice. In addition, further measure the respiration quotient and energy expenditure of αTSC2^{KO} and control mice.

Increased glucagon levels increase gluconeogenesis and glycogenolysis in control mice; however αTSC2^{KO} mice were hyperglucagonemic, but had reduced fasting glycemia. These data were puzzling and therefore we examined if the increased glucagon levels detected in αTSC2^{KO} mice were result of abnormal proglucagon processing. We did not detect any changes in fed or fasting active GLP-1 levels between αTSC2^{KO} and control mice, suggesting lack of abnormal proglucagon processing. Further analysis of PC2 mRNA and protein expression in α-cells from αTSC2^{KO} and control mice is needed to fully exclude the role of abnormal proglucagon processing as result of increased mTORC1 signaling in α-cells. Based on our data, we suggest that chronic hyperglucagonemia in αTSC2^{KO} mice may lead to decrease in hepatic glucagon signaling and gluconeogenesis, contributing to decreased fasting blood glucose levels and improved glucose tolerance. In addition, our data suggest that the role of glucagon in inhibiting glucokinase and suppressing glycogenolysis and glucagon's suppression of plasma free fatty acid levels is preserved and consistent with increased levels of fed glucagon in αTSC2^{KO} mice. Hepatic insulin sensitivity was not increased in αTSC2^{KO} and therefore does not contribute to the improvement in glucose tolerance. Additional studies will determine the adaptation of fasting on hepatic glycogen content and the expression of these genes in αTSC2^{KO} and controls. We will further measure glucagon signaling by exogenous administration of glucagon in controls and αTSC2^{KO} and analyze glucagon-signaling activation in the liver. In addition, we will evaluate the role of hyperglucagonemia on β-cell function to test whether alterations in insulin secretion are contributing to the improved glycemia in this mouse model.

The present data suggest that chronic hyperglucagonemia in αTSC2^{KO} mice leads to decreased hepatic glucagon signaling and gluconeogenesis contributing to decreased fasting blood glucose levels and improved glucose tolerance; however, the mechanism responsible for these effects is unknown. Recent study has shown that elevated plasma glucagon levels as a result of high-protein feeding lower blood glucose levels and

hepatic glucose production *via* the CNS (LaPierre et al., 2015). These data show that elevated circulating glucagon levels act in the brain to lower plasma glucose levels and the same mechanisms could be play a role in the decreased hepatic production of αTSC2^{KO} mice. The actions of glucagon to reduce body weight through decreased adipose tissue expansion and increase energy expenditure requires FGF-21 in mice. Activation of the glucagon receptor leads to increased plasma FGF-21 levels and hepatic *FGF-21* RNA (Habegger et al., 2013). Interestingly, a recent study has shown that pancreatic β and α-cells produce and secrete FGF21 (Omar et al., 2014). Inhibition of the glucagon receptor in the global glucagon receptor knock out mice results in α-cell hyperplasia and hyperglucagonemia and increased plasma FGF21 levels, which improved glucose tolerance in these mice in an insulin-independent manner. It is possible that the improvement in glucose homeostasis in the αTSC2^{KO} mice could be mediated by increase in FGF21 levels. Future studies will be designed to determine if the effects on body weight, improved glucose tolerance and decreased hepatic production of αTSC2^{KO} mice are dependent on glucagon signaling and the regulation of plasma, α-cell and hepatic expression levels of FGF21.

Previous data showed that complete ablation of β-cells and insulin levels by Streptozotocin (STZ) administration results in significant increase in α-cell mass and glucagon levels and the development of severe hyperglycemia in control mice (Chapter 2, Figure 11). The increase in α-cell mass was associated with increased mTORC1/phospho-S6 signaling in α-cells of control mice treated with STZ. Surprisingly, β-cell ablation after Streptozotocin (STZ) treatment of αTSC2^{KO} lead to an increase in glucagon levels but lower blood glucose levels compared to the hyperglycemic STZ-treated controls. The mRNA expression levels of glucagon receptor and gene targets involved in gluconeogenesis (*GCGR*, *PEPCK*, *G6Pase*), glycolysis (glucokinase) and fatty acid synthesis (fatty acid synthase) had a trend of increased expression in αTSC2^{KO} mice compared to controls after STZ. Ultimately, the number of animals in this experiment will need to be increased for complete analysis of the role of hyperglycemia-hyperinsulinemia in the glycemic response of this model of hyperglucagonemia.

CHAPTER 5

Clinical Implications

Rapalogs (rapamycin analogs) are FDA-approved drugs that suppress mTORC1 activity and are routinely used as immunosuppressants in transplantation surgeries and for the treatment of several malignancies. The findings presented in these studies show that rapamycin treatment decreases islet glucagon content and glucagon secretion in response to hypoglycemia. These data could have major clinical implications in responses to hypoglycemia in post-transplant diabetics. Further, these data could perhaps explain the defects in counterregulation of blood glucose in response to hypoglycemia in patients after islet transplantation surgeries that are under chronic immunosuppression therapy with rapamycin analogs (Paty et al., 2002; Rickels et al., 2007).

Rapalogs have also been linked to the development of new-onset diabetes by clinical and animal studies (Bussiere et al., 2006; Gyurus et al., 2011; Kulke et al., 2009; Larsen et al., 2006). Based on our data, we rapalogs do not cause hyperglycemia and new-onset diabetes by increasing glucagon levels. However, it is important to highlight that inhibiting mTORC1 in α-cells leads to decreased glucagon content and glucagon secretion in hypoglycemia, because that proposes a major challenge in employing insulin therapy and maintenance proper glucose control of these patients.

Despite the increasing number of oral medications becoming available, Sulfonylurea derivatives have been a mainstay approach for enhancing insulin secretion in diabetic patients. Sulfonylureas increase insulin secretion by blocking ATP-sensitive K^+ (K_{ATP}) channels *via* binding to SUR subunit of the channels. Sulfonylurea therapy has also been linked to increased episodes of hypoglycemia, which has been attributed to the increased insulin levels. However, clinical and animal studies have shown that acute administration of Sulfonylurea derivatives blunts the glucagon response to hypoglycemia (Efendic et al., 1979; Ostenson et al., 1986; ter Braak et al., 2002). Therefore, it should be noted that further consideration should be taken into the treatment approach of new-onset diabetes in patients who are undergoing immunosuppressive treatment by rapalogs, as these may create a dangerous predisposition to hypoglycemic episodes.

REFERENCES

Artner, I., Le Lay, J., Hang, Y., Elghazi, L., Schisler, J.C., Henderson, E., Sosa-Pineda, B., and Stein, R. (2006). MafB: an activator of the glucagon gene expressed in developing islet alpha- and beta-cells. Diabetes *55*, 297-304.

Asplin, C.M., Paquette, T.L., and Palmer, J.P. (1981). In vivo inhibition of glucagon secretion by paracrine beta cell activity in man. The Journal of clinical investigation *68*, 314-318.

Bar-Peled, L., Schweitzer, L.D., Zoncu, R., and Sabatini, D.M. (2012). Ragulator is a GEF for the rag GTPases that signal amino acid levels to mTORC1. Cell *150*, 1196-1208.

Bensley S.H., W.C.A. (1939). The effect of continuous intravenous injection of an extract of the alpha cells of the guinea pig pancreas on the intact guinea pig. Anat Rec, 413.

Bentzinger, C.F., Romanino, K., Cloëtta, D., Lin, S., Mascarenhas, J.B., Oliveri, F., Xia, J., Casanova, E., Costa, C.F., Brink, M., et al. (2008). Skeletal muscle-specific ablation of raptor, but not of rictor, causes metabolic changes and results in muscle dystrophy. Cell metabolism *8*, 411-424.

Bernal-Mizrachi, E., Cras-Méneur, C., Ye, B.R., Johnson, J.D., and Permutt, M.A. (2010). Transgenic overexpression of active calcineurin in beta-cells results in decreased beta-cell mass and hyperglycemia. PLoS ONE *5*, e11969.

Bernal-Mizrachi, E., Fatrai, S., Johnson, J.D., Ohsugi, M., Otani, K., Han, Z., Polonsky, K.S., and Permutt, M.A. (2004). Defective insulin secretion and increased susceptibility to experimental diabetes are induced by reduced Akt activity in pancreatic islet beta cells. The Journal of clinical investigation *114*, 928-936.

Bernal-Mizrachi, E., Wen, W., Stahlhut, S., Welling, C.M., and Permutt, M.A. (2001). Islet beta cell expression of constitutively active Akt1/PKB alpha induces striking hypertrophy, hyperplasia, and hyperinsulinemia. The Journal of clinical investigation *108*, 1631-1638.

Bloom, S.R., Edwards, A.V., and Hardy, R.N. (1978). The role of the autonomic nervous system in the control of glucagon, insulin and pancreatic polypeptide release from the pancreas. J Physiol *280*, 9-23.

Blouet, C., Jo, Y.H., Li, X., and Schwartz, G.J. (2009). Mediobasal hypothalamic leucine sensing regulates food intake through activation of a hypothalamus-brainstem circuit. The Journal of neuroscience : the official journal of the Society for Neuroscience *29*, 8302-8311.

Blouet, C., Ono, H., and Schwartz, G.J. (2008). Mediobasal hypothalamic p70 S6 kinase 1 modulates the control of energy homeostasis. Cell metabolism *8*, 459-467.

Blouet, C., and Schwartz, G.J. (2012). Brainstem nutrient sensing in the nucleus of the solitary tract inhibits feeding. Cell metabolism *16*, 579-587.

Bonner-Weir, S., and Orci, L. (1982). New perspectives on the microvasculature of the islets of Langerhans in the rat. Diabetes *31*, 883-889.

Brown, E.J., Albers, M.W., Shin, T.B., Ichikawa, K., Keith, C.T., Lane, W.S., and Schreiber, S.L. (1994). A mammalian protein targeted by G1-arresting rapamycin-receptor complex. Nature *369*, 756-758.

Brubaker, P.L., and Drucker, D.J. (2004). Minireview: Glucagon-like peptides regulate cell proliferation and apoptosis in the pancreas, gut, and central nervous system. Endocrinology *145*, 2653-2659.

Brunicardi, F.C., Kleinman, R., Moldovan, S., Nguyen, T.H., Watt, P.C., Walsh, J., and Gingerich, R. (2001). Immunoneutralization of somatostatin, insulin, and glucagon causes alterations in islet cell secretion in the isolated perfused human pancreas. Pancreas *23*, 302-308.

Bussiere, C.T., Lakey, J.R., Shapiro, A.M., and Korbutt, G.S. (2006). The impact of the mTOR inhibitor sirolimus on the proliferation and function of pancreatic islets and ductal cells. Diabetologia *49*, 2341-2349.

Cabrera, O., Berman, D.M., Kenyon, N.S., Ricordi, C., Berggren, P.O., and Caicedo, A. (2006). The unique cytoarchitecture of human pancreatic islets has implications for islet cell function. Proceedings of the National Academy of Sciences of the United States of America *103*, 2334-2339.

Cabrera, O., Jacques-Silva, M.C., Speier, S., Yang, S.N., Kohler, M., Fachado, A., Vieira, E., Zierath, J.R., Kibbey, R., Berman, D.M., et al. (2008). Glutamate is a positive autocrine signal for glucagon release. Cell metabolism *7*, 545-554.

Campbell, J.E., and Drucker, D.J. (2015). Islet alpha cells and glucagon--critical regulators of energy homeostasis. Nat Rev Endocrinol *11*, 329-338.

Campos, R.V., Lee, Y.C., and Drucker, D.J. (1994). Divergent tissue-specific and developmental expression of receptors for glucagon and glucagon-like peptide-1 in the mouse. Endocrinology *134*, 2156-2164.

Cantley, J., Choudhury, A.I., Asare-Anane, H., Selman, C., Lingard, S., Heffron, H., Herrera, P., Persaud, S.J., and Withers, D.J. (2007). Pancreatic deletion of insulin receptor substrate 2 reduces beta and alpha cell mass and impairs glucose homeostasis in mice. Diabetologia *50*, 1248-1256.

Chen, L., Philippe, J., and Unger, R.H. (2011). Glucagon responses of isolated alpha cells to glucose, insulin, somatostatin, and leptin. Endocrine practice : official journal of the American College of Endocrinology and the American Association of Clinical Endocrinologists *17*, 819-825.

Collombat, P., Mansouri, A., Hecksher-Sorensen, J., Serup, P., Krull, J., Gradwohl, G., and Gruss, P. (2003). Opposing actions of Arx and Pax4 in endocrine pancreas development. Genes & development *17*, 2591-2603.

Collombat, P., Xu, X., Ravassard, P., Sosa-Pineda, B., Dussaud, S., Billestrup, N., Madsen, O.D., Serup, P., Heimberg, H., and Mansouri, A. (2009). The ectopic expression of Pax4 in the mouse pancreas converts progenitor cells into alpha and subsequently beta cells. Cell *138*, 449-462.

Conrad, E., Dai, C., Spaeth, J., Guo, M., Cyphert, H.A., Scoville, D., Carroll, J., Yu, W.M., Goodrich, L.V., Harlan, D.M., et al. (2015). The MAFB transcription factor impacts islet alpha-cell function in rodents and represents a unique signature of primate islet beta-cells. American journal of physiology. Endocrinology and metabolism, ajpendo 00285 02015.

Cota, D., Proulx, K., Smith, K.A., Kozma, S.C., Thomas, G., Woods, S.C., and Seeley, R.J. (2006). Hypothalamic mTOR signaling regulates food intake. Science *312*, 927-930.

Courtney, M., Gjernes, E., Druelle, N., Ravaud, C., Vieira, A., Ben-Othman, N., Pfeifer, A., Avolio, F., Leuckx, G., Lacas-Gervais, S., et al. (2013). The inactivation of Arx in pancreatic alpha-cells triggers their neogenesis and conversion into functional beta-like cells. PLoS Genet *9*, e1003934.

Cryer, P.E. (2002). Hypoglycaemia: the limiting factor in the glycaemic management of Type I and Type II diabetes. Diabetologia *45*, 937-948.

Dai, X.Q., Plummer, G., Casimir, M., Kang, Y., Hajmrle, C., Gaisano, H.Y., Manning Fox, J.E., and MacDonald, P.E. (2011). SUMOylation regulates insulin exocytosis downstream of secretory granule docking in rodents and humans. Diabetes *60*, 838-847.

Dan, H.C., Sun, M., Yang, L., Feldman, R.I., Sui, X.M., Ou, C.C., Nellist, M., Yeung, R.S., Halley, D.J., Nicosia, S.V., et al. (2002). Phosphatidylinositol 3-kinase/Akt pathway regulates tuberous sclerosis tumor suppressor complex by phosphorylation of tuberin. J. Biol. Chem. *277*, 35364-35370.

Daniel, P.M., Pratt, O.E., and Spargo, E. (1977). The mechanism by which glucagon induces the release of amino acids from muscle and its relevance to fasting. Proc R Soc Lond B Biol Sci *196*, 347-365.

Dinneen, S., Alzaid, A., Turk, D., and Rizza, R. (1995). Failure of glucagon suppression contributes to postprandial hyperglycaemia in IDDM. Diabetologia *38*, 337-343.

Dowling, R.J.O., Topisirovic, I., Fonseca, B.D., and Sonenberg, N. (2010). Dissecting the role of mTOR: lessons from mTOR inhibitors. Biochim Biophys Acta *1804*, 433-439.

Drucker, D.J., and Asa, S. (1988). Glucagon gene expression in vertebrate brain. The Journal of biological chemistry *263*, 13475-13478.

Efendic, S., Enzmann, F., Nylen, A., Uvnas-Wallensten, K., and Luft, R. (1979). Effect of glucose/sulfonylurea interaction on release of insulin, glucagon, and somatostatin from isolated perfused rat pancreas. Proceedings of the National Academy of Sciences of the United States of America *76*, 5901-5904.

Efeyan, A., Zoncu, R., and Sabatini, D.M. (2012). Amino acids and mTORC1: from lysosomes to disease. Trends Mol Med *18*, 524-533.

Egan, D., Kim, J., Shaw, R.J., and Guan, K.L. (2011). The autophagy initiating kinase ULK1 is regulated via opposing phosphorylation by AMPK and mTOR. Autophagy *7*, 643-644.

Ellingsgaard, H., Ehses, J.A., Hammar, E.B., Van Lommel, L., Quintens, R., Martens, G., Kerr-Conte, J., Pattou, F., Berney, T., Pipeleers, D., et al. (2008). Interleukin-6 regulates pancreatic alpha-cell mass expansion. Proceedings of the National Academy of Sciences of the United States of America *105*, 13163-13168.

Farah, A.E. (1983). Glucagon and the circulation. Pharmacological reviews *35*, 181-217.

Fava, G.E., Dong, E.W., and Wu, H. (2016). Intra-islet glucagon-like peptide 1. J Diabetes Complications.

Filippi, B.M., Abraham, M.A., Yue, J.T., and Lam, T.K. (2013). Insulin and glucagon signaling in the central nervous system. Reviews in endocrine & metabolic disorders.

Finak, G., McDavid, A., Yajima, M., Deng, J., Gersuk, V., Shalek, A.K., Slichter, C.K., Miller, H.W., McElrath, M.J., Prlic, M., et al. (2015). MAST: a flexible statistical framework for assessing transcriptional changes and characterizing heterogeneity in single-cell RNA sequencing data. Genome Biol *16*, 278.

Foa PP, S.L., Weinstein H, Berger S, Smith JA (1952). Secretion of the hyperglycemic-glycogenolytic factor in normal dog. Am J Physiol, 32-36.

Franklin, I., Gromada, J., Gjinovci, A., Theander, S., and Wollheim, C.B. (2005). Beta-cell secretory products activate alpha-cell ATP-dependent potassium channels to inhibit glucagon release. Diabetes *54*, 1808-1815.

Furuta, M., Zhou, A., Webb, G., Carroll, R., Ravazzola, M., Orci, L., and Steiner, D.F. (2001). Severe defect in proglucagon processing in islet A-cells of prohormone convertase 2 null mice. The Journal of biological chemistry *276*, 27197-27202.

Gao, N., White, P., Doliba, N., Golson, M.L., Matschinsky, F.M., and Kaestner, K.H. (2007). Foxa2 controls vesicle docking and insulin secretion in mature Beta cells. Cell metabolism *6*, 267-279.

Gerich, J.E., Langlois, M., Noacco, C., Karam, J.H., and Forsham, P.H. (1973). Lack of glucagon response to hypoglycemia in diabetes: evidence for an intrinsic pancreatic alpha cell defect. Science *182*, 171-173.

Gerich, J.E., Lorenzi, M., Schneider, V., Kwan, C.W., Karam, J.H., Guillemin, R., and Forsham, P.H. (1974). Inhibition of pancreatic glucagon responses to arginine by somatostatin in normal man and in insulin-dependent diabetics. Diabetes *23*, 876-880.

Gilon, P., Bertrand, G., Loubatieres-Mariani, M.M., Remacle, C., and Henquin, J.C. (1991). The influence of gamma-aminobutyric acid on hormone release by the mouse and rat endocrine pancreas. Endocrinology *129*, 2521-2529.

Gonzalez-Munoz, C., Nieto-Ceron, S., Cabezas-Herrera, J., and Hernandez-Cascales, J. (2008). Glucagon increases contractility in ventricle but not in atrium of the rat heart. Eur J Pharmacol *587*, 243-247.

Gopel, S.O., Kanno, T., Barg, S., Weng, X.G., Gromada, J., and Rorsman, P. (2000). Regulation of glucagon release in mouse -cells by KATP channels and inactivation of TTX-sensitive Na+ channels. J Physiol *528*, 509-520.

Gosmain, Y., Cheyssac, C., Masson, M.H., Guerardel, A., Poisson, C., and Philippe, J. (2012). Pax6 is a key component of regulated glucagon secretion. Endocrinology *153*, 4204-4215.

Gromada, J., Franklin, I., and Wollheim, C.B. (2007). Alpha-cells of the endocrine pancreas: 35 years of research but the enigma remains. Endocrine reviews *28*, 84-116.

Gyurus, E., Kaposztas, Z., and Kahan, B.D. (2011). Sirolimus therapy predisposes to new-onset diabetes mellitus after renal transplantation: a long-term analysis of various treatment regimens. Transplant Proc *43*, 1583-1592.

Habegger, K.M., Stemmer, K., Cheng, C., Muller, T.D., Heppner, K.M., Ottaway, N., Holland, J., Hembree, J.L., Smiley, D., Gelfanov, V., et al. (2013). Fibroblast growth factor 21 mediates specific glucagon actions. Diabetes *62*, 1453-1463.

Hauge-Evans, A.C., King, A.J., Carmignac, D., Richardson, C.C., Robinson, I.C., Low, M.J., Christie, M.R., Persaud, S.J., and Jones, P.M. (2009). Somatostatin secreted by islet delta-cells fulfills multiple roles as a paracrine regulator of islet function. Diabetes *58*, 403-411.

Heddad Masson, M., Poisson, C., Guerardel, A., Mamin, A., Philippe, J., and Gosmain, Y. (2014). Foxa1 and Foxa2 regulate alpha-cell differentiation, glucagon biosynthesis, and secretion. Endocrinology *155*, 3781-3792.

Heimberg, H., De Vos, A., Moens, K., Quartier, E., Bouwens, L., Pipeleers, D., Van Schaftingen, E., Madsen, O., and Schuit, F. (1996). The glucose sensor protein glucokinase is expressed in glucagon-producing alpha-cells. Proceedings of the National Academy of Sciences of the United States of America *93*, 7036-7041.

Hernandez, O., Way, S., McKenna, J., 3rd, and Gambello, M.J. (2007). Generation of a conditional disruption of the Tsc2 gene. Genesis *45*, 101-106.

Hosokawa, N., Hara, T., Kaizuka, T., Kishi, C., Takamura, A., Miura, Y., Iemura, S., Natsume, T., Takehana, K., Yamada, N., et al. (2009). Nutrient-dependent mTORC1 association with the ULK1-Atg13-FIP200 complex required for autophagy. Mol Biol Cell *20*, 1981-1991.

Inoki, K., Li, Y., Zhu, T., Wu, J., and Guan, K.L. (2002). TSC2 is phosphorylated and inhibited by Akt and suppresses mTOR signalling. Nature cell biology *4*, 648-657.

Inoki, K., Ouyang, H., Zhu, T., Lindvall, C., Wang, Y., Zhang, X., Yang, Q., Bennett, C., Harada, Y., Stankunas, K., et al. (2006). TSC2 integrates Wnt and energy signals via a coordinated phosphorylation by AMPK and GSK3 to regulate cell growth. Cell *126*, 955-968.

Inoki, K., Zhu, T., and Guan, K.L. (2003). TSC2 mediates cellular energy response to control cell growth and survival. Cell *115*, 577-590.

Ishihara, H., Maechler, P., Gjinovci, A., Herrera, P.L., and Wollheim, C.B. (2003). Islet beta-cell secretion determines glucagon release from neighbouring alpha-cells. Nature cell biology *5*, 330-335.

Jiang, G., and Zhang, B.B. (2003). Glucagon and regulation of glucose metabolism. American journal of physiology. Endocrinology and metabolism *284*, E671-678.

Jung, C.H., Jun, C.B., Ro, S.H., Kim, Y.M., Otto, N.M., Cao, J., Kundu, M., and Kim, D.H. (2009). ULK-Atg13-FIP200 complexes mediate mTOR signaling to the autophagy machinery. Mol Biol Cell *20*, 1992-2003.

Kaestner, K.H., Katz, J., Liu, Y., Drucker, D.J., and Schutz, G. (1999). Inactivation of the winged helix transcription factor HNF3alpha affects glucose homeostasis and islet glucagon gene expression in vivo. Genes & development *13*, 495-504.

Karlsson, S., and Ahren, B. (1987). Inhibition of 2-deoxy-glucose-induced glucagon secretion by muscarinic and alpha-adrenoceptor blockade in the mouse. Diabetes Res Clin Pract *3*, 239-242.

Karpe, F., Dickmann, J.R., and Frayn, K.N. (2011). Fatty acids, obesity, and insulin resistance: time for a reevaluation. Diabetes *60*, 2441-2449.

Katz, L.S., Gosmain, Y., Marthinet, E., and Philippe, J. (2009). Pax6 regulates the proglucagon processing enzyme PC2 and its chaperone 7B2. Mol Cell Biol *29*, 2322-2334.

Kawamori, D., and Kulkarni, R.N. (2009). Insulin modulation of glucagon secretion: the role of insulin and other factors in the regulation of glucagon secretion. Islets *1*, 276-279.

Kawamori, D., Kurpad, A.J., Hu, J., Liew, C.W., Shih, J.L., Ford, E.L., Herrera, P.L., Polonsky, K.S., McGuinness, O.P., and Kulkarni, R.N. (2009). Insulin signaling in alpha cells modulates glucagon secretion in vivo. Cell metabolism *9*, 350-361.

Khamzina, L., Veilleux, A., Bergeron, S., and Marette, A. (2005). Increased activation of the mammalian target of rapamycin pathway in liver and skeletal muscle of obese rats: possible involvement in obesity-linked insulin resistance. Endocrinology *146*, 1473-1481.

Kim, D.H., Sarbassov, D.D., Ali, S.M., King, J.E., Latek, R.R., Erdjument-Bromage, H., Tempst, P., and Sabatini, D.M. (2002). mTOR interacts with raptor to form a nutrient-sensitive complex that signals to the cell growth machinery. Cell *110*, 163-175.

Kim, J., Kundu, M., Viollet, B., and Guan, K.L. (2011). AMPK and mTOR regulate autophagy through direct phosphorylation of Ulk1. Nature cell biology *13*, 132-141.

Kim, J.G., Baggio, L.L., Bridon, D.P., Castaigne, J.P., Robitaille, M.F., Jette, L., Benquet, C., and Drucker, D.J. (2003). Development and characterization of a glucagon-like peptide 1-albumin conjugate: the ability to activate the glucagon-like peptide 1 receptor in vivo. Diabetes *52*, 751-759.

Kulke, M.H., Bergsland, E.K., and Yao, J.C. (2009). Glycemic control in patients with insulinoma treated with everolimus. The New England journal of medicine *360*, 195-197.

Lane, M.A. (1907). The cytological characters of the areas of Langerhans. Am J Anat, 409-422.

Lantz, K.A., Vatamaniuk, M.Z., Brestelli, J.E., Friedman, J.R., Matschinsky, F.M., and Kaestner, K.H. (2004). Foxa2 regulates multiple pathways of insulin secretion. The Journal of clinical investigation *114*, 512-520.

LaPierre, M.P., Abraham, M.A., Filippi, B.M., Yue, J.T., and Lam, T.K. (2014). Glucagon and lipid signaling in the hypothalamus. Mamm Genome *25*, 434-441.

LaPierre, M.P., Abraham, M.A., Yue, J.T., Filippi, B.M., and Lam, T.K. (2015). Glucagon signalling in the dorsal vagal complex is sufficient and necessary for high-protein feeding to regulate glucose homeostasis in vivo. EMBO reports *16*, 1299-1307.

Laplante, M., and Sabatini, D.M. (2012). mTOR signaling in growth control and disease. Cell *149*, 274-293.

Larsen, J.L., Bennett, R.G., Burkman, T., Ramirez, A.L., Yamamoto, S., Gulizia, J., Radio, S., and Hamel, F.G. (2006). Tacrolimus and sirolimus cause insulin resistance in normal sprague dawley rats. Transplantation *82*, 466-470.

Leclerc, I., Sun, G., Morris, C., Fernandez-Millan, E., Nyirenda, M., and Rutter, G.A. (2011). AMP-activated protein kinase regulates glucagon secretion from mouse pancreatic alpha cells. Diabetologia *54*, 125-134.

Lee, C.H., Inoki, K., and Guan, K.L. (2007). mTOR pathway as a target in tissue hypertrophy. Annu Rev Pharmacol Toxicol *47*, 443-467.

Lee, C.S., Sund, N.J., Behr, R., Herrera, P.L., and Kaestner, K.H. (2005). Foxa2 is required for the differentiation of pancreatic alpha-cells. Developmental biology *278*, 484-495.

Lefebvre, P.J. (1995). Glucagon and its family revisited. Diabetes Care *18*, 715-730.

Liss, B., Bruns, R., and Roeper, J. (1999). Alternative sulfonylurea receptor expression defines metabolic sensitivity of K-ATP channels in dopaminergic midbrain neurons. EMBO J *18*, 833-846.

Liu, Z., Kim, W., Chen, Z., Shin, Y.K., Carlson, O.D., Fiori, J.L., Xin, L., Napora, J.K., Short, R., Odetunde, J.O., et al. (2011). Insulin and glucagon regulate pancreatic alpha-cell proliferation. PLoS One *6*, e16096.

Longuet, C., Robledo, A.M., Dean, E.D., Dai, C., Ali, S., McGuinness, I., de Chavez, V., Vuguin, P.M., Charron, M.J., Powers, A.C., et al. (2013). Liver-specific disruption of the murine glucagon receptor produces alpha-cell hyperplasia: evidence for a circulating alpha-cell growth factor. Diabetes *62*, 1196-1205.

Longuet, C., Sinclair, E.M., Maida, A., Baggio, L.L., Maziarz, M., Charron, M.J., and Drucker, D.J. (2008). The glucagon receptor is required for the adaptive metabolic response to fasting. Cell metabolism *8*, 359-371.

MacDonald, P.E., De Marinis, Y.Z., Ramracheya, R., Salehi, A., Ma, X., Johnson, P.R.V., Cox, R., Eliasson, L., and Rorsman, P. (2007). A K ATP channel-dependent pathway within alpha cells regulates glucagon release from both rodent and human islets of Langerhans. PLoS biology *5*, e143.

Manning, B.D., Tee, A.R., Logsdon, M.N., Blenis, J., and Cantley, L.C. (2002). Identification of the tuberous sclerosis complex-2 tumor suppressor gene product tuberin as a target of the phosphoinositide 3-kinase/akt pathway. Mol Cell *10*, 151-162.

Marroqui, L., Alonso-Magdalena, P., Merino, B., Fuentes, E., Nadal, A., and Quesada, I. (2014). Nutrient regulation of glucagon secretion: involvement in metabolism and diabetes. Nutr Res Rev *27*, 48-62.

Marty, N., Dallaporta, M., Foretz, M., Emery, M., Tarussio, D., Bady, I., Binnert, C., Beermann, F., and Thorens, B. (2005). Regulation of glucagon secretion by glucose transporter type 2 (glut2) and astrocyte-dependent glucose sensors. The Journal of clinical investigation *115*, 3545-3553.

Maruyama, H., Hisatomi, A., Orci, L., Grodsky, G.M., and Unger, R.H. (1984). Insulin within islets is a physiologic glucagon release inhibitor. The Journal of clinical investigation *74*, 2296-2299.

Mastracci, T.L., Wilcox, C.L., Arnes, L., Panea, C., Golden, J.A., May, C.L., and Sussel, L. (2011). Nkx2.2 and Arx genetically interact to regulate pancreatic endocrine cell development and endocrine hormone expression. Developmental biology *359*, 1-11.

Mery, P.F., Brechler, V., Pavoine, C., Pecker, F., and Fischmeister, R. (1990). Glucagon stimulates the cardiac Ca2+ current by activation of adenylyl cyclase and inhibition of phosphodiesterase. Nature *345*, 158-161.

Mezza, T., Muscogiuri, G., Sorice, G.P., Clemente, G., Hu, J., Pontecorvi, A., Holst, J.J., Giaccari, A., and Kulkarni, R.N. (2014). Insulin resistance alters islet morphology in nondiabetic humans. Diabetes *63*, 994-1007.

Mighiu, P.I., Yue, J.T., Filippi, B.M., Abraham, M.A., Chari, M., Lam, C.K., Yang, C.S., Christian, N.R., Charron, M.J., and Lam, T.K. (2013). Hypothalamic glucagon signaling inhibits hepatic glucose production. Nat Med *19*, 766-772.

Mizushima, N., Yamamoto, A., Matsui, M., Yoshimori, T., and Ohsumi, Y. (2004). In vivo analysis of autophagy in response to nutrient starvation using transgenic mice expressing a fluorescent autophagosome marker. Mol Biol Cell *15*, 1101-1111.

Mori, H., Inoki, K., Munzberg, H., Opland, D., Faouzi, M., Villanueva, E.C., Ikenoue, T., Kwiatkowski, D., MacDougald, O.A., Myers, M.G., Jr., et al. (2009a). Critical role for hypothalamic mTOR activity in energy balance. Cell metabolism *9*, 362-374.

Mori, H., Inoki, K., Opland, D., Munzberg, H., Villanueva, E.C., Faouzi, M., Ikenoue, T., Kwiatkowski, D.J., Macdougald, O.A., Myers, M.G., Jr., et al. (2009b). Critical roles for the TSC-mTOR pathway in beta-cell function. American journal of physiology. Endocrinology and metabolism *297*, E1013-1022.

Morley, M.G., Leiter, E.H., Eisenstein, A.B., and Strack, I. (1982). Dietary modulation of alpha-cell volume and function in strain 129/J mice. Am J Physiol *242*, G354-359.

Murakami, M., Ichisaka, T., Maeda, M., Oshiro, N., Hara, K., Edenhofer, F., Kiyama, H., Yonezawa, K., and Yamanaka, S. (2004). mTOR is essential for growth and proliferation in early mouse embryos and embryonic stem cells. Mol Cell Biol *24*, 6710-6718.

Murlin JR, C.H., Gibbs CBF, Stokes AM (1923). Aqueous extracts of the pancreas. 1. Influence on the carbohydrate metabolism of the depancreatized animals. The Journal of biological chemistry, 253-296.

Olsen, H.L., Theander, S., Bokvist, K., Buschard, K., Wollheim, C.B., and Gromada, J. (2005). Glucose stimulates glucagon release in single rat alpha-cells by mechanisms that mirror the stimulus-secretion coupling in beta-cells. Endocrinology *146*, 4861-4870.

Omar, B.A., Andersen, B., Hald, J., Raun, K., Nishimura, E., and Ahren, B. (2014). Fibroblast growth factor 21 (FGF21) and glucagon-like peptide 1 contribute to diabetes resistance in glucagon receptor-deficient mice. Diabetes *63*, 101-110.

Orci, L., Baetens, D., Rufener, C., Amherdt, M., Ravazzola, M., Studer, P., Malaisse-Lagae, F., and Unger, R.H. (1976). Hypertrophy and hyperplasia of somatostatin-containing D-cells in diabetes. Proceedings of the National Academy of Sciences of the United States of America *73*, 1338-1342.

Ostenson, C.G., Nylen, A., Grill, V., Gutniak, M., and Efendic, S. (1986). Sulfonylurea-induced inhibition of glucagon secretion from the perfused rat pancreas: evidence for a direct, non-paracrine effect. Diabetologia *29*, 861-867.

Paty, B.W., Ryan, E.A., Shapiro, A.M., Lakey, J.R., and Robertson, R.P. (2002). Intrahepatic islet transplantation in type 1 diabetic patients does not restore hypoglycemic hormonal counterregulation or symptom recognition after insulin independence. Diabetes *51*, 3428-3434.

Philippe, J. (1989). Glucagon gene transcription is negatively regulated by insulin in a hamster islet cell line. The Journal of clinical investigation *84*, 672-677.

Philippe, J., Morel, C., and Prezioso, V.R. (1994). Glucagon gene expression is negatively regulated by hepatocyte nuclear factor 3 beta. Mol Cell Biol *14*, 3514-3523.

Pipeleers, D.G., Schuit, F.C., Van Schravendijk, C.F., and Van de Winkel, M. (1985). Interplay of nutrients and hormones in the regulation of glucagon release. Endocrinology *117*, 817-823.

Plesner, A., Ten Holder, J.T., and Verchere, C.B. (2014). Islet remodeling in female mice with spontaneous autoimmune and streptozotocin-induced diabetes. PLoS One *9*, e102843.

Polak, P., Cybulski, N., Feige, J.N., Auwerx, J., Rüegg, M.A., and Hall, M.N. (2008). Adipose-specific knockout of raptor results in lean mice with enhanced mitochondrial respiration. Cell metabolism *8*, 399-410.

Rahier, J., Goebbels, R.M., and Henquin, J.C. (1983). Cellular composition of the human diabetic pancreas. Diabetologia *24*, 366-371.

Ramracheya, R., Ward, C., Shigeto, M., Walker, J.N., Amisten, S., Zhang, Q., Johnson, P.R., Rorsman, P., and Braun, M. (2010). Membrane potential-dependent inactivation of voltage-gated ion channels in alpha-cells inhibits glucagon secretion from human islets. Diabetes *59*, 2198-2208.

Reaven, G.M., Chen, Y.D., Golay, A., Swislocki, A.L., and Jaspan, J.B. (1987). Documentation of hyperglucagonemia throughout the day in nonobese and obese patients with noninsulin-dependent diabetes mellitus. The Journal of clinical endocrinology and metabolism *64*, 106-110.

Rickels, M.R., Schutta, M.H., Mueller, R., Kapoor, S., Markmann, J.F., Naji, A., and Teff, K.L. (2007). Glycemic thresholds for activation of counterregulatory hormone and

symptom responses in islet transplant recipients. The Journal of clinical endocrinology and metabolism *92*, 873-879.

Ritz-Laser, B., Estreicher, A., Gauthier, B.R., Mamin, A., Edlund, H., and Philippe, J. (2002). The pancreatic beta-cell-specific transcription factor Pax-4 inhibits glucagon gene expression through Pax-6. Diabetologia *45*, 97-107.

Ritz-Laser, B., Mamin, A., Brun, T., Avril, I., Schwitzgebel, V.M., and Philippe, J. (2005). The zinc finger-containing transcription factor Gata-4 is expressed in the developing endocrine pancreas and activates glucagon gene expression. Molecular endocrinology *19*, 759-770.

Rolin, B., Larsen, M.O., Gotfredsen, C.F., Deacon, C.F., Carr, R.D., Wilken, M., and Knudsen, L.B. (2002). The long-acting GLP-1 derivative NN2211 ameliorates glycemia and increases beta-cell mass in diabetic mice. American journal of physiology. Endocrinology and metabolism *283*, E745-752.

Rorsman, P., Berggren, P.O., Bokvist, K., Ericson, H., Mohler, H., Ostenson, C.G., and Smith, P.A. (1989). Glucose-inhibition of glucagon secretion involves activation of GABAA-receptor chloride channels. Nature *341*, 233-236.

Rorsman, P., Ramracheya, R., Rorsman, N.J., and Zhang, Q. (2014). ATP-regulated potassium channels and voltage-gated calcium channels in pancreatic alpha and beta cells: similar functions but reciprocal effects on secretion. Diabetologia *57*, 1749-1761.

Rorsman, P., Salehi, S.A., Abdulkader, F., Braun, M., and MacDonald, P.E. (2008). K(ATP)-channels and glucose-regulated glucagon secretion. Trends Endocrinol Metab *19*, 277-284.

Salem, V., Izzi-Engbeaya, C., Coello, C., Thomas, D.B., Chambers, E.S., Comninos, A.N., Buckley, A., Win, Z., Al-Nahhas, A., Rabiner, E.A., et al. (2016). Glucagon increases energy expenditure independently of brown adipose tissue activation in humans. Diabetes Obes Metab *18*, 72-81.

Sancak, Y., Bar-Peled, L., Zoncu, R., Markhard, A.L., Nada, S., and Sabatini, D.M. (2010). Ragulator-Rag complex targets mTORC1 to the lysosomal surface and is necessary for its activation by amino acids. Cell *141*, 290-303.

Sancak, Y., Peterson, T.R., Shaul, Y.D., Lindquist, R.A., Thoreen, C.C., Bar-Peled, L., and Sabatini, D.M. (2008). The Rag GTPases bind raptor and mediate amino acid signaling to mTORC1. Science *320*, 1496-1501.

Sancak, Y., and Sabatini, D.M. (2009). Rag proteins regulate amino-acid-induced mTORC1 signalling. Biochem Soc Trans *37*, 289-290.

Sanchez, A.M., Csibi, A., Raibon, A., Cornille, K., Gay, S., Bernardi, H., and Candau, R. (2012). AMPK promotes skeletal muscle autophagy through activation of forkhead FoxO3a and interaction with Ulk1. J Cell Biochem *113*, 695-710.

Sarbassov, D.D., Guertin, D.A., Ali, S.M., and Sabatini, D.M. (2005). Phosphorylation and regulation of Akt/PKB by the rictor-mTOR complex. Science *307*, 1098-1101.

Schinner, S., Barthel, A., Dellas, C., Grzeskowiak, R., Sharma, S.K., Oetjen, E., Blume, R., and Knepel, W. (2005). Protein kinase B activity is sufficient to mimic the effect of insulin on glucagon gene transcription. The Journal of biological chemistry *280*, 7369-7376.

Segel, S.A., Paramore, D.S., and Cryer, P.E. (2002). Hypoglycemia-associated autonomic failure in advanced type 2 diabetes. Diabetes *51*, 724-733.

Sengupta, S., Peterson, T.R., Laplante, M., Oh, S., and Sabatini, D.M. (2010). mTORC1 controls fasting-induced ketogenesis and its modulation by ageing. Nature *468*, 1100-1104.

Shen, X.X., Li, H.L., Pan, L., Hong, J., Xiao, J., Hermansen, K., Jeppesen, P.B., and Li, G.W. (2012). Glucotoxicity and alpha cell dysfunction: involvement of the PI3K/Akt pathway in glucose-induced insulin resistance in rat islets and clonal alphaTC1-6 cells. Endocrine research *37*, 12-24.

Sherwin, R.S., Fisher, M., Hendler, R., and Felig, P. (1976). Hyperglucagonemia and blood glucose regulation in normal, obese and diabetic subjects. The New England journal of medicine *294*, 455-461.

Shigeyama, Y., Kobayashi, T., Kido, Y., Hashimoto, N., Asahara, S., Matsuda, T., Takeda, A., Inoue, T., Shibutani, Y., Koyanagi, M., et al. (2008). Biphasic response of pancreatic beta-cell mass to ablation of tuberous sclerosis complex 2 in mice. Mol Cell Biol *28*, 2971-2979.

Shih, D.Q., Navas, M.A., Kuwajima, S., Duncan, S.A., and Stoffel, M. (1999). Impaired glucose homeostasis and neonatal mortality in hepatocyte nuclear factor 3alpha-deficient mice. Proceedings of the National Academy of Sciences of the United States of America *96*, 10152-10157.

Shimobayashi, M., and Hall, M.N. (2014). Making new contacts: the mTOR network in metabolism and signalling crosstalk. Nature reviews Molecular cell biology *15*, 155-162.

Shiota, C., Prasadan, K., Guo, P., El-Gohary, Y., Wiersch, J., Xiao, X., Esni, F., and Gittes, G.K. (2013). alpha-Cells are dispensable in postnatal morphogenesis and maturation of mouse pancreatic islets. American journal of physiology. Endocrinology and metabolism *305*, E1030-1040.

Shiota, C., Rocheleau, J.V., Shiota, M., Piston, D.W., and Magnuson, M.A. (2005). Impaired glucagon secretory responses in mice lacking the type 1 sulfonylurea receptor. American journal of physiology. Endocrinology and metabolism *289*, E570-577.

Solloway, M.J., Madjidi, A., Gu, C., Eastham-Anderson, J., Clarke, H.J., Kljavin, N., Zavala-Solorio, J., Kates, L., Friedman, B., Brauer, M., et al. (2015). Glucagon Couples

Hepatic Amino Acid Catabolism to mTOR-Dependent Regulation of alpha-Cell Mass. Cell Rep *12*, 495-510.

Sosa-Pineda, B., Chowdhury, K., Torres, M., Oliver, G., and Gruss, P. (1997). The Pax4 gene is essential for differentiation of insulin-producing beta cells in the mammalian pancreas. Nature *386*, 399-402.

Soulard, A., Cohen, A., and Hall, M.N. (2009). TOR signaling in invertebrates. Curr. Opin. Cell Biol. *21*, 825-836.

Spigelman, A.F., Dai, X., and MacDonald, P.E. (2010). Voltage-dependent K(+) channels are positive regulators of alpha cell action potential generation and glucagon secretion in mice and humans. Diabetologia *53*, 1917-1926.

St-Onge, L., Sosa-Pineda, B., Chowdhury, K., Mansouri, A., and Gruss, P. (1997). Pax6 is required for differentiation of glucagon-producing alpha-cells in mouse pancreas. Nature *387*, 406-409.

Stagner, J.I., Samols, E., and Marks, V. (1989). The anterograde and retrograde infusion of glucagon antibodies suggests that A cells are vascularly perfused before D cells within the rat islet. Diabetologia *32*, 203-206.

Stoffers, D.A., Kieffer, T.J., Hussain, M.A., Drucker, D.J., Bonner-Weir, S., Habener, J.F., and Egan, J.M. (2000). Insulinotropic glucagon-like peptide 1 agonists stimulate expression of homeodomain protein IDX-1 and increase islet size in mouse pancreas. Diabetes *49*, 741-748.

Sutherland, E.W., and De Duve, C. (1948a). A glycogenolytic factor from pancreas. Federation proceedings *7*, 195.

Sutherland, E.W., and De Duve, C. (1948b). Origin and distribution of the hyperglycemic-glycogenolytic factor of the pancreas. The Journal of biological chemistry *175*, 663-674.

ter Braak, E.W., Appelman, A.M., van der Tweel, I., Erkelens, D.W., and van Haeften, T.W. (2002). The sulfonylurea glyburide induces impairment of glucagon and growth hormone responses during mild insulin-induced hypoglycemia. Diabetes Care *25*, 107-112.

Thorel, F., Damond, N., Chera, S., Wiederkehr, A., Thorens, B., Meda, P., Wollheim, C.B., and Herrera, P.L. (2011). Normal glucagon signaling and β-cell function after near-total α-cell ablation in adult mice. Diabetes *60*, 2872-2882.

Um, S.H., Frigerio, F., Watanabe, M., Picard, F., Joaquin, M., Sticker, M., Fumagalli, S., Allegrini, P.R., Kozma, S.C., Auwerx, J., et al. (2004). Absence of S6K1 protects against age- and diet-induced obesity while enhancing insulin sensitivity. Nature *431*, 200-205.

Walker, J.N., Ramracheya, R., Zhang, Q., Johnson, P.R., Braun, M., and Rorsman, P. (2011). Regulation of glucagon secretion by glucose: paracrine, intrinsic or both? Diabetes Obes Metab *13 Suppl 1*, 95-105.

Wang, H., Gauthier, B.R., Hagenfeldt-Johansson, K.A., Iezzi, M., and Wollheim, C.B. (2002). Foxa2 (HNF3beta) controls multiple genes implicated in metabolism-secretion coupling of glucose-induced insulin release. The Journal of biological chemistry *277*, 17564-17570.

Wang, Q., Li, L., Xu, E., Wong, V., Rhodes, C., and Brubaker, P.L. (2004). Glucagon-like peptide-1 regulates proliferation and apoptosis via activation of protein kinase B in pancreatic INS-1 beta cells. Diabetologia *47*, 478-487.

Wang, S., Jensen, J.N., Seymour, P.A., Hsu, W., Dor, Y., Sander, M., Magnuson, M.A., Serup, P., and Gu, G. (2009). Sustained Neurog3 expression in hormone-expressing islet cells is required for endocrine maturation and function. Proceedings of the National Academy of Sciences of the United States of America *106*, 9715-9720.

Weir, G.C., Atkins, R.F., and Martin, D.B. (1976). Glucagon secretion from the perfused rat pancreas following acute and chronic streptozotocin. Metabolism: clinical and experimental *25*, 1519-1521.

Wendt, A., Birnir, B., Buschard, K., Gromada, J., Salehi, A., Sewing, S., Rorsman, P., and Braun, M. (2004). Glucose inhibition of glucagon secretion from rat alpha-cells is mediated by GABA released from neighboring beta-cells. Diabetes *53*, 1038-1045.

Wierup, N., Yang, S., McEvilly, R.J., Mulder, H., and Sundler, F. (2004). Ghrelin is expressed in a novel endocrine cell type in developing rat islets and inhibits insulin secretion from INS-1 (832/13) cells. The journal of histochemistry and cytochemistry : official journal of the Histochemistry Society *52*, 301-310.

Xu, E., Kumar, M., Zhang, Y., Ju, W., Obata, T., Zhang, N., Liu, S., Wendt, A., Deng, S., Ebina, Y., et al. (2006). Intra-islet insulin suppresses glucagon release via GABA-GABAA receptor system. Cell metabolism *3*, 47-58.

Yang, J., MacDougall, M.L., McDowell, M.T., Xi, L., Wei, R., Zavadoski, W.J., Molloy, M.P., Baker, J.D., Kuhn, M., Cabrera, O., et al. (2011). Polyomic profiling reveals significant hepatic metabolic alterations in glucagon-receptor (GCGR) knockout mice: implications on anti-glucagon therapies for diabetes. BMC Genomics *12*, 281.

Yoon, K.H., Ko, S.H., Cho, J.H., Lee, J.M., Ahn, Y.B., Song, K.H., Yoo, S.J., Kang, M.I., Cha, B.Y., Lee, K.W., et al. (2003). Selective beta-cell loss and alpha-cell expansion in patients with type 2 diabetes mellitus in Korea. The Journal of clinical endocrinology and metabolism *88*, 2300-2308.

Yue, J.T., Riddell, M.C., Burdett, E., Coy, D.H., Efendic, S., and Vranic, M. (2013). Amelioration of hypoglycemia via somatostatin receptor type 2 antagonism in recurrently hypoglycemic diabetic rats. Diabetes *62*, 2215-2222.

Zhang, Q., Ramracheya, R., Lahmann, C., Tarasov, A., Bengtsson, M., Braha, O., Braun, M., Brereton, M., Collins, S., Galvanovskis, J., et al. (2013). Role of KATP Channels in Glucose-Regulated Glucagon Secretion and Impaired Counterregulation in Type 2 Diabetes. Cell metabolism *18*, 871-882.

Zhang, Y., Zhang, Y., Bone, R.N., Cui, W., Peng, J.B., Siegal, G.P., Wang, H., and Wu, H. (2012). Regeneration of pancreatic non-beta endocrine cells in adult mice following a single diabetes-inducing dose of streptozotocin. PLoS One *7*, e36675.